UNSW SYDNEY

Highly Accurate Ultrasonic Positioning and Tracking Systems

Author:
Khyam, Mohammad

Publication Date:
2015

DOI:
https://doi.org/10.26190/unsworks/2706

License:
https://creativecommons.org/licenses/by-nc-nd/3.0/au/
Link to license to see what you are allowed to do with this resource.

Downloaded from http://hdl.handle.net/1959.4/54259 in https://unsworks.unsw.edu.au on 2024-04-30

Highly Accurate Ultrasonic Positioning and Tracking Systems

by

Mohammad Omar Khyam

A thesis submitted in fulfilment of the requirements

for the degree of

Doctor of Philosophy

School of Engineering and Information Technology

The University of New South Wales

Canberra, Australia

August, 2014

Originality Statement

'I hereby declare that this submission is my own work and to the best of my knowledge and belief, it contains no material previously published or written by another person, nor material which to a substantial extent has been accepted for the award of any other degree or diploma at UNSW or any other educational institution, except where due acknowledgement is made in the thesis. Any contribution made to the research by colleagues, with whom I have worked at UNSW or elsewhere, during my candidature, is fully acknowledged. I also declare that the intellectual content of this thesis is the product of my own work, except to the extent that assistance from others in the project's design and conception or in style, presentation and linguistic expression is acknowledged.'

Signed..

Date........................

Dedication

My late father; the best man that I have ever known.

Not forgetting my mother, the living encouragement for me

My wife Mutmainnah Hasib, who is constantly very supportive to all my plans

Acknowledgements

"Patience is not passive waiting. Patience is active acceptance of the process required to attain your goals and dreams."–Ray Davis

Thanks to

• God, the Almighty, *Alhamdulillah*, for bestowing His unlimited Mercy and Blessings on me to accomplish this task.

• My supervisor, Associate Professor Dr. Mark Pickering, for his continuous guidance and encouragement throughout my PhD journey. His energy and enthusiasm still continue to amaze me. Whenever I have felt down, I could simply knock on his door and discuss different issues. During the countless discussions I had with him, I always felt that I was his only student, although he had about ten students. He has always given me the courage to continue and see my work until the end. I have learnt many things from him, which will indeed be useful for my future career. Without his assistance this thesis would not have been possible.

• My co-supervisor, Senior Lecturer, Dr. Andrew Lambert, for his help and support throughout my PhD candidature.

• Dr. Jahangir Alam, for his valuable directions in my research and for his closest guideline.

• Denise Russel for proofreading my thesis.

• The University of New South Wales for supporting me with Tuition Fee Remission Scholarship, Completion Scholarship and Post-graduate Research Support Schemes.

• All the UNSW, Canberra, school office members for their cordial assistance throughout my research journey.

• Dr. Apel Mahamud, as my local guardian in Australia.

• Younger, elders, and friends in the University and community who have made my life in the Australian Capital Territory fruitful and pleasurable.

• My house mates Habibullah Habib, Md Asikuzzaman and Mohiuddin Ahmed for their support like family members.

• Mutmainnah Hasib, my wife, for being so understanding about the life of a graduate student. I will happily support her in whatever she decides to pursue for the rest of our lives.

• My brother and sister, for giving me their unconditional support.

• The amazing lady my mother, the living encouragement for me. She has always been with me with her prayers and well wishes.

• My late father, for teaching me the value of education. He would have been the happiest person today, if he would have been alive. May Allah rest him in peace and place him in heaven!

Abstract

Localization is the process of determining the current location of a target(s) within given coordinates using a location system. The localization process has two main phases: firstly, the measurement phase, that establishes a relationship in terms of the distance and/or angle between the targets(s) to be localized and the system infrastructure; and secondly, the positioning phase, that exploits the measured information to calculate the absolute or relative location coordinates of the target(s). So far the most widely used positioning system is the Global Positioning System (GPS). However, in a GPS system, the receiver requires line-of-sight (LOS) reception from different satellites, which is usually difficult to obtain indoors. Therefore, as there is a need for alternate location systems in these GPS-obstructed environments, indoor positioning has drawn considerable attention from both academia and industry. Indoor environments, which are characterized by obstacles such as walls, floors, ceilings, and furniture, provide countless opportunities for a wide range of applications requiring different levels of accuracy. High-accuracy applications, such as gait analysis, usually use optical motion capture systems (MCSs), which are cost-prohibitive for many users, and also require complex arrangements of expensive equipment. In addition, they are responsive to changes in lighting and shadow. Therefore, with the aim of overcoming these limitations, ultrasonic positioning systems (UPSs) have drawn considerable attention. Usually, a narrowband UPS uses either a single tone or narrowband chirp signal in the measurement

phase in which accurate estimations of distance, through time-of-flight (TOF) techniques, are fundamental. Generally, cross-correlation, which produces a peak at the time delay between a transmitted and received signal, is considered the optimal TOF estimation technique. Since their accuracy depends on the width of the correlation peak, which is inversely proportional to the signal's bandwidth, these systems can only be said to be highly accurate if the reflected or multipath signal at the receiver is separated in time by more than the width of the correlation peak; otherwise, errors are introduced into the system. To improve the accuracy of such systems, the bandwidth of the signal must be increased, which increases the cost of the system. In the first part of this thesis, a new phase-correlation-based TOF estimation technique, that uses a narrowband chirp signal working in a closely spaced multipath environment, is proposed. In this system, the correlation peak becomes narrower by virtually, rather than physically, increasing the signal's bandwidth, which reduces system cost. The performance of the proposed method is evaluated experimentally.

As the correlation technique finds matches between transmitted and received signals, both signals need to be stored at the receiver, which increases hardware cost and computational complexity. In the second part of this thesis, firstly, to solve the limitations of the correlation technique, a narrowband orthogonal frequency division multiplexing (OFDM)-based TOF technique is introduced in which the TOF is estimated based on a pre-defined threshold. The proposed technique has advantages in terms of computational complexity and hardware cost when compared to the correlation technique, as in this approach TOF estimation decisions are made using threshold detection and only the received signal needs to be stored. An additional feature of this technique is that it has good noise cancelation properties. In the positioning phase, existing UPSs generally use the lateration algorithm to obtain a target's location information. For the accurate positioning of reference points in an indoor environment, it is logistically simpler if they are installed in a fixed plane. This means that the distances between the reference points will usually be smaller than the distances between the reference points and the target(s). In this configuration, when lateration is used for positioning target(s), the surfaces of the spheres centered at the reference points will be almost parallel. This results in larger errors in the positions of the intersecting points of the spheres for directions tangential to the surfaces of the spheres than for those normal to these surfaces. This phenomenon is known as dilution of precision (DOP). To overcome this DOP problem, a steepest descent optimization algorithm is proposed. The proposed algorithm places the reference points at positions which best correspond to their measured distances from the target utilizing a three-dimensional (3D) rigid-body transformation. An additional feature of this algorithm is that it allows errors to be ignored in the distance measurements of the receivers corresponding to one complete cycle of the transmitted signal. Experimental results demonstrate the improvement obtained by the proposed methods over the traditional lateration based positioning systems that use cross-correlation techniques with a transmitted chirp signal.

Finally, when UPSs use single tone or narrowband chirp signals, they cannot simultaneously localize multiple targets due to signal interference. This is generally overcome by either using the time division multiplexing (TDM) technique, which reduces the positioning update rate, or introducing a broadband transducer, which increases system cost. In the last part of this thesis, the proposed OFDM-based steepest descent optimization algorithm is first extended to handle multiple target positioning utilizing the orthogonal property of the OFDM signal. Since TDM techniques and broadband transducers are not required, this system can maintain the single target system update rate without increasing system cost. For the positioning of a moving target(s), most of the existing localization systems use the matched filtering technique, where a bank of correlators is used to estimate the Doppler shift associated with the target's movement. This requirement increases computational complexity and system cost. The proposed OFDM-based steepest decent optimization algorithm is further extended for tracking a moving target. The Doppler shift is estimate by introducing a pilot carrier to the transmitted OFDM signal. As it does not require matched filters to estimate the Doppler shift, the proposed system does not require extra computational complexity or system cost. The accuracy of the proposed system is compared with an optical motion capture system, Vicon, and it is shown to have the same order of precision while incurring less cost and complexity.

Contents

List of Figures

List of Tables

List of Abbreviations

Abbreviations	**Description**
2D	Two-dimensional
3D	Three-dimensional
AENSBox	Acoustic Embedded Networked Sensing Box
AHLoS	Ad-hoc Localization System
AOA	Angle-of-Arrival
AWGN	Additive White Gaussian Noise
BLPA	Bluetooth Local Positioning Application
BPSK	Binary Phase Shift Keying
BS	Base Station
CAN	Controller Area Network
CDM	Code Division Multiplexing
CID	Cell Identification
CO	Cell Origin
CODA	Cartesian Optoelectronic Dynamic Anthropometer
DAQ	Data Acquisition
DGPS	Differential Global Positioning System
DLL	Dynamic-Link Library
DOLPHIN	Distributed Object Locating System for Physical Space Internetworking

DOP	Dilution of Precision
DR	Dead Reckoning
DSCDMA	Direct Sequence Code Division Multiple Access
DSSS	Direct Sequence Spread Spectrum
EKF	Extended Kalman Filter
EM	Electromagnetic
ETOA	Elapsed Time Between Two Time-of-Arrivals
FDM	Frequency Division Multiplexing
FFT	Fast Fourier Transform
FHSS	Frequency Hopped Spread Spectrum
FM	Frequency-modulated
FMCW	Frequency-modulated Continuous Wave
GA	Genetic Algorithm
GPS	Global Positioning System
HA	Hybrid Algorithm
ICI	Inter Sub-carrier Interference
ID	Identification
IMM	Interacting Multiple Model
IR	Infrared
KF	Kalman Filter
k-NN	k-Nearest-Neighbors
LAN	Local Area Network
LANDMARC	Location ID based on Dynamic Active Rfid Calibration
LED	Light-Emitting Diode
LORAN	Long-Range Navigation
LOS	Line-of-Sight
LPR	Local Positioning Radar

LSE	Least Squares Estimation
MCS	Motion Capture System
MCU	Motion Capture unit
MD	Mobile Device
MLP	Multilayer Perceptron
MS	Mobile Station
NIR	Near-Infrared
NLOS	Non-Line-of-Sight
OFDM	Orthogonal Frequency Division Multiplexing
PD	Phase Difference
PDA	Personal Digital Assistant
PF	Particle Filter
PN	Pseudo-noise
RADAR	Radio Detection and Ranging
REKF	Robust Extended Kalman Filter
RF	Radio Frequency
RFID	Radio Frequency Identification
RIPS	Radio Interferometric Positioning System
RSS	Received Signal Strength
RSSI	Received Signal Strength Indicator
RTT	Round-Trip-Time
SDM	Space Division Multiplexing
SDK	Software Development Kit
SMP	Smallest M-vertex Polygon
SNR	Signal-to-Noise Ratio
SONAR	Sound Navigation and Ranging
SS	Signal Strength

SVC	Support Vector Classification
SVD	Singular Value Decomposition
SVM	Support Vector Machine
SVR	Support Vector Regression
TDM	Time Division Multiplexing
TDOA	Time-Difference-of-Arrival
TOA	Time-of-Arrival
TOF	Time-of-Flight
UNSW	University of New South Wales
US	Ultrasonic
UPS	Ultrasonic Positioning System
UTC	Coordinated Universal Time
UWB	Ultra Wideband
WLAN	Wireless Local Area Network
WSN	Wireless Sensor Network

Chapter 1

Introduction

This chapter presents an introduction to localization, surveys the uses of localization applications and discusses the types of signals used in this thesis. It concludes by providing the contributions of this thesis, including a list of publications that present the main results of the thesis and the organization of the remaining chapters.

The question "Where am I?" has existed from the time when mankind began to seek somewhere to dwell. Throughout human history, finding one's own location has been a central problem, whether to rediscover recently explored food resources or determine the way back home. To achieve this, people have developed different tactics; for example, scrutinizing the environment and discovering conspicuous features, such as river shores, mountains or particular trees, they used to determine their positions when exploring an area [10]. Also, they have taken the Earth as a frame of reference to ascertain their location by calculating the angles of different celestial bodies relative to the horizon, which act as a set of natural reference points moving in predictable paths, using tools such as the quadrant and sextant [11].

Throughout the evolution of mankind, great scientific and technological developments have been achieved. In the twentieth century, advances in electronics and telecommunications brought a range of new inventions that enabled technologies such as Long-range Navigation (LORAN), Radio Detection and Ranging (RADAR) and Sound Navigation and Ranging (SONAR) which are used to provide navigational guidance to aircrafts, ships and submarines [12]. In the latter half of the twentieth century, following new demands for location sensing, the Global Positioning System (GPS) [13], which is used not only for navigational purposes but also in missile guidance, vehicle and person tracking, clock synchronization in cellular systems, geographical information systems, surveying, mapping, etc., was designed and provisioned.

In the GPS system, its receiver requires line-of-sight (LOS) receptions from different satellites which are inherently impossible to obtain indoors, underwater or in urban locations. In addition, the presence of building materials and metallic objects in an indoor environment places fundamental limitations on the propagation of GPS radio signals [14] which considerably undermines their localization performances. Therefore, in these GPS-obstructed environments, there is a need for alternate location systems. As a result, indoor positioning has drawn considerable attention from both academia and industry.

To determine the position of a target(s) in two- or three-dimensional (2D or 3D respectively) space, an indoor positioning system requires a predefined set of reference points and a signal which could be instigated by any of them, to establish a relationship in terms of distance and/or angle between the target and the reference points. This part of the location system is known as the measurement phase and, using it, the system is able to calculate the target's position using a localization algorithm through what is known as the positioning phase. Generally,

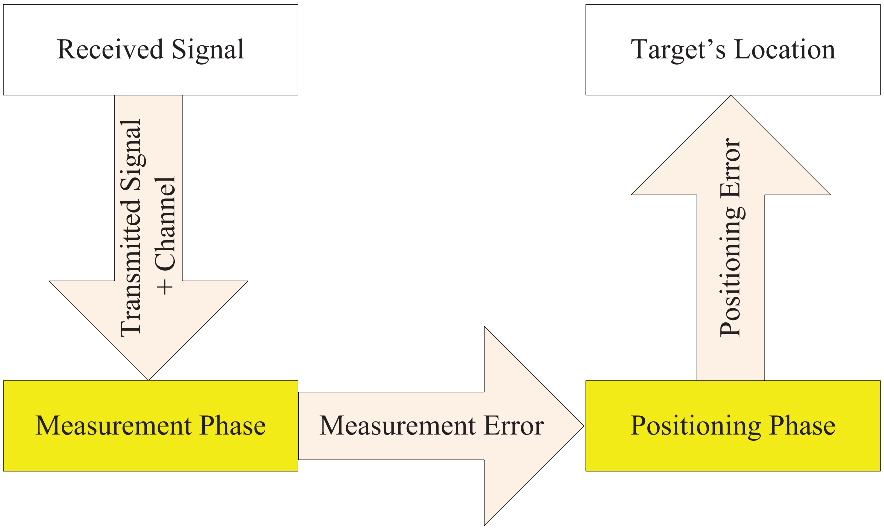

Figure 1.1: Location cycle of a positioning system.

in the measurement phase, it is more common to use distance information with the time-of-flight (*TOF*)[1] than angle information [15, 16] and, in the positioning phase, *tri(or multi)lateration*[2] is widely used [17]. A small amount of error in either of these two phases gives an erroneous target(s) location. Generally, an error in the measurement phase is caused by an environmental factor such as reflection and, in the positioning phase, by two types of error, one introduced in the measurement phase and another introduced by itself either during installation of the reference points or due to the relative configuration of reference points and target(s), both of which bias the positioning results. The location cycle of a positioning system is shown in Figure 1.1.

[1]The TOF is the travel time taken by a physical signal to propagate between a transmitter and receiver; its details are discussed in Section 2.3.1.1, Chapter 2.

[2]An algorithm for determining the position of an object in 3D space from at least three reference points is called trilateration and, from more than three, multilateration; a detailed description is given in Section 2.3.2.1, Chapter 2.

1.1 Applications of Indoor Positioning Systems

There is a wide range of promising indoor applications and evolving technologies, which require different levels of accuracy, that can benefit from location knowledge.

Indoor positioning applications requiring low accuracy can use wireless sensor networks (WSNs). Such applications include those which: provide safety and topical information to the public about cinemas, concerts or events in the vicinity; navigate people to the right places in stores in malls, offices and large museums; find products of interest for people in a store or a robot in industry; determine the assets and staff members required to optimize processes in complex systems; and monitor environmental phenomena, such as heat, pressure, humidity, air pollution and deformations of objects and structures.

High-accuracy applications include those which: in the entertainment industry, especially films and video games, require accurate positioning to create life-like models that move like real human beings; in the robotics and computer science industry, use 3D positioning to produce human-like actions in robots; in sports science, require 3D positioning to analyse the movements of athletes in order to help them improve their techniques; in rehabilitation processes, require accurate positioning in order to establish normal movement models for the patients whose central nervous systems are damaged.

Usually, all the abovementioned high-accuracy applications use optical systems in which optical markers are mounted on the subject at specified limb positions and their movements captured through special cameras. From the captured images, the markers coordinates are identified and, finally, their 3D trajectories created. Although these systems are able to provide sub-millimeter accuracy, their cost is prohibitive for many users and they also require complex arrangements of expensive equipment. Moreover, they are generally not invariant to changes in lighting and shadow [18, 19].

Having high-accuracy applications in mind, especially gait analysis [20], this thesis attempts to develop highly accurate indoor positioning systems. Generally, there are two types of waves used for indoor positioning, electromagnetic (EM) and ultrasonic (US). Given the aim of developing a highly accurate indoor positioning systems, it was decided to use an US rather than EM wave because of its following advantages.

1.2 Advantages of US over EM Wave

Firstly, as the frequencies of an US signal are lower (normally in the order of Hz/kHz) than those of an EM signal (usually in the order of MHz/GHz) and the speed of an US signal is radically slower (almost 10^6 times) than that of an EM signal, hence, the cost, complexity and signal processing time of the ranging hardware in an US-based positioning system is much less than for an EM based system. If the speed of sound in air is approximately 343 m/s at 20°C, a resolution of 1 mm in distance corresponds to a resolution in time of 2.94 μs. As, for an EM wave traveling at the speed of light, the required resolution is 3.33 ps, a very complex system would be required to measure the time delays associated with its TOF. However, besides its lower cost, complexity and signal processing time, there is another advantage of an US wave over EM wave in terms of the power needed. Relative to EM-based approaches, an US transducer can be operated at lower power because most of the energy required to operate it can be drawn from the signal itself while the cost of a *narrowband*[3] US transducer, which operates at a narrowband of frequencies centered around 40 kHz, is approximately $10.00.

Secondly, the use of US waves allows for more control over the signal, i.e., an US transducer can be easily designed according to any specifications.

Finally, for medical applications, an US signal provides a safer solution than an EM signal as there is a potential (albeit, minute) for RF waves to disrupt other medical equipment situated nearby.

1.3 Motivation and Contributions

In the past, a number of ultrasonic positioning systems (UPSs) have been developed for workplaces, homes, public spaces and medical settings for applications including body tracking [21–39], laparoscopic surgery [40], indoor navigation [41–50], robot navigation [44, 51–53], multiple device location [54], and short-range applications such as paper thickness measurements [55]. Generally, in an UPS, cross-correlation is considered the optimal solution for distance measurement using TOF information [56]. Cross-correlation calculates the number of samples required to shift a transmitted signal so that it is aligned with the received signal and produces the maximum value of cross-correlation at that time delay. However, for a single tone signal, cross-correlation performs poorly in terms of TOF estimations because, in a particular signal length, there are several cycles which produce very similar peaks adjacent to the main peak when it is cross-correlated with the received signal and, in a noisy environment, a false peak may be detected [57, 58]. Cross-correlation provides improved accuracy when the waveform is a

[3] If the ratio of the bandwidth to the center frequency of a signal is less than or equal to 0.2, the signal is considered narrowband.

frequency-modulated (FM) signal, such as a linear chirp [16, 58, 59], with its accuracy dependent on the width of the peak which is inversely proportional to the signal's bandwidth. Therefore, this technique can be said to be highly accurate if the reflected or multipath signals at the receivers are separated in time by more than the width of the correlation peak; otherwise, errors are introduced into the system. Therefore, to improve the accuracy of the cross-correlation technique, it is necessary to use a *broadband*[4] signal [16, 59] which increases the system cost.

The first contribution of this dissertation is a new phase-correlation-based TOF estimation technique using a narrowband chirp signal which works in a closely spaced multipath environment. Its unique features are: its capability to narrow the correlation peak by increasing the signal's bandwidth virtually, rather than physically in a moderate signal-to-noise ratio (SNR) ($\approx$ 6 dB) environment which reduces the system cost; it helps to accurately determine the TOF in a closely spaced multipath environment; and additionally it can separate the individual multipath components. The proposed approach is tested in an indoor environment and compared with the cross-correlation technique. The experimental results shows that the proposed approach achieved higher accuracy (almost sub-millimeter) than the cross-correlation technique.

The correlation technique is also known as a matched filtering technique as it finds matches between transmitted and received signals by storing both which increases the computational complexity and hardware cost. Most importantly, for the accurate positioning of the reference points in indoors, it is simpler logistically if they are installed in a fixed plane. This means that, if the distance between reference points is less than the distance between them and localizing target(s) (which is likely to happen) and, with this configuration if lateration is used for

[4]If the ratio of the bandwidth to the center frequency of a signal is greater than 0.2, the signal is considered broadband.

positioning, this will produce larger errors in position estimations which will be explained later.

In the second part of this thesis, two algorithms are proposed for the measurement and positioning phases. In the former, a narrowband orthogonal frequency division multiplexing (OFDM)-based TOF technique is introduced which has the following unique advantages when compared with the chirp-based correlation technique: less computational complexity as TOF estimation decisions are made on a threshold basis; efficient use of memory as only the received signal needs to be stored; and good noise cancelation properties as the frequency components other than those present in an OFDM signal are forcefully set to zero during *equalization*[5]. In the positioning phase, a steepest descent optimization algorithm is proposed, which has the following advantages over the traditional lateration algorithm: it is capable of overcoming the error due to the reference points' configuration; and it can compensate for errors in distance measurements of the receivers which correspond to one complete cycle of the transmitted signal. The proposed approach is evaluated in an indoor environment and its performance is compared with the traditional cross-correlation-based multilateration algorithm which uses a narrowband chirp or single tone signal. The experimental results show that the proposed approach achieved higher accuracy (sub-millimeter) than the traditional approach.

When a single tone or narrowband chirp signal is used by an UPS for static and dynamic transducer positioning, it suffers from two major problems. Firstly, it cannot simultaneously localize multiple transducers due to signal interference. Although this can be solved either by the time division multiplexing (TDM) technique or by introducing a broadband transducer, it reduces the positioning update

[5]The process of removing the transducer effect and reducing noise from the received signal is called equalization, as detailed in Section 4.3, Chapter 4.

rate and increases the system cost respectively. Secondly, for moving transducer positioning, to estimate and compensate the *Doppler shift*[6], it uses a matched filtering technique whereby a bank of transmitted signals is created and stored by shifting the frequency of the transmitted signal to different values and then cross-correlating it with the received signal which requires a large amount of computation.

Therefore, with gait analysis in mind as well as the abovementioned problems, the previously introduced OFDM-based steepest descent optimization algorithm is initially extended to handle multiple transducer positioning utilizing the orthogonal nature of the OFDM signal. Then, it is further extended for tracking using a pendulum model, with Doppler shift compensation performed by introducing a pilot carrier, the strength of which is greater than those of the other sub-carriers in the OFDM signal. The unique features of this proposed system are: it can simultaneously localize multiple transducers without using either a TDM technique or a broadband transducer; and it can compensate the Doppler shift without using a matched filter. Hence there are no negative impacts on system update rate or system cost and complexity. The experimental results shows that the proposed system is able to calculate the 3D locations of multiple transducers with sub-millimeter accuracy and the 3D trajectory of a moving transducer with millimeter precision, which is significantly better than that of the alternative traditional method. The experimental results of various pendulum trajectories obtained using the proposed method are compared with that obtained using a commercially available optical MCS, Vicon, and it is shown that proposed system has the same order of precision but incurs less cost and complexity than the Vicon MCS.

[6]The Doppler shift is the apparent frequency difference between the frequency at which signals leave the transmitter and that at which they arrive at a receiver.

The above contributions resulted in the following papers which have already been published or are currently under review.

1.4 List of Publications

M. Khyam, M. J. Alam, A. J. Lambert, C. R. Benson and M. R. Pickering, "High Precision Mobile Transducer Tracking using a Robust Optimization Approach", submitted to *IEEE Transactions on Instrumentation and Measurement.*

M. Khyam, M.J. Alam, A.J. Lambert, C.R. Benson and M.R. Pickering, "High Precision Ultrasonic Positioning using Phase Correlation", in *Proceedings of the 6th International Conference on Signal Processing and Communication Systems (ICSPCS),* Gold Coast, Queensland, Australia, December 12-14, 2012, pp. 1–6.

M. Khyam, M. J. Alam, A. J. Lambert, C. R. Benson and M. R. Pickering, "High Precision Ultrasonic Positioning using a Robust Optimization Approach", in *Proceedings of the 18th International Conference on Digital Signal Processing (DSP),* Santorini, Greece, July 1-3, 2013, pp. 1–6.

M. Khyam, M.J. Alam, A. J. Lambert, C. R. Benson and M. R. Pickering, "High Precision Multiple Ultrasonic Transducer Positioning using a Robust Optimization Approach", in *Proceedings of the 13th IEEE International Symposium on Signal Processing and Information Technology (ISSPIT),* Athens, Greece, December 12-15, 2013, pp. 192–197.

M. Khyam, M. J. Alam and M. R. Pickering, "OFDM-based Low-complexity Time of Arrival Estimation in Active Sonar", Accepted in *OCEANS'14 MTS/IEEE Conference,* Taiwan, Taipei, April 7-10, 2014.

The remaining chapters in this thesis are organized as follows. Chapter 2 provides an overview of the two phases of a positioning system and includes a review of the literature in relation to both outdoor and indoor positioning systems. A new TOF measurement technique using phase-correlation is presented in Chapter 3. Chapter 4 introduces two new techniques, one for TOF estimation using an OFDM signal and another for positioning using a steepest descent optimization algorithm. In Chapter 5, the new algorithm proposed in Chapter 4 is initially extended from single to simultaneous multiple transducer positioning and then is further extended for tracking a moving target using a complex pendulum model. Chapter 6 provides a summary of this thesis and outlines some directions for future research.

Chapter 2

Background and Related Work

This chapter begins with an introduction to localization. The underlying body of knowledge in these areas serves as the foundation of the proposed localization techniques. The chapter concludes with a literature review on localization for both outdoor and indoor.

2.1 Localization

The process of determining the current location of a target(s) within given coordinates using a location system is called localization which has two phases: firstly, the measurement phase that establishes a relationship in terms of the distance and/or angle between the targets(s) to be localized and the system infrastructure; and secondly, the positioning phase that exploits the measured information to calculate the absolute or relative location coordinates of the object(s). Of course, calibration steps are added to the measurement and positioning phases to compensate the error occurring due to environmental and manufacturing effects and installation process of the system infrastructure.

In the positioning phase, the algorithm that generates the location coordinates, can be categorized by the following three mechanisms [16].

• **Reference-based localization:** This requires a well-known set of fixed or mobile reference points which are also referred to as anchors or landmarks. Using the distance information between the target and reference points, the location of the target is measured using a localization algorithm (e.g., trilateration). In the case of moving reference points, (e.g., the global positioning system (GPS)) [13], the points must follow a trajectory which is already known so that their coordinates can be determined at any given instant [60–62].

• **Reference-free localization:** Without any previous knowledge of reference points the locations of targets are determined here using only the knowledge of the targets separation distances [61–63]. The underlying algorithm searches in a defined coordinate space to determine the optimal coordinates for targets that satisfy the calculated distance constraints. These are called virtual coordinates as none of the objects is tagged within a global location coordinate system. Generally, some form of non-linear optimization approaches are used by these localization algorithms to solve an equation system formed by the distance constraints and these algorithms may be trapped in a local minima, which results in erroneous location estimation. Additionally, this method becomes complex due to the absence of reference points.

• **Localization from dead reckoning (DR):** This is a process which calculates the location of a target by means of the target's motion dynamics, such as velocity, acceleration and orientation [64–66]. For example, if a target begins moving from a point (P) along a direction (θ) at a constant velocity (v), its location coordinates at time t are given by ($vt \cos\theta$ and $vt \sin\theta$). In DR, a target's current location is calculated based on its previously estimated locations and suffers from the cumulative error or 'drift' arising from time or traveled distances. Because of this limitation, the majority of location systems employ landmarks or a combination of landmarks and DR [67, 68].

Generally, the performance of a location system depend on its architecture which is discussed in the following section.

2.2 Location System Architectures

The scalability, privacy and tracking performance of a location system depend on its architecture which can be either active mobile or passive mobile [69, 70], as shown in Figure 2.1 and Figure 2.2 respectively. In the former, fixed receivers at well-known positions periodically receive wireless signals (e.g., ultrasonic (US) or electromagnetic signals at radio frequencies (RF)) from a mobile device (MD) and each computes its distance from the MD using these received signals. On the contrary, in a passive mobile architecture, beacons fixed at well-known positions periodically transmit their location information on a wireless channel, the MDs listening to each beacon estimate their distances from the beacons. Both architectures have their pros and cons. The tracking performance of the active architecture is better than that of the passive mobile architecture (of course, if the number of MDs is less than the number of reference points) since a receiver in the latter can listen to only one beacon at a time and may move between two successive beacon transmissions. As a result, it fails to obtain simultaneous distance measurements whereas, in an active mobile case, multiple receivers simultaneously obtain estimates of their distances from a moving device. However, a passive mobile architecture offers better scalability as the concentration of its

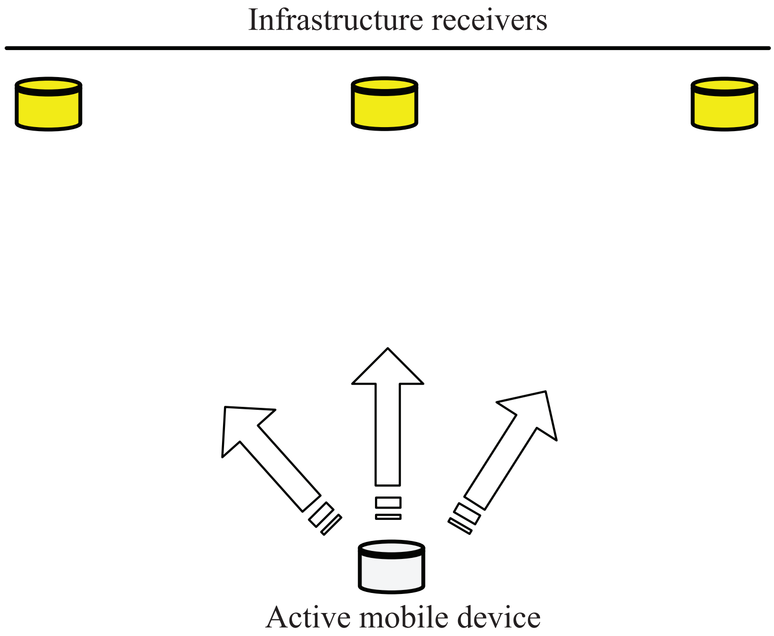

Figure 2.1: Active mobile architecture.

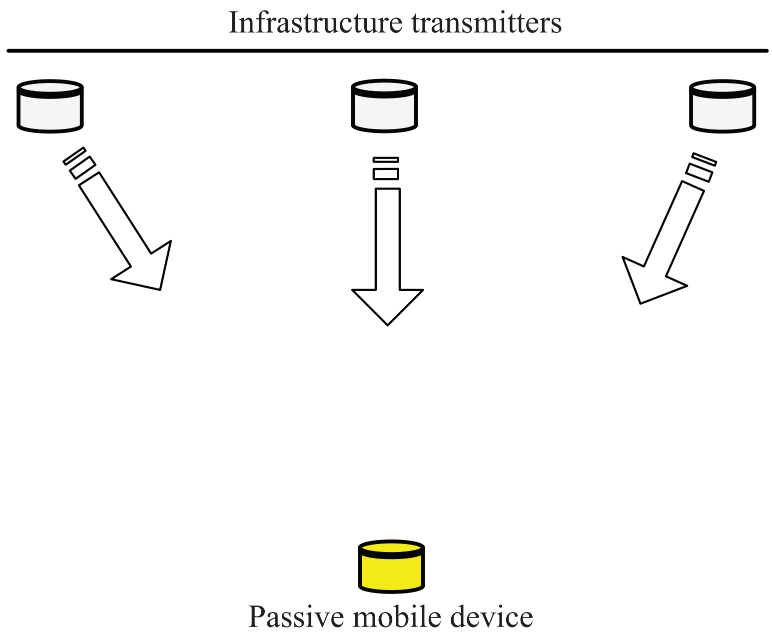

Figure 2.2: Passive mobile architecture.

devices increases because the wireless channel (RF or US) is not dependent on the number of MDs. This architecture has an increased level of privacy as each MD estimates its own location.

As discussed earlier a localization system has two phases, measurement and positioning. In the following section, the measurement techniques which establish relationships in terms of the distances and/or angles between targets and reference points, and the localization algorithms that utilize this information to calculate the location coordinates of the targets are discussed.

2.3 Overview of the Localization Process

To establish the relationship between objects (targets and reference points) in the measurement phase, a physical signal must be sent by the object which can be sent by either the target(s) or reference points. The taxonomy shown in Figure 2.3 describes the various methods and signals that may be used in the location process.

2.3.1 Overview of Measurement Phase

For location estimations, the distance or angle or both between a target and a set of given reference points is used. Generally, distance-based is more popular than angle-based localization and involves obtaining an estimate of any of the following three parameters: time, phase difference (PD) and signal strength (SS) which are described below.

2.3.1.1 Time

Time-based methods estimate the distance between a pair of objects (target and the reference points which are configured as transmitters and receivers) by measuring the travel time (known as the time-of-flight (TOF)) of a physical signal

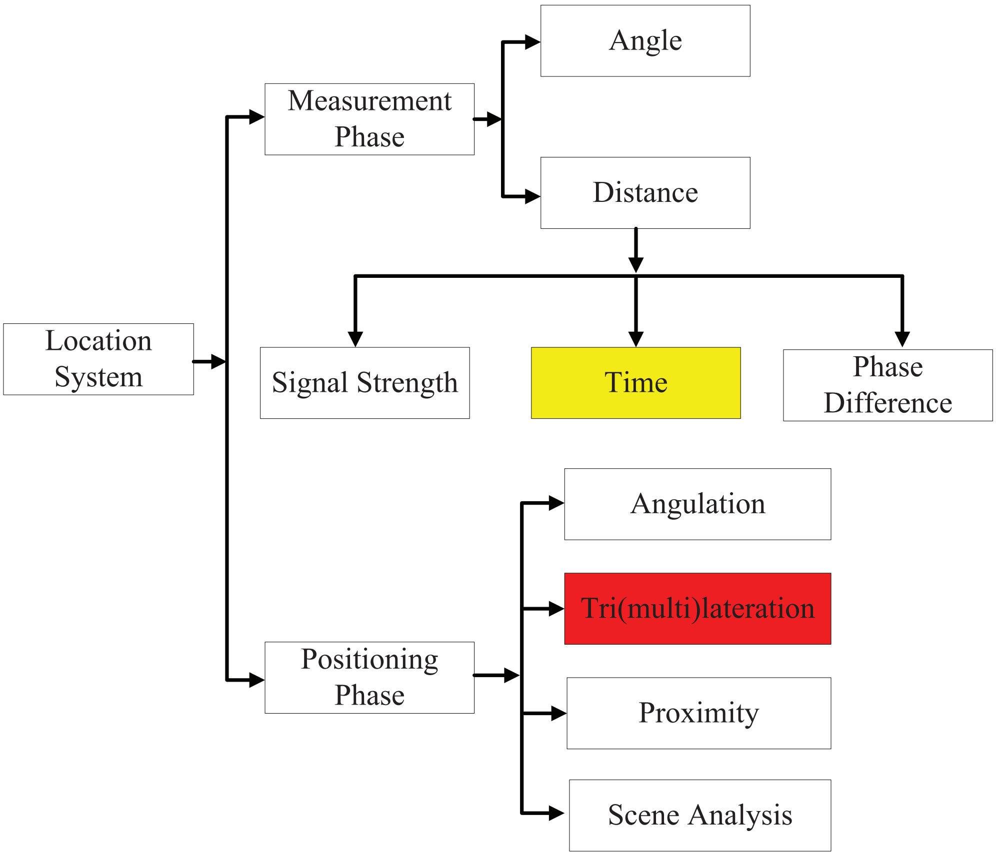

Figure 2.3: Taxonomy of location systems.

propagating between them. The TOF is directly related to the velocity of the transmitted signal [41, 71–75]. If the velocity of the signal is v and TOF is t_F, then the distance between transmitter and receiver is given by $d = vt_F$. Obviously, this is valid for the pitch-catch method whereby the transmitter and receiver are independent. However, in the pulse-echo method, also known as the return-trip-time (RTT) method, where a single transducer transmits and receives, the above distance measurement equation is modified to be $d = \frac{vt_F}{2}$ as the signal travels the distance between the transmitter and receiver twice. Time-based methods can be classified in two ways: based on either clock synchronization or signal sensing and detection.

Clock synchronization

Based on clock differences, the TOF can be estimated in any of the following ways.

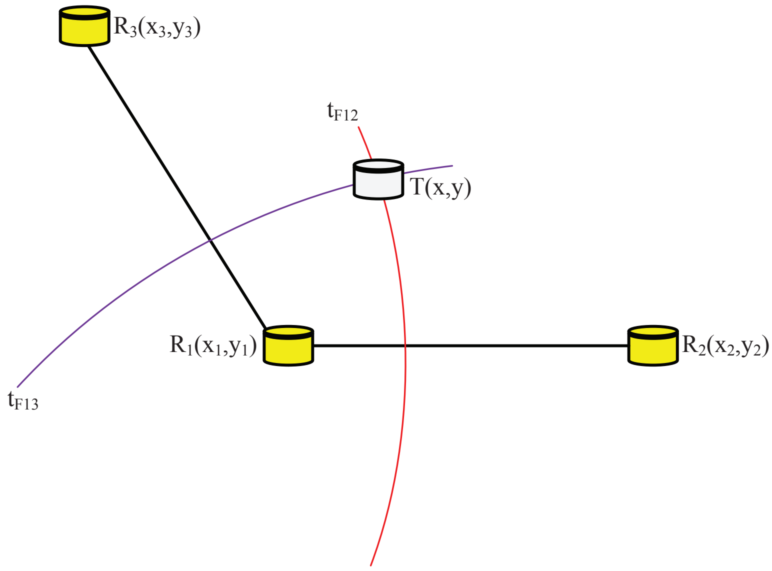

Figure 2.4: Hyperbolic TDOA technique.

• **Time-of-arrival (TOA):** If the transmitter(s) and receiver(s) share a common clock and the starting time of the transmitted signal is known, the time stamp of the incoming signal at the receiver is called the TOA [76–79].

• **Time-difference-of-arrival (TDOA):** To avoid the requirement for precise clock synchronization between the transmitter and receiver, the TDOA technique was introduced for range solutions and can be implemented in the following two ways.

(a) Hyperbolic TDOA: In this approach, the location of a transmitter can be determined by calculating the differences in time at which a signal arrives at multiple measuring units. In order to determine the TDOA between two reference points, the transmitter must lie on a hyperboloid with a constant range difference between the two reference points [80, 81]. Usually, two TDOA measurements, which require at least three reference points, can determine the transmitter's location by finding the intersection of the two hyperbolas, as shown in Figure 2.4.

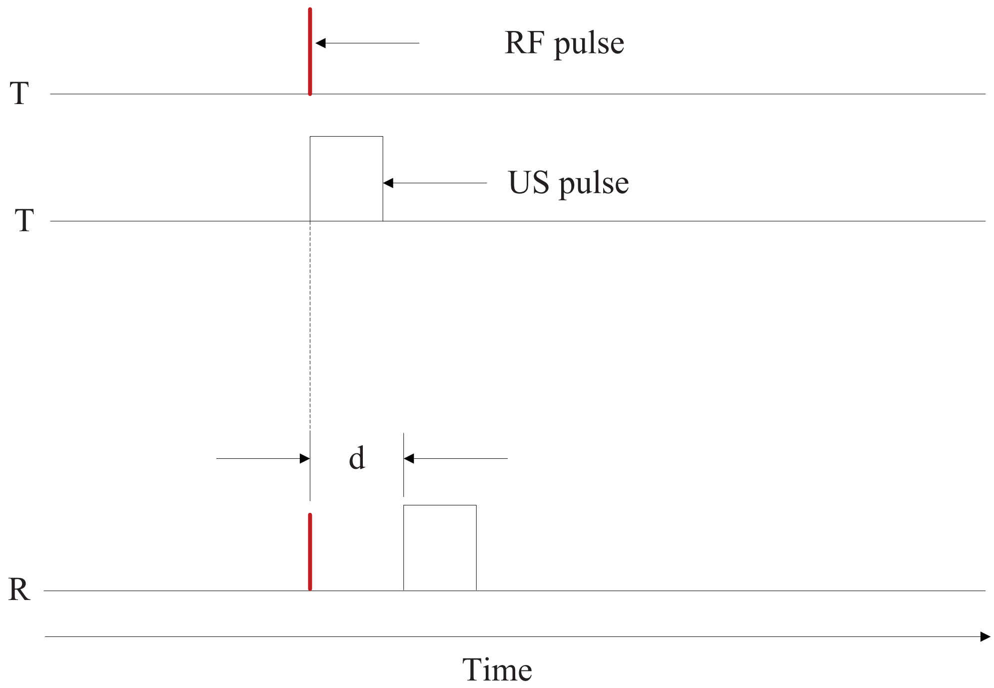

Figure 2.5: Velocity-difference TDOA technique.

(b) Velocity-difference TDOA: In this method, the distance between the transmitter and receiver is determined by simultaneously transmitting two different signals (e.g., RF and US) with significantly different velocities that traverse the same path from the transmitter to receiver which results in a time lag at the receiving end [3, 15, 38, 41, 43, 69–71, 82–84]. In Figure 2.5, considering two signals (s_1 (such as RF) and s_2 (such as US)), with speeds of v_1 and v_2 respectively, sent simultaneously by a transmitter (T), if $v_1 > v_2$, signal s_2 lags behind signal s_1 as they propagate and, if t_F denotes this time lag at a receiver (R) located at a distance (d) from the transmitter then this distance is given by:

$$d = \frac{t_F}{\frac{1}{v_2} - \frac{1}{v_1}}$$

• **Elapsed time between two TOA (ETOA):** The underlying idea of ETOA [72, 85] is shown in Figure 2.6. In two-way sensing, the first device (A) transmits an US signal which is recorded by the recorders of both devices (A and B) and

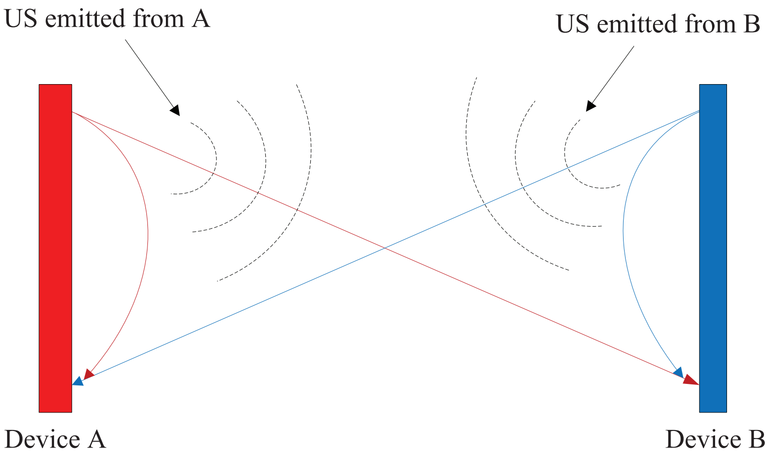

Figure 2.6: ETOA technique.

then, after a time span, the same task is performed by B sending an echo. Both devices check their recorded data and find the sample points of time at which the two previously transmitted signals arrived and compute the elapsed time between them.

Signal sensing and detection

In this category, generally two approaches are available which measure the TOF based on signal energy. These two methods are described below.

- **Threshold detection:** This method, which is one of the simplest ways of measuring the TOF, calculates the time when the received signal exceeds a given threshold level for the first time [86]. Although it requires only simple circuitry and calculations, as a TOF measurement technique, it has two major sources of error: i) in a low signal-to-noise ratio (SNR) environment, the noise level may exceed the preset threshold level which increases the likelihood of false positives being detected; and ii) the likelihood of false positives is also increased as the receiving transducer acquires energy before the output signals can be detected with proper noise immunity. Figure 2.7 illustrates the estimation of TOF using the threshold detection method which returns an incorrect delay at t_0 whereas the true delay is

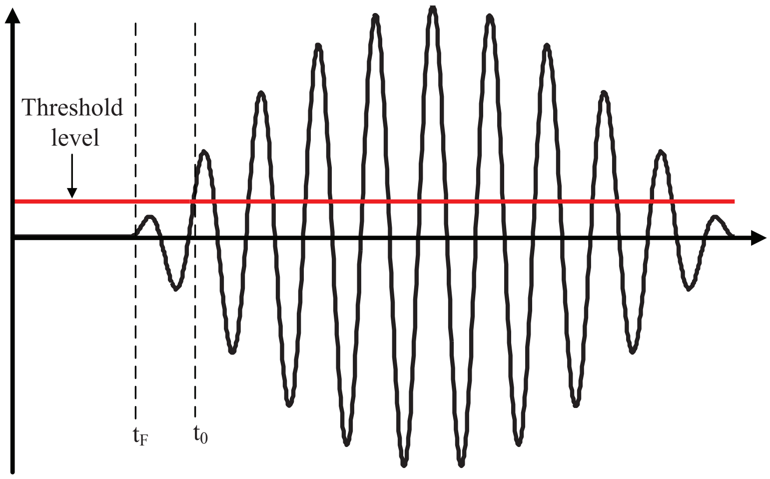

Figure 2.7: Threshold detection.

at t_F. In order to improve the accuracy of this method, different techniques have been proposed, including creating an analytical signal via the Hilbert transform [86], curve fitting [87–89] and sliding window [90].

- **Cross-correlation/Matched filter:** This is the standard digital signal processing technique for measuring the TOF which evaluates the similarity of two signals as a function of time delay [86, 91]. The desired TOF is estimated by finding the time instance at which the reference signal (i.e., a locally stored copy of the original transmitted signal) produces the largest cross-correlation with the received signal, which is indicated by the peak height in the output of the matched filter and (equivalent) time-shift in the correlator bank (Figure 2.8). The mathematical model of the cross-correlation in the discrete time domain is given below. Initially, the transmitted and received signals are sampled and simultaneously digitized to measure the TOF using their cross-correlation ($c[n]$) which is given by:

$$c[n] = \sum_{k=0}^{n-1} s_R[k] s_T[n-k] \tag{2.1}$$

where $s_T[n]$ is the sampled transmitted signal, $s_R[n]$ the sampled received signal and n the number of samples. Usually, when the transmitted and received signals

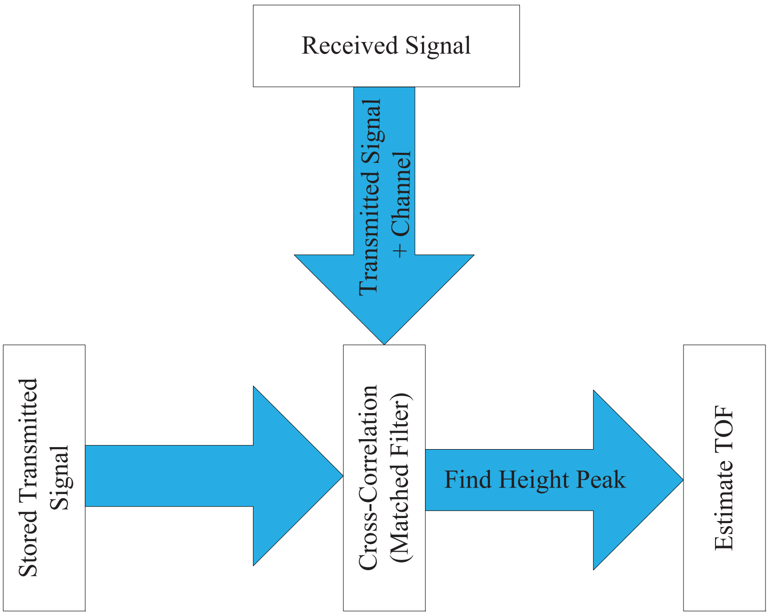

Figure 2.8: Cross-correlation technique.

are perfectly aligned in time, the cross-correlation output is a maximum. If the transmitted signal needs to be shifted by n_F sample times to generate the maximum value of $c[n]$, the TOF between the transmitted and received signals can be represented by $\frac{n_F}{F_s}$, where F_s is the sampling rate.

Although it requires higher computational complexity and needs to store both transmitted and received signals, this method is considered to be the optimal solution for TOF estimation [56, 59, 92, 93]. The cross-correlation technique is typically used with two types of signals: a single tone and a chirp. For a single tone signal the cross-correlation method shows poor performance in the TOF estimation because, in a particular signal length for a single tone signal, there will be several cycles which produce very similar peaks adjacent to the main peak when it is cross-correlated with the received signal. As a results, false peaks may be detected in a noisy environment [59, 94]. Cross-correlation provides improved accuracy when the waveform is not a single tone signal but a frequency-modulated (FM) signal, such as a linear chirp [49, 54, 59, 82, 95, 96]. The accuracy of the cross-correlation technique depends on the width of the peak (the narrower the peak the higher the accuracy) which is inversely proportional to the signal's bandwidth. Therefore, the technique can be said to be highly accurate if the reflected or multipath signals at the receiver are separated in time by more than the width of the correlation peak; otherwise errors can be introduced into the system [57]. Hence, to improve the accuracy of the cross-correlation technique, a broadband signal is required which increases the system cost. Moreover, when a chirp signal is used along with cross-correlation for static and dynamic target positioning, it suffers from two major problems which are: a) simultaneous multiple target positioning is not possible due to signal interference. This can be solved either by the time division multiplexing (TDM) technique, i.e., share the whole available bandwidth among the multiple transmitters at different time slots which reduces the positioning update rate or by frequency division multiplexing (FDM) technique, i.e., transmitting different bands of chirp at the same time which requires higher bandwidth resulting in higher system cost and; b) for moving target positioning, to estimate and compensate the Doppler shift, a matched filtering technique is used where a bank of transmitted signals is created and stored by shifting the frequency of the transmitted signal to different values and then each signal is cross-correlated with the received signal [16, 47, 51, 58, 97–101]. This approach requires a large amount of computational effort.

2.3.1.2 Phase difference (PD)

It is also possible to determine the distance between objects (target(s) and reference points) of both transmitted and received signals from the phase difference as discussed below.

In a narrowband ranging technique, the distance between a transmitter and receiver can be determined using the phase difference between the transmitted and received signals. If a transmitter transmits a sine wave with a zero phase offset, the receiver will receive the wave after a time interval which causes a difference in phase at the receiving end. The phase difference, θ, and the TOF, t_F, are related by $t_F = \frac{\theta}{\omega_c}$, where ω_c is the carrier frequency in radians. The problem with this approach is that, due to the repetition of the waves, ambiguity exists when the measured range is larger than the wavelength (λ) of the transmitted signal [57]. However, it can measure a maximum phase difference of 2π radians without ambiguity; in other words, a distance of up to a wavelength (λ). For example, an US positioning system (UPS) operating at 40 kHz at 25° C (i.e., its velocity is 346 m/s) can only measure distances of up to 8.65 mm without ambiguity, which is quite small for most applications. If it was possible to operate a system at a low frequency, e.g., 1 kHz, the unambiguous measurable distance would be 346 mm but a narrowband single frequency phase method would not be able to directly provide this range as it operates at approximately 40 kHz unless coupled with other methods [102].

2.3.1.3 Received signal strength (RSS)

This technique estimates the distance between a transmitter and receiver using the attenuation of the transmitted signal, the power level of which is known. If this transmitted power and gain of the transmitter are P_t and G_t respectively, the distance between the transmitter and receiver is (d), the aperture (surface) area of the receiver is (A_r) and attenuation coefficient is (γ), the RSS is given by:

$$\text{RSS} = \frac{P_t G_t A_r}{(4\pi d)^\gamma} \tag{2.2}$$

This equation is commonly over-idealized by assuming that $\gamma = 2$ which can be significantly higher in real situations and it also does not consider environmental effects (e.g., reflection). Therefore, by combining this theoretical model with empirical observations, a more realistic model called the log-normal model is widely used [103–106] and given by:

$$\mathrm{RSS}(d) = \mathrm{RSS}(d_0) + 10\gamma \log_{10}\left(\frac{d}{d_0}\right) + \chi_\sigma \tag{2.3}$$

where χ_σ is a zero-mean Gaussian random variable, d_0 a reference distance and, in contrast to the theoretical model, the attenuation coefficient (γ) is derived from empirical data.

The radio frequency RSS (RF RSS) method is considered to be an appealing method, mainly in wireless (sensor) networks, primarily because RSS information can be achieved at almost no additional cost for each radio message sent and received [107, 108]. However, although this method is comparatively simple and inexpensive to implement in hardware, reliably implementing it in the real world is difficult because of the dynamic variations in SS due to noise, multipath reflections from the environment and the presence of non-stationary objects, such as people, doors and furniture. Additionally, as the transmission power and measured SS are also influenced by manufacturing differences in the hardware, knowledge of the channel characteristics and extensive calibrations are essential at the time of system deployment. It has also been shown that SS models need to adapt, even in apparently static environments [109], which habitually makes the ranging task non-trivial for even the simplest scenario.

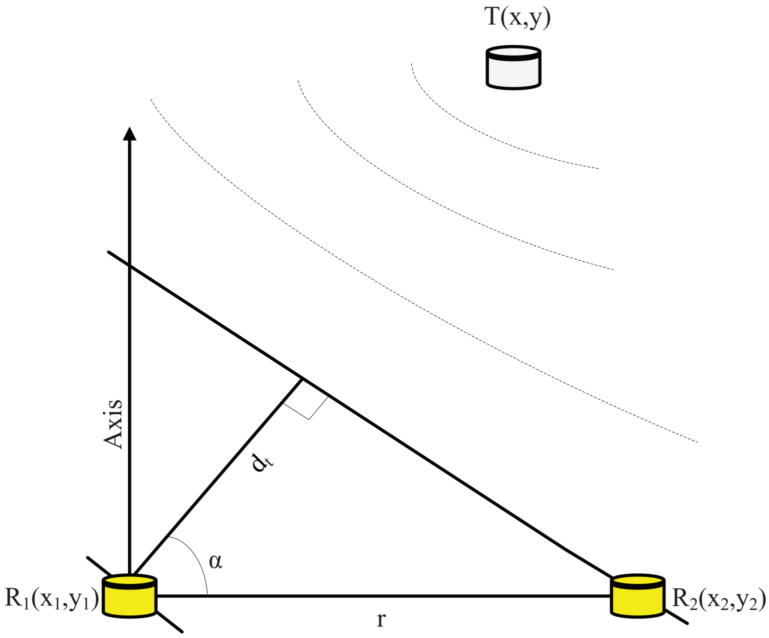

Figure 2.9: Estimation of AOA of transmitter T with respect to axis of receiver R_1.

2.3.1.4 Angle

In this approach, the location of the target is estimated by measuring the angle between the direction of propagation of an incident wave and some reference direction, which is known as the angle-of-arrival (AOA). Using the positioning information of the reference points, the position of the target can be easily calculated utilizing geometrical methods [110–113]. When a signal propagates through a medium, it spreads across the direction of travel in the form of a spherical wave which becomes a plane wave at a point known as the far-field of that signal, the general assumption for far-field operation is $D > 2d/\lambda$ from the transmitter, where D is the radial distance between the transmitter and receiver, d the distance between receivers R_1 and R_2 (shown in Figure 2.9), and λ the wavelength. The waveform remains spherical at all points below the far-field condition which is known as the near-field. The underlying idea of the AOA technique is described as follows.

In Figure 2.9, let the receiving node (R_1) calculate an AOA (α) of the transmitting node (T) which is located in the far-field region with respect to its axis. The transmitting node transmits a signal in the direction of the co-linear receivers (R_1 and R_2) which intersects both receivers at different times, in other words, at a difference in distance of d_t and an angle of α with respect to the line joining R_1 and R_2. Now, d_t can be expressed as:

$$d_t = r \sin \alpha \tag{2.4}$$

where the co-linear distance between R_1 and R_2 (r) can be calculated using prior knowledge of the receivers' coordinates.

Alternatively, if the plane wave impinges on R_1 and R_2 at a time delay (Δt) and the speed of the wave is v, the difference in distance between the wave reaching R_1 and R_2 is d_t which is given by:

$$d_t = v \Delta t \tag{2.5}$$

Combining equations (2.4) and (2.5), the solution to α is given by:

$$\alpha = \cos^{-1} \left(\frac{v \Delta t}{r} \right) \tag{2.6}$$

There are several other approaches available in [71, 106, 114] which use either the RSS indicator (RSSI) across an antenna array or the phase delay instead of time delay.

However, the use of the AOA for localization is not an efficient solution when considered from the perspective of a practical system because angle measurements are simply much more difficult and expensive than distance measurements for receiving nodes with tremendous constraints in terms of cost, form factor and energy.

Summary of the measurement phase: The distance between target(s) and reference points could be measured either using the travel time information of the physical signal propagating between a transmitter and receiver, known as the TOF or using the attenuation information at the receiving end of the transmitted signal known as the RSS. The TOF can be measured using both time and phase domain methods. The time domain method approaches include clock synchronization and, signal sensing and detection. The most widely used clock synchronization method is the velocity-difference TDOA method that measures the TOF by transmitting two synchronized signals with significantly different speeds (e.g., US and RF) that traverse the same path between transmitter and receiver. The most widely used signal sensing and detection methods are threshold detection and cross-correlation. Threshold detection calculates the time when the received signal exceeds a given threshold level, whereas cross-correlation calculates the number of samples required to shift the transmitted signal so that it is aligned with the received signal and produces the maximum value of cross correlation. In time-based approaches, when a single signal (e.g., US) is used, the cross-correlation method is considered to be the optimal solution for TOF measurement. The phase domain method calculates the phase difference between transmitted and received signal to estimate the TOF which suffers from phase ambiguity problems. The angle measurement technique involves determining the angle between the direction of propagation of an incident wave and some reference direction known as the AOA.

2.3.2 Overview of Localization Phase

Once the distance or angle information is available, the location of an object can easily be determined using any of the following localization algorithms.

2.3.2.1 Lateration

This is the most widely used localization algorithm and it's principle is illustrated in Figure 2.10. The position of a target in three-dimensional (3D) space can be determined by measuring its distance from at least three reference points (at least two non-colinear) [61, 115–118], known as trilateration. The distance from the target to each reference point is taken as the radius of a sphere centered at the reference points. If two measurements are taken into account, two spheres (R_1 and R_2) intersect at one circle (C). The third sphere (R_3) intersects with this circle at two points (P_1 and P_2), which are mirror images of each other on opposite sides of the reference plane. The trilateration result can easily be found as one of the intersecting points will lie on the desired positioning volume, i.e., in front of the reference plane, so the remaining intersecting point is discarded. The position of the target can only be located correctly if the coordinates of the reference points and the distances from target to reference points are accurate. However, in practical situations errors in the distance measurement are introduced due to multipath and environmental uncertainty, which results in inaccurate estimation of the target's location. Whenever possible, to reduce the influence of distance errors, more than three reference points are used for coordinate calculation which is known as multilateration [118–121] as shown in Figure 2.11. The mathematical model of the lateration algorithm is given below.

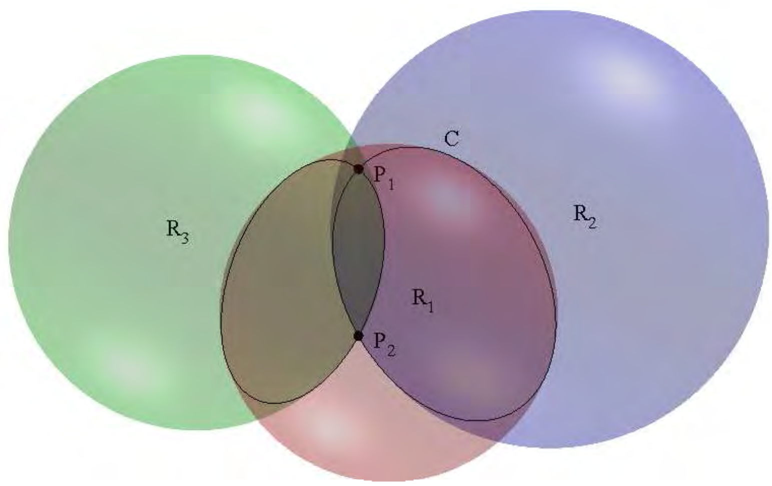

Figure 2.10: A visualization of trilateration for location estimation.

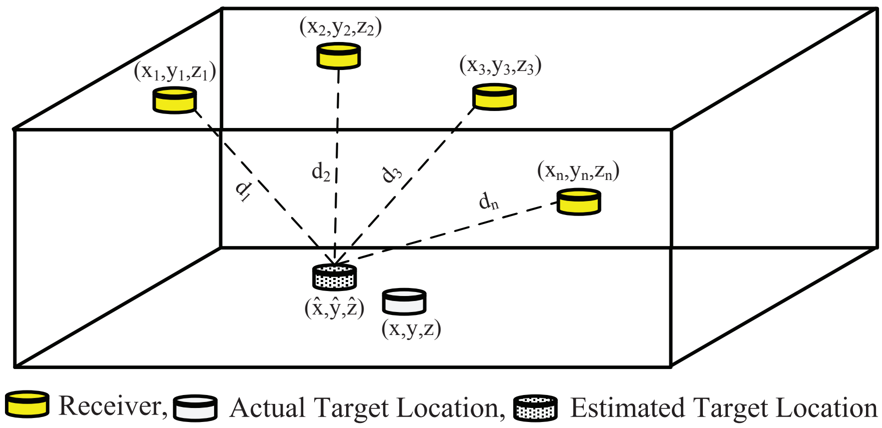

Figure 2.11: A visualization of multilateration to estimate the location of a target in real environment.

If we denote the unknown location of the target as (x, y, z), the i-th sensor as (x_i, y_i, z_i) and range estimate as d_i, then the following set of equations will hold true $\forall_i$, assuming no range error

$$d_i^2 = (x_i - x)^2 + (y_i - y)^2 + (z_i - z)^2 \tag{2.7}$$

For each reference node included in the lateration, a corresponding equation is used. This set of quadratic equations can be solved by subtracting the last equation from the others one by one which gives a set of linear equations. Subsequently, singular value decomposition (SVD) [122, 123] or an iterative algorithm (e.g. least squares estimation (LSE)) [124] can be used for solving the set. When assuming n suitable reference nodes, the equation set can be presented as:

$$\mathbf{PX} = \mathbf{Q} \tag{2.8}$$

where,

$$\mathbf{P} = \begin{bmatrix} (x_1 - x_n) & (y_1 - y_n) & (z_1 - z_n) \\ ... & ... & ... \\ (x_{n-1} - x_n) & (y_{n-1} - y_n) & (z_{n-1} - z_n) \end{bmatrix} \tag{2.9}$$

$$\mathbf{Q} = \frac{1}{2} \begin{bmatrix} (x_1^2 - x_n^2) + (y_1^2 - y_n^2) + (z_1^2 - z_n^2) - (d_1^2 - d_n^2) \\ ... \\ (x_{n-1}^2 - x_n^2) + (y_{n-1}^2 - y_n^2) + (z_{n-1}^2 - z_n^2) - \\ (d_{n-1}^2 - d_n^2) \end{bmatrix} \tag{2.10}$$

and the vector of unknown coordinates is given by:

$$\mathbf{X} = \begin{bmatrix} x \\ y \\ z \end{bmatrix} \tag{2.11}$$

The estimation of the unknown location is:

$$\hat{\mathbf{X}} = (\mathbf{P^T P})^{-1} \mathbf{P^T Q} \tag{2.12}$$

Theoretically, only four receivers are required to determine the position of the target and multilateration is advantageous when a large number of reference points are introduced into the system as it deals with linear equations instead of quadratic equations as in equation (2.7). However, both trilateration and multilateration techniques produce a large amount of error in position calculations when the reference points are placed on a single plane, which is logistically simpler for indoor applications and their distance from the target is larger than the distance between them which is likely to happen. This configuration means that, when trilateration or multilateration is used, the surface of the spheres centered at the reference points will be almost parallel. This will produce larger errors in the position of the intersecting point of the spheres for directions tangential to the surface of the spheres than for directions normal to the surface of the spheres. This phenomenon is known as dilution of precision (DOP).

2.3.2.2 Angulation

Rather than using distance information, the angulation technique estimates the location of an object by using AOA information with respect to two and three reference points for two-dimensional (2D) and 3D location estimations respectively [106, 125–127]. The mathematical formulation for the angulation algorithm is shown below.

In Figure 2.12, if the location of the target (T) is to be determined with respect to receivers R_1 and R_2 located on the same plane using angles α_1 and α_2, the receivers ($R_1(x_1, y_1)$ and $R_2(x_2, y_2)$) estimate the distances (d_1 and d_2) from T using TOF information and the angles (α_1 and α_2) using the AOA technique. Now, the location of $T(x, y)$ can be given by:

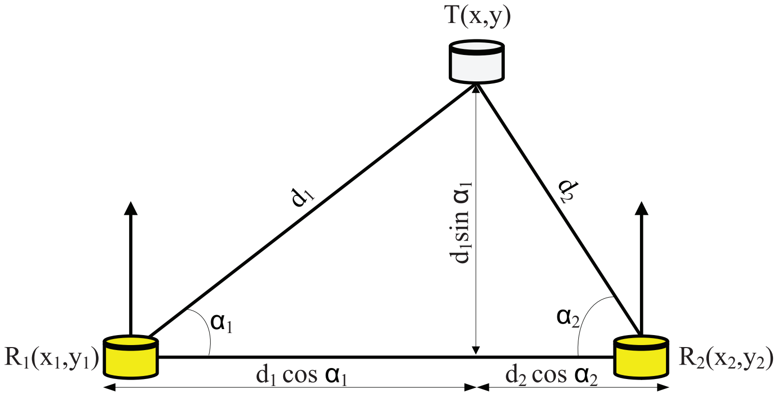

Figure 2.12: Estimation of the location of transmitter T using the angulation technique based on AOA information for R_1 and R_2.

$$x = d_1 \cos \alpha_1 \qquad \text{and} \qquad y = d_1 \sin \ \alpha_1 \tag{2.13}$$

$$x = x_2 + d_1 \cos \alpha_2 \qquad \text{and} \qquad y = y_2 + d_1 \sin \alpha_2 \tag{2.14}$$

Similarly, when more reference points are introduced into the system, the equation for any other n-th reference point is:

$$x = x_n + d_1 \cos \alpha_n \qquad \text{and} \qquad y = y_n + d_1 \sin \alpha_n \tag{2.15}$$

The matrix representation related to the linear equation $\mathbf{PX} = \mathbf{Q}$ is:

$$\mathbf{P} = \begin{bmatrix} 1 & 0 \\ 0 & 1 \\ ---- & ---- \\ 1 & 0 \\ 0 & 1 \\ ---- & ---- \\ \cdots\cdots & \cdots\cdots \\ ---- & ---- \\ 1 & 0 \\ 0 & 1 \end{bmatrix}$$

$$\mathbf{X} = \begin{bmatrix} x \\ y \end{bmatrix}$$

and

$$\mathbf{Q} = \begin{bmatrix} d_1 cos\alpha_1 \\ d_1 sin\alpha_1 \\ ------ \\ x_1 + d_1 cos\alpha_1 \\ y_1 + d_1 sin\alpha_1 \\ ------ \\ \cdots\cdots \\ x_n + d_1 cos\alpha_1 \\ y_n + d_1 sin\alpha_1 \end{bmatrix}$$

The estimation of the unknown location is $\hat{\mathbf{X}} = (\mathbf{P^T P})^{-1}\mathbf{P^T Q}$.

The advantage of this method is that it does not have the issue of co-linearity between reference nodes in localization as two reference nodes are sufficient to uniquely determine the location. However, as the AOA is dependent on the distances between the target and reference nodes, in a practical situation, an error in distance measurement is introduced due to multipath and environmental uncertainties which results in an inaccurate estimation of the AOA. The same amount of distance error leads to a larger number of localization errors in angulation than in lateration [128–130]. Angulation technique determine the 3D position of a target by introducing one or more reference points on the 3rd rather than x and y planes which increases complexity in terms of mathematical formulation and practical implementation [17].

2.3.2.3 Scene analysis

In a complex indoor environment where line-of-sight (LOS) is not always available, most positioning systems find the locations of mobile targets using a scene analysis algorithm. A scene analysis algorithm usually uses a passive mobile architecture and works in a two-stage process [106, 131–137].

In the first stage, known as the off-line stage, a mobile station extracts fingerprints, i.e., features from one or more metrics of the signal measured at predefined points in the environment. Generally, these metrics include the TOF or AOA or RSS of the incoming signal which is proportional to the distance between the mobile receiver and emitting station. At each location, along with the corresponding spatial coordinates, a database or map of fingerprints is generated which stores the values of the signal's feature.

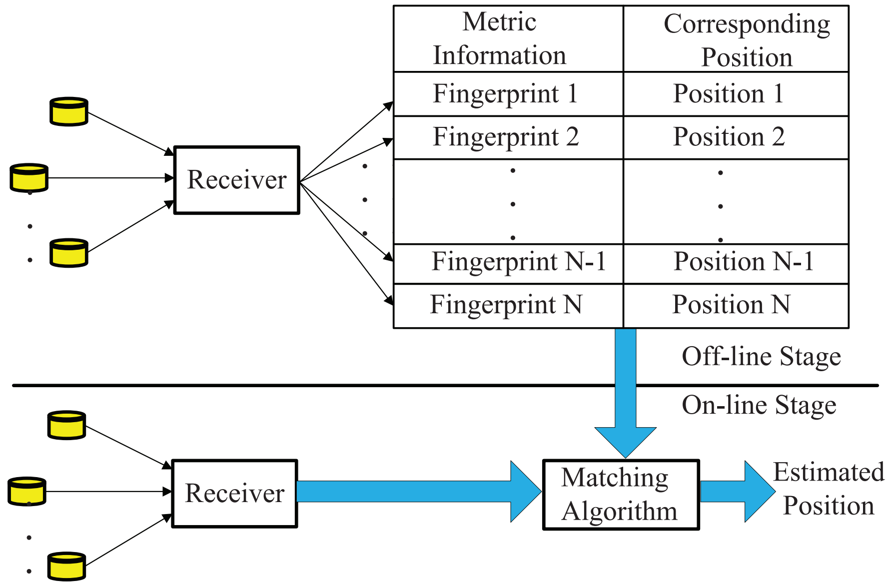

Figure 2.13: Scene analysis algorithm for location estimation.

The second stage, known as the on-line stage, involves the active localization process whereby the mobile receiver extracts a fingerprint of the signal at an unknown location and, localization is achieved by finding the closest match between the features of the received signal and those stored in the database. The steps in the scene analysis algorithm are shown in Figure 2.13.

Although the scene analysis algorithm works well in a complex indoor environment where LOS is not available, the vital challenge is due to the fact that the radio map is non-stationary, hence, variations occur in the measured signals during the on- and off-line phases at the same location. Due to the dynamic aspects of the environment, such as the presence or absence of people, elevators, moving doors and other environmental changes, there is a mismatch between on-line and off-line phase data which leads to errors in positioning [106, 134, 138].

Algorithms developed to find the closest match or matches from the map include probabilistic methods, k-nearest-neighbor (k-NN), neural networks, support vector machine (SVM) and smallest M-vertex polygon (SMP) [102, 139, 140] algorithms which are described below.

Probabilistic methods

Assuming that that there are n location candidates $(X_1, X_2, X_3, ..., X_n)$ and the most appropriate one is chosen based on the posteriori probability, throughout the duration of the off-line stage, the fingerprints (e.g., RSS) from nearby base stations are measured in these n locations, sampled and stored. If we also assume that the observed fingerprint vector during the on-line stage is Y, the decision rule can be obtained based on the posteriori probability as:

select X_i if $P(X_i \mid Y) > P(X_j \mid Y)$ for $i, j \;=\; 1, 2, 3, ..., n, j \neq i$.

From Bayes' theorem,

$$P(X_i \mid Y) = \frac{P(Y \mid X_i)P(X_i)}{P(Y)}, \tag{2.16}$$

the posteriori probability $(P(X_i \mid Y))$ is the combination of likelihood $(P(Y \mid X_i))$, prior probability $(P(X_i))$ and observed evidence $(P(Y))$. As $P(Y)$ remains the same during one location process and assuming that $P(X_i) = P(X_j)$ for $i, j = 1, 2, 3, ..., n$, the following decision rule can be obtained based on the likelihood that $P(Y|X_i)$ is the probability of receiving fingerprint Y given that the mobile node is located in location X_i, that is,

select X_i if $P(Y \mid X_i) > P(Y \mid X_j)$ for $i, j = 1, 2, 3, ..., n, j \neq i$.

Assuming the likelihood that each location candidate is a Gaussian distribution for which the mean and standard deviation can be calculated from the sample data, if the base stations in the environment are independent, the overall likelihood of obtaining one location candidate can be calculated by directly multiplying the likelihoods of all the base stations by:

$$P(Y \mid X_i) = P(Y_1 \mid X_i)P(Y_2 \mid X_i)...P(Y_n \mid X_i) \tag{2.17}$$

In addition to the histogram approach, a kernel technique can be used to calculate likelihood. As a mobile unit cannot be bounded on the discrete location candidates, interpolation is performed to locate a mobile unit in-between the discrete location candidates more accurately. The estimated location $(\hat{x}, \hat{y})$ is given by the following equation which is a weighted average of the coordinates of all sampling locations.

$$(\hat{x}, \hat{y}) = \sum_{i=1}^{n} (P(X_i \mid Y)(x_{X_i}, y_{X_i})) \tag{2.18}$$

where (x_{X_i} and y_{X_i}) are the location coordinates of the i-th candidate. Probabilistic modelling techniques for location applications involve not only the actual positioning problem but also pragmatically important concerns such as calibration, active learning, error estimation and tracking with history. Therefore, in [141], a Bayesian network-based and/or tracking-assisted positioning is proposed.

k-nearest-neighbor (kNN)

This technique [106, 142, 143] calculates the distances between the observed fingerprint in the on-line stage and all the fingerprints previously stored during the off-line stage. The generalized weighted distance ($d(x, \acute{x})$) between a measured fingerprint vector during the on-line phase (x) and the off-line phase ($\acute{x}$) is given by:

$$d(x, \acute{x}) = \frac{1}{d} \Big(\sum_{k=1}^{d} \frac{1}{w_k} \left| x_k - \acute{x}_k \right|^p \Big)^{1/p} \tag{2.19}$$

The following are two algorithms based on the measured signal distance for locating a target.

(a) The location corresponding to the fingerprint with the smallest distance to the calculated fingerprint is chosen considering the Manhattan distance ($p = 1$) and Euclidean distance ($p = 2$), with $w = 1$ for all entries and measurements [106].

(b) A set of k data samples with the smallest signal distances is chosen from the database and, by averaging their location coordinates, the target location is estimated.

Although the weight (w_k) can be used to bias the distance by a factor that indicates the reliability of the database entry or fingerprint measurement ($\acute{x}$), the improvement is not very significant [106].

Neural network

In a neural network [135, 136], a fingerprint and corresponding location coordinates are adopted as the inputs and targets for training purposes throughout the off-line stage. Proper weights are achieved after the training of the neural network. The multilayer perceptron (MLP) shown in Figure 2.14, which has one or more hidden layers, is one of the most widely used neural networks that adopt supervised learning algorithms. It consists of a set of source nodes comprising the input layer, one or more hidden layers and an output layer of neurons. The input connection propagates only in the forward direction, i.e., from the input to hidden layers, hidden to output layers, etc. The output of the i-th neuron at the m-th layer can be described as:

$$a_i(m) = \sum_{j=1}^{N_{m-1}} w_{ij}(m) y_j(m-1) + b_i(m) \tag{2.20}$$

$$y_i(m) = f(a_i(m)) \tag{2.21}$$

where $a_i(m)$ and $y_i(m)$ are the activation and output values respectively of neuron i in the m-th hidden layer. The activation is the weighted sum of the outputs from the neurons in the $(m-1)$-th layer plus the bias layer while $w_{ij}(l)$ refers to the weight connecting the output from the j-th neuron in the $(m-1)$-th layer to the

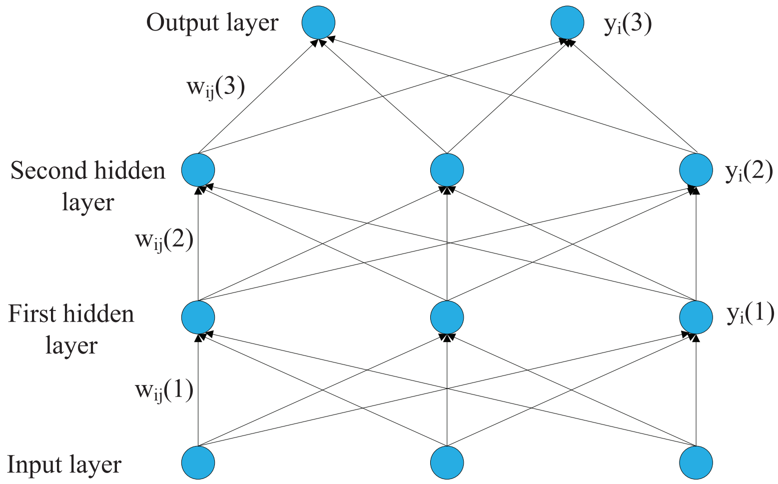

Figure 2.14: A multilayer perceptron.

input of the i-th neuron in the m-th layer.

The transfer function (f) for the hidden layers is the sigmoidal function which is differentiable over all layers and given by:

$$f(x) = \frac{1}{1+e^{-x}} \tag{2.22}$$

or the hyperbolic tangent function:

$$f(x) = \tanh\left(\frac{x}{2}\right) = \frac{1-e^{-x}}{1+e^{-x}} \tag{2.23}$$

The output from the system is the 2D or 3D estimated location which is contained in a two- or three-element vector respectively. However, this method requires a high number of calibration samples which is very undesirable [102, 140].

Support vector machine (SVM)

The SVM is a supervised learning model with an associated learning algorithm which is used for data classification and regression. It is a means of statistical analysis and machine learning, and performs very well in many classification and regression applications; for example, when classifying images, it attains much higher search accuracies than conventional query refinement schemes after just three to four rounds of relevance feedback [102]. SVMs have been used in a wide range of science, medicine and engineering applications, and produced excellent empirical performances [144, 145]. The theory of SVM is found in [146, 147], and in [148, 149], support vector classification (SVC) of multiple classes and support vector regression (SVR) were used successfully for localization.

Smallest M-vertex polygon (SMP)

SMP uses the online fingerprint values to search for candidate locations in signal space with respect to each signal transmitter separately. Based on the database of stored samples, during the on-line stage, each transmitter promotes a cluster of candidate locations which have the same fingerprint. Then, for each of M transmitters, a M-vertex polygon is formed by choosing at least one candidate from each transmitter for M number of transmitters. Averaging the coordinates of the vertices of the smallest polygon (the one with the shortest perimeter) gives the estimated position of a target. SMP has been used in [143] for localization.

2.3.2.4 Proximity

A proximity location algorithm provides the location of a target with respect to a well-known position or area and usually relies on a dense grid of detectors, each with a well-known position. When a mobile target is detected in a certain detector's coverage area, its position is considered to be in the proximity of this area and, when it is detected by more than one detector, it is considered to be in the proximity of a detector that has a height of the RSS [139].

Let D be a detector which has the proximity area shown by the square in Figure 2.15. The locations of mobile devices MD1 and MD2 are to be estimated

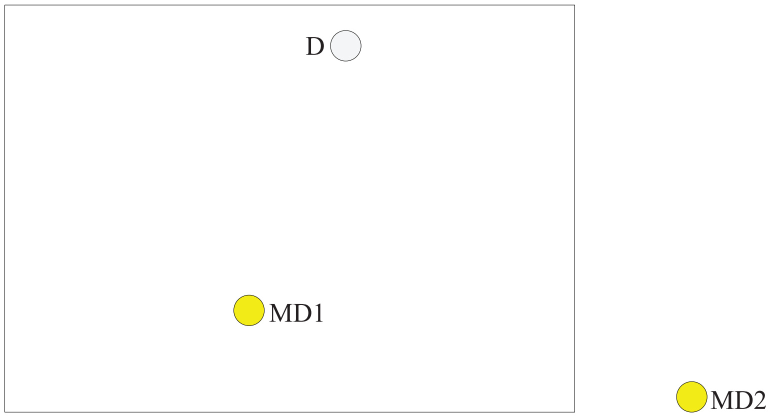

Figure 2.15: Proximity positioning technique.

based on whether they are in the proximity area or not. The Figure 2.15 clearly shows that MD1 is in the proximity area of detector D whereas MD2 is outside the area. This is how the proximity algorithm makes the decision, whether a MD is in a room or not. Therefore, the proximity location sensing technique is unable to provide absolute or relative position estimations as with the other positioning techniques described earlier. This technique is useful only for some specific location-based services and applications. For example, when a sensing area of a location measuring element is a room. This method is relatively simple to implement and systems using RF identification (RFID) and infrared (IR) radiation are often based on it. One more example is the cell identification (Cell-ID) or cell of origin (COO) method which is most commonly used nowadays to approximate the position of a mobile handset by knowing which cell site the device is using at a given time.

Summary of localization algorithms: To estimate the location of an object in 2D or 3D space, angulation uses AOA information with respect to two or three reference points whereas lateration uses distance information utilizing TOF from at least three or four reference points. Lateration with three reference points is called trilateration and with more than three points is called multilateration. The angulation technique is more complex and sensitive than the lateration technique as it deals with angle information to calculate the position of an object. Rather than providing precise location information, the proximity algorithm provides only a rough location of an object (e.g., an object is located nearest to a specific room in a floor or building). Scene analysis uses metrics (including AOA or RSS or TOF) to build a fingerprint for the target environment and then estimates the location of the target by matching on-line measurements with the closest stored fingerprint. A range of pattern recognition techniques have been developed for fingerprint-based positioning systems, such as probabilistic methods and the kNN, neural network, SVM and SMP. Of all the localization algorithms, lateration is more attractive as it provides a better trade-off between system complexity, accuracy, scalability and cost.

2.4 Related Work

Localization technologies hold promise for many ambient intelligence applications which require accurate, reliable and real-time positioning in both outdoor and indoor environments. This section describes a number of existing localization systems.

2.4.1 Outdoor Positioning Systems

Basically, most location systems were built for outdoor navigation, such as for the military, commercial ships and aircraft. Also, knowledge of location was a precious resource for early navigators who, using the Earth as a frame of reference, determined their locations by calculating the angles of different celestial bodies relative to the horizon, which act as a set of natural reference points moving in predictable paths, using tools such as the quadrant and sextant [11]. During the twentieth century, outdoor location systems radically improved in terms of quality and accuracy, and three major systems, SONAR, RADAR and GPS, are described in the following sections.

2.4.1.1 Sound navigation and ranging (SONAR)

During World War I, two types of SONAR systems, active and passive, were developed for underwater navigation by submarines which use different working principles to achieve the same functions.

Active sonar consists of a sound transmitter and receiver which emit sound pulses and wait for a reflection from an obstacle, such as a ship in the water, and then the elapsed time, i.e., TOF, is calculated to determine their distances from the obstacle. To measure the bearing, several hydrophones are used which measure the relative arrival time to each. Using the distance and bearing information the position of the target is determined [150, 151].

Passive sonar listens to any sound made by a target but does not transmit. It uses a directional hydrophone to estimate the bearing of the received signal and listens to the background noise generated in the ocean to provide estimates of its depth using cross-correlation [152–155]. Although the use of passive sonar was limited to military applications, it has recently been widely used for depth estimations of the seabed, bottom profiling and detecting underwater objects and fish.

2.4.1.2 Aircraft radio detection and ranging (RADAR)

A RADAR system uses almost the same principle as a SONAR system. It consists of a radio transmitter which emits RF pulses and a receiver with a rotating antenna which receives an echo from a target, such as an aircraft, and then its distance from the target is calculated using the speed of the RF signal and TOF. The orientation of the target with respect to the Earth is obtained using the angle of rotation information obtained from the RADAR's antenna at the time of reflection [144].

2.4.1.3 Global positioning system (GPS)

To fulfil the military and civilian needs for navigation and target tracking, real-time location systems have drawn considerable attention from both academia and industry. As a result, a GPS has been developed which consists of a constellation of 31 satellites (as of May 2013) that follow well-known orbits [156]. Each satellite broadcasts an RF signal preset with a unique bit pattern synchronized to the global Coordinated Universal Time (UTC). After receiving data streams from different satellites, the GPS receivers calculate the distances using their propagation delays. With a set of at least three distances, the receiver computes its position in 2D or 3D and, in unobstructed outdoor environments, is able to obtain a position precision of about 15-30 m using GPS signals. The errors due to obstructions of signals in the ionosphere and atmosphere can be reduced to about 5 m using differential GPS (DGPS) but at a higher cost [157]. DGPS uses ground-based reference stations which transmit the differences between the positions specified by the satellite systems and their known fixed positions to other nearby GPS receivers. These GPS receivers then use this error information to make a more accurate estimate of their positions. GPS applications are not confined to the navigational field as they are also widely used in missile guidance, vehicle and person tracking, clock synchronization in cellular systems, geographical information systems, surveying, mapping, etc. So far this is the most widely used positioning system.

2.4.2 Indoor Positioning Systems

To provide the location information of targets, traditional outdoor location systems, such as RADAR and GPS, use expensive infrastructures as reference points, such as RF ground stations, satellites, etc., and RF signals which provide an accuracy of several meters. Although this accuracy is sufficient for outdoor location applications, it is not for indoor ones (e.g., indoor navigation, robot navigation, device finding and body tracking). Indoor positioning systems operate in harsher environments which obstruct RF propagation, and also require higher accuracy. Moreover, as indoor applications typically operate in a smaller coverage area, it is often desirable to restrict this area to a single organization. Therefore, indoor positioning systems, with different technologies and using different types of signals, have drawn a considerable amount of attention from both academia and industry.

Indoor localization systems can be classified according to several aspects, one of which is the type of signal emitted which might be an electromagnetic (EM) (RF, IR and visible light), US or audible sound, as described below. A taxonomy of indoor localization technologies based on the signals they use is shown in Figure 2.16.

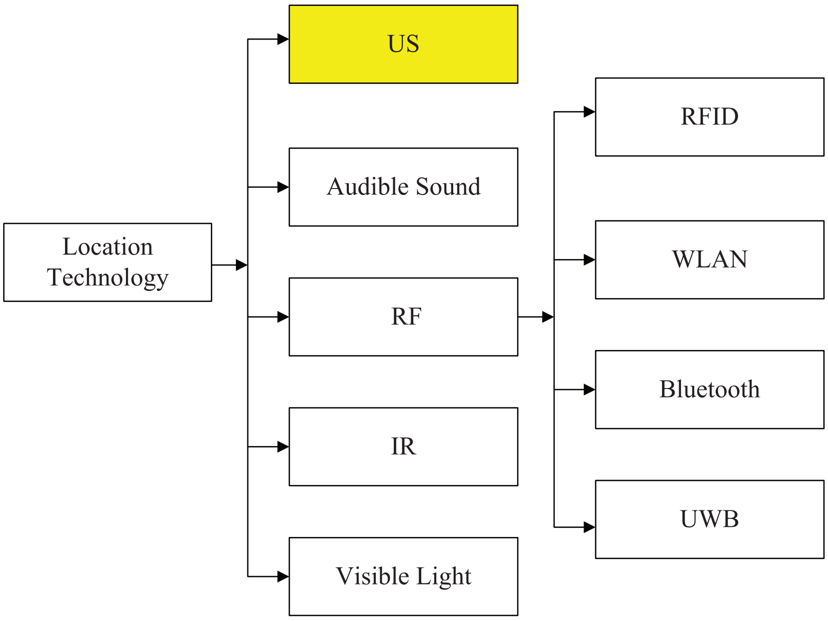

Figure 2.16: Taxonomy of indoor localization technologies based on signals used.

2.4.2.1 US positioning systems (UPSs)

Inspired by the technique adopted by bats to navigate at night, many indoor positioning systems which use US signals have been introduced. Due to the slower propagation speed of an US signal, compared to RF signals, UPSs have opened a new dimension in the area of indoor positioning as they can avoid the need for sophisticated hardware and provide high accuracy, as described in Chapter 1, Section 1.2. Several existing commercial and non-commercial UPSs are described in Appendix A, Section A.1.

The major advantages of US-based positioning are cost effectiveness and high accuracy. To measure the TOF, they generally use an additional RF signal where clock synchronization is necessary. However, when this is not required, threshold detection, cross-correlation or phase deference techniques are typically used. Lateration is the most widely used positioning algorithm for US-based indoor positioning.

2.4.2.2 Audible sound positioning systems

Due to its capability to transmit audible sound, almost every personal device, such as a mobile phone, personal digital assistant (PDA), etc., is a possible technology for indoor positioning and, as these devices can be reused, system costs are reduced. Although these systems are able to provide longer range information than US signals due to their lower frequencies, they are easily affected by the noise present in the environment. Some audible sound positioning systems are described Appendix A, Section A.2.

Though audible sound is an available service in almost every personal devices used in our daily lives, because of the properties of audible sound, it is affected by the noise present in the environment. In addition, as transmitting audible sound is a type of noise transmission in the environment which is uncomfortable for people who hear it, this is not a comfortable positioning solution.

2.4.2.3 RF-based positioning systems

Due to the availability of existing RF infrastructure, such as wireless access points (APs) and WLANs, RF-based positioning systems are very common, with trilateration and scene analysis algorithms generally adopted for positioning. RF technology can be further sub-categorized according to its underlying hardware technology, as discussed below.

RF identification (RFID)

RFID is a wireless technology that transfers data through EM fields for the purposes of automatically identifying and tracking tags electronically attached to objects that store information [138]. Due to its flexible and inexpensive approach to identification of individual persons or devices, it is generally used in complex indoor environments, such as workplaces, hospitals, etc. A RFID system generally consists of one or more reading devices which can wirelessly obtain the IDs of tags present in the operating environment. The reader broadcasts a RF signal and the tags present in the environment return the signal, modulating it by adding a unique identification code [138, 158]. Two types of RFID technologies are available [138, 159, 160], active, which is powered by a battery, and passive which draws energy from the incoming radio signals. Active RFID provides a higher range of coverage than passive RFID but increases the system cost as its tags are larger and less power efficient than those of a passive system. There are currently a small number of RFID-based positioning systems, as described in Appendix A, Section A.3.

The advantages of RFID-based positioning systems include that, due to the light weights of their tags, people can easily carry them, and they can uniquely identify equipment and persons tracked in the operating environment. However, their maintenance is difficult because of numerous infrastructure components installed in the operating environment.

Wireless local area network (WLAN)

One of the most popular positioning systems is a WLAN-based approach. As WLANs are now available in public areas, such as universities, hospitals, shopping centers, train stations, etc., WLAN-based positioning systems are dominant in the field of indoor positioning. Generally, they use the RSSI method for positioning which degrades accuracy as the RSS is adversely affected by changes in the physical environment, such as the movement and orientation of a human body, and rearrangement of furniture, walls, doors, etc. The influences of these types of changes and their impacts on positioning are discussed and analysed in [106, 161–164]. In Appendix A, Section A.4, some WLAN-based positioning systems are introduced.

Like any other indoor positioning system, WLAN-based methods have a goal of cost reduction and, as they use the existing infrastructure of a WLAN, this is achieved. However, the accuracy of this type of system is limited to a range of several centimeters to several meters because of the influences of the environmental sources previously mentioned. In addition, although the scene analysis algorithm works well in complex indoor environments, it makes a WLAN-based positioning system complex and costly if the number of users significantly increases.

Radio interferometric localization system (RILS)

In the field of radio interferometry, phase difference is a popular technique for range measurement. Conventional radio interferometry has a wide range of applications in physics, geodesy and astronomy. Radio interferometry requires an expensive device called a radio interferometer. However, in the field of indoor localization, it was first introduced by Maróti et al. [165] using low-cost and low-power platforms in a wireless sensor network (WSN) architecture. The underlying idea of RILS is as follows.

A pair of transmitting nodes (i and j) transmit signals simultaneously at slightly different frequencies (f_i and f_j) and a pair of receiving nodes (k and l) receives the beat signal from the resultant composite signal with a beat frequency ($|f_i - f_j|$). Then, at receiving nodes k and l, the phase difference of the beat signal is a function of the distance between the four nodes (i, j, k and l) and is given by:

$$\Phi_{i,j,k,l} = \frac{2\pi}{(c/f)}(d_{il} - d_{jl} + d_{jk} - d_{ik})(\mathrm{mod}\ 2\pi) \tag{2.24}$$

where c is the signal speed, $f = \frac{f_i+f_j}{2}$ and d_{XY} denotes the Euclidean distance between X and Y. The linear combination of the distances between two transmitters (i, j) and two receivers (k, l) is called the $q - range$ quantity. Once the required amount of $q - ranges$ is achieved from the radio interferometric phase measurements, the position of the target is determined by finding the optimum of a set of constrained non-linear equations. To minimize the system cost, the transmitting nodes (i and j) transmit at nearly the same frequency so that the composite signal has a low-frequency envelope that can be determined by cheap and simple hardware. The platform description and measured performance of four interferometric-based positioning systems is given in Appendix A, Section A.5.

Although RILS methods have high location accuracy with respect to their coverage ranges, all the above systems require precise time synchronization among their nodes and a configuration mechanism for adjusting their carrier frequencies which also lead to the need for system tuning and calibration.

Bluetooth

Although Wi-Fi-based location systems show fairly accurate results, a Wi-Fi device is not as cheap and widely installed in MDs. In addition, despite laptops and newer smart phones having integrated Wi-Fi components, not all have Wi-Fi features but do have Bluetooth installed. Additionally, if a device has both, Bluetooth is more beneficial than Wi-Fi for positioning in terms of energy consumption, and its chipsets cost less. Therefore, researchers have been motivated to introduce Bluetooth-based positioning systems, a few of which are described in Appendix A, Section A.6.

These systems not only re-use devices already containing Bluetooth technology but are also an effective solution for indoor positioning due to their low-cost chipsets and low-power technology. However, a Bluetooth-based positioning system suffers with a lower accuracy (2-3 m) and lower update rate (20-30 sec) than other systems.

Ultra wideband (UWB)-based positioning systems

Due to the ultra-short pulses (typically less than 1 ns) of a UWB signal, UWB-based positioning systems have become quite interesting to researchers and industry. Unlike conventional RF-based positioning systems which suffer from multi-path distortions reflected by walls in indoor environments, the shorter pulses of UWB signals make it possible to detect reflected signals from an original signal and achieve high accuracy. In addition, UWB signals propagate over multiple bands of frequencies simultaneously, from 3.1 to 10.6 GHz. A few UWB-based positioning systems are described in Appendix A, Section A.7.

Although a UWB-based positioning system is capable of providing high accuracy using a super-high-resolution signal, it requires high-speed clocks and highly sophisticated dedicated hardware to take advantage of this ultra-short signal. Also, metallic and liquid materials cause signal interference in UWB-based positioning system.

2.4.2.4 IR-based positioning systems

IR-based positioning technology is a popular choice when high positioning accuracy (sub-millimeter) is required, particularly for human motion capture. As this research is concerned with gait analysis, a subfield of human motion capture, a brief description of gait analysis and the existing systems used for gait analysis are given below.

Biomechanics is a field of Classical or Newtonian mechanics, a branch of physical science that is concerned with the behaviour of bodies under the action of forces. A popular subject of this field is human motion capture which has a long history dating back to the 1800s. Film photography based motion analyses was generally used in these early experiments. However, these approaches suffered from the limitations of automated data reduction (i.e., reduction of multitudinous amounts of data down to the meaningful parts). Afterwards, a frame by frame manual digitization procedure, which was time consuming and laborious, was introduced to obtain the motion data. In the late 20th century, it became achievable to capture and process information regarding the 3D motion in real time. Motion analysis covers a wide range of applications and gait analysis, a subfield of biomechanics is one of them.

- **Gait analysis:** According to the definition of [20], "gait analysis is the systematic measurement, description, and assessment of those quantities thought to characterize human locomotion". It has been used for many different application areas from the entertainment industry to robotics, sports science and medical science. Generally, the gait data are captured throughout gait analysis via different measuring techniques, and then processed and analysed to obtain the gait parameters (such as variations in joint angles, resultant forces and moments occurring in the joints and the muscle activity) required for the assessment of a subject's gait.

In almost all fields of human movement, gait analysis has been used for a wide variety of applications, for both clinical and research purposes. In the clinical decision making processes such as diagnoses of disorders, as well as future treatment plans in physical medicine, rehabilitation gait analysis plays an important role. Gait analysis also allows the quantification of the effects of rehabilitation and orthopaedic surgery. Aside from clinical applications it is extensively used in the entertainment industry, robotic science and sports science. In the entertainment industry, it is used particularly for making films and games in which realistic models that move like real humans are created. In the robotics and computer science industries, human like actions are incorporated in robots using human pose estimations. In sports science, athletes can advance their techniques by capturing and analysing their current movements.

- **Gait analysis system:** Since gait analysis has a wide range of application involving both clinical and research purposes, various methods have been developed to perform gait analysis. These include electrogoniometers, accelerometers, electromagnetic systems and optical motion capture system (MCS) among which the optical MSC is most widely used. Nowadays, a variety of optical MCSs are available in the market. They use active or passive architectures, depending on the type of markers used by the system. Both systems require at least three markers to define a segment of an object.

In active marker systems, generally light-emitting diodes (LEDs) are employed which are triggered and pulsed successively by a computer which helps the system to identify the markers used by the system automatically, hence marker tracking is not a problem. In these systems, a large number of markers can be used by placing the closely to each other so no marker merging occurs; hence more information can be obtained about the subject. However, these systems are not flexible, and measurements are cumbersome as wire connection from LEDs to the datastation (where data would be stored) has to be delivered on the subject's body. Additionally, batteries are required here for LEDs and for long duration experiments heat generated by the LEDs might be an issue. MCSs which use active markers are called optoelectronic systems.

On the contrary, passive marker systems use lightweight reflective markers which require an illumination source (typically IR) which is usually mounted around each camera lens. As these systems use lightweight reflective markers they do not need cables and batteries on the user. At each marker, the illumination source, the IR light, sent out from the camera is reflected back into the lens. At each camera lens, an IR filter along with a threshold value is used to discriminate the marker automatically from the background noise. As all markers are visible at any given time, potential merging of markers creates limitations on how close together markers may be placed. Each marker trajectory must be recognized with a label and tracked during the test. This requires the use of sophisticated algorithms to recognize the center marker positions for precise tracking. Four (two active and two passive) commercial optical MCSs are described in Appendix A, Section A.8.

2.4.2.5 Vision-based positioning systems

The easiest way of tracking and identifying a person or device without using markers in a complex environment is a vision-based positioning system which estimates a location from the images captured by one or multiple cameras. In this approach, using one or multiple cameras of the functioning environment, a pre-measured database of images is created and the stored information is used in the real-time phase to locate and identify the target. In addition, it is able to provide a valuable location context for services, e.g., a person drinking water sitting in a particular place. In Appendix A, Section A.9, a popular vision-based system is discussed.

Although a cheap camera can cover a large area and person or device to be tracked, and does not require any tags/markers, these positioning systems have some drawbacks. Firstly, since they work on previously stored information of the functioning environment, a small change in the environment, such as the introduction of another table, leads to the database being updated. Secondly, they are greatly affected by sources of interference, for example, the turning off and on of a light in the operating environment. Finally, tracking multiple persons is challenging and highly computationally complex.

2.5 Conclusions

This chapter described the underlying principles of localization systems, and reviewed the extensive efforts undertaken by researchers to design various outdoor and indoor positioning technologies, from large global systems such as GPS to small specific indoor systems like Cricket. The systems reviewed tackle the localization problem in an indoor environment using both active and passive mobile architectures. Although these efforts undoubtedly form a strong foundation for various localization techniques, there is still no one system which can fulfil all requirements as there are some limitations in each category of existing techniques. Despite EM-based positioning, more specifically, IR-based positioning systems showing high precision (sub-millimeter) in terms of localization, they require complex setups and involve significant initial costs. The best alternative for obtaining high accuracy with a relatively low cost and complexity are US-based positioning systems as they use slower speed and readily available devices. Generally, in US-based positioning systems, cross-correlation is considered to be the optimal solution for TOF estimation. The accuracy of cross-correlation improves when the signal bandwidth is increased which also increases the system cost.

Hence, to solve this problem, in Chapter 3, a phase-correlation approach is proposed which is capable of delivering a narrower peak without increasing the bandwidth physically. Although the phase-correlation approach provides higher accuracy than cross-correlation, it must find matches between the stored transmitted and received signals. Thus, increasing the computational complexity and hardware cost. Moreover, most UPSs use the lateration algorithm for positioning target(s). However, they suffer from DOP errors when reference points are installed on a fixed plane

To disentangle these problems, in Chapter 4, two algorithms are proposed for the measurement and positioning phases. In the former, a narrowband orthogonal frequency division multiplexing (OFDM)-based TOF technique is introduced. In the positioning phase, a steepest descent optimization algorithm is proposed which does not suffer from DOP errors like the traditional lateration algorithm.

Finally, when exiting UPSs use a single tone or narrowband chirp signal for static and dynamic target positioning they suffer from two major problems. Firstly, they cannot localize multiple targets simultaneously due to signal interference. Although efforts must be made by using either aTDM technique which reduces the system update rate or by introducing a broadband transducer which increases system cost. Secondly, they use a matched filtering technique to estimate the Doppler shift associated with the target's movement whereby a bank of transmitted signals is created and stored by shifting the frequency of the transmitted signal to different values. Thus, computational complexity and system cost is increased. To solve these problems, in Chapter 5, the OFDM-based steepest decent optimization algorithm introduced in Chapter 4 is initially extended for simultaneous multiple transducer positioning and then for tracking. The accuracy of these systems are compared with an optical motion capture system, Vicon.

Chapter 3

Highly Accurate Ultrasonic Positioning using Phase-correlation

Highly accurate three-dimensional (3D) indoor ultrasonic positioning systems (UPSs) are used in many applications, including industrial, robotic, scientific, military and medical, in which accurate estimations of distance through time-of-flight (TOF) techniques are fundamental. Generally, cross-correlation is considered to be the optimal TOF estimation technique which produces a peak at the time delay between a transmitted and received signal. However, as its accuracy depends on the width of the peak, which is inversely proportional to the signal's bandwidth, it can only be said to be highly accurate if the reflected or multipath signal at the receiver is separated in time by more than the width of the correlation peak; otherwise, errors are introduced into the system. To improve its accuracy, the bandwidth of the transmitted signal must be increased which increases the system cost. In this chapter, a phase-correlation technique for solving the abovementioned problem of the chirp-based cross-correlation technique, which is able to provide a much narrower peak than cross-correlation without increasing the signal's physical bandwidth, is proposed. The experimental results show that the accuracy obtained using this technique, along with the multilateration algorithm, is acceptable for medical applications in which high accuracy ($\approx$ 0.5 mm) is required and which is generally achieved using optical motion capture systems (MCSs). The system cost and complexity of this proposed UPS is expected to be much less than that of an equivalent optical system.

3.1 Introduction

The location of a radiating source can be determined using information regarding its distances from at least three reference points, the locations of which are known [94]. This technique has been extensively used in research and production fields in many and varied applications, such as robot navigation [44, 51–53], the precise location of instruments during laparoscopic surgery [40], and human movement tracking [21–39]. The general rationale for the system presented in this chapter is the opportunity offered by ultrasound to conceive rather simple measurement methods or build comparatively cheap meters characterized by suitable accuracy, reduced measurement time and, above all, a high level of inherent safety [56].

The process of obtaining distance information is begun by sending an ultrasonic (US) burst from a transmitter to a receiver. Ideally, one would send a continuous wave signal, for instance, a sine wave, from the transmitter. Then, using the phase-shift information between the transmitted and received signals, the distance information could be obtained. This technique can measure distances up to a wavelength (λ) because a phase variation of a signal from $0°$ to $360°$ corresponds to a distance variation from 0 to λ. However, if the measured distance is longer than a wavelength, this technique is limited to short-range applications as the integer number of wavelengths within the distance is unknown.

Therefore, for distances longer than a wavelength, it is common to measure the TOF which employs the following concept. A transmitter sends an US pulse which travels through the air to a receiver and this traveling time (t_F) is used to obtain the distance (d) between the transmitter and receiver using the common, straightforward law [166]:

$$d = vt_F \tag{3.1}$$

where v is the speed of sound.

The simplest way of determining the TOF involves transmitting and detecting the arrival of an US signal by triggering the event when the received signal exceeds a predefined threshold level for the first time which, of course, must be above the noise level. Although it is computationally simple and can be implemented with low-cost single frequency US transducers, for low signal-to-noise ratio (SNR) signals, it is not the most suitable method because, on average, it estimates a false positive TOF compared with the actual one [56].

A more standard and proper TOF estimation technique is cross-correlation in which transmitted and received signals are cross-correlated to produce the maximum value at the time delay and performs better than the threshold technique for low SNR signals. It is considered as the optimal TOF estimation technique as it uses all the information contained in the signals [56] and has noise reduction properties because, theoretically, the result is zero when random noise is cross-correlated which means that the additive noise is reduced. The accuracy of cross-correlation depends mainly on the width of the correlation peak which is inversely proportional to the bandwidth, that is, the narrower the peak, the higher the TOF estimation accuracy. So a larger the bandwidth translates to a higher the accuracy although this results in an increased system cost. Above all, this technique can be said to be highly accurate if the reflected or multipath signal at the receiver is separated in time by more than the width of the correlation peak [57, 58] which might not always happen in an indoor environment due to the presence of numerous obstacles which can introduce errors into the system.

Therefore, a technique for improving system accuracy in an indoor multipath environment called phase-correlation, which is able to produce a narrower peak without increasing the system bandwidth physically while fulfilling the above criteria, is introduced.

The remainder of this chapter is organized as follows: Section 3.2 presents the system design; in Section 3.3, a general system model of an UPS is described; the cross-correlation method in the frequency domain discussed in Section 3.4 is then modified to improve system accuracy in Section 3.5; a comparison of the performances of the cross-correlation and proposed methods from simulations is presented in Section 3.6; Section 3.7 describes the experimental procedure for determining the accuracy of the proposed system; the experimental results are discussed in Section 3.8; and Section 3.9 presents the conclusions drawn from this study.

3.2 System Design

The aim of this dissertation was to develop such UPSs which would be able to provide the sub-millimeter accuracy required for sensitive medical applications such as gait analysis. When designing such types of UPSs, several characteristics needed to be considered which are described below.

3.2.1 System-level Architecture

As low cost 40 kHz US transmitters and receivers are readily available commercially, it was decided that the systems developed in this dissertation would operate at or around a frequency of 40 kHz. The transmitters and receivers used in the proposed UPSs were the Piezotite MA40S4S and MA40S4R [167] which can effectively utilize 10% of the frequencies centered around 40 kHz.

In line with the goals of applying the proposed system for sensitive medical application, accuracy was a high priority. For such a positioning and tracking system which requires a very high degree of accuracy (sub-millimeter), the selection of its data acquisition (DAQ) module is an important issue. In order to determine an appropriate interface for the positioning system, potential detection errors are studied under a specific scenario which involves investigating how many errors will be introduced if the time detection is delayed by one sample which helps to ascertain the sampling rate to be used to maintain an accuracy of less than 0.5 mm.

Using the common audio interface UA-25EX [168], the sampling rate of which is 96 kHz, i.e., a sampling time of $t_s = \frac{1}{96\ \text{kHz}} = 10\ \mu s$, if the detection is out by one sample period, when the speed of sound is 344 m/s, the prospective error in the predicted distance (d_e) will be:

$$d_e = v \times t_s = 10\ \mu s \times 344\ \text{m/s} \approx 3.6\ \text{mm} \tag{3.2}$$

Although this error is too large for the system's desired accuracy, it can be either physically or virtually reduced by increasing the sampling rate. As, if the sampling rate is increased virtually, e.g., through interpolation, the complexity and uncertainty in the system's software is increased, the choice was to increase it physically. As the desired accuracy is less than 0.5 mm, according to equation (3.2), the sampling rate has to be $t_s = \frac{0.5 \text{ mm}}{344 \text{ m/s}} = 1.45$ μs which corresponds to a minimum sampling frequency of $f_{s_{\min}} = \frac{1}{1.45\ \mu\text{s}} \approx$ 0.7 MHz.

Therefore, in order to obtain accurate data simultaneously at each receiver, the minimum sampling frequency must be 0.7 MHz. After conducting market research, the USB-1604HS-2AO DAQ module [169] was selected as it has simultaneous 1.33 MHz sampling at each of its four input channels and 1 MHz sampling at its output channel which means that the error (d_e) incurred by one sample's false detection is reduced to 0.344 mm, a huge improvement compared with typical audio interfaces and exceeds the desired accuracy of 0.5 mm. After selecting the I/O of the system, the focus is then on software development of the positioning algorithms.

3.2.2 Software Development

Three main steps are involved in the software development of an UPS. Firstly, a signal must be sent by the transmitter which will also be used to trigger the receivers to determine the TOF. Secondly, once a signal is transmitted by the transmitter and received by the receivers, these signals need to be captured by the DAQ module to determine their TOFs. Finally, using these TOFs, a 3D position needs to be established. Figure 3.1 shows these components and their context.

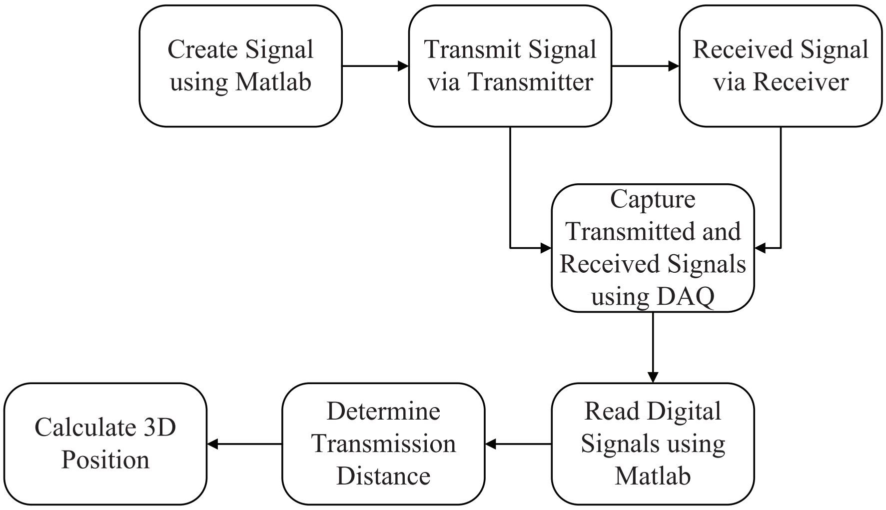

Figure 3.1: Block diagram of basic components of the proposed UPSs.

In the following section, a general system model of an UPS which considers all real environmental factors is presented.

3.3 System Model

If, in an UPS, a number of transmitters transmit signals with a frequency of f_a, the signal received by a receiver in the system is [170]:

$$r(t) = \sum_{q=1}^{a} \sum_{l=0}^{M} A_{q,l}\ e^{j2\pi(f_a - f_{d_{q,l}})t}\ \delta(t - t_{F_{q,l}}) h_{tx_a} h_{rx} + \tilde{n}(t) h_{rx} \tag{3.3}$$

where a represents the number of transmitters, h_{tx} and h_{rx} the impulse responses of the transmitter and receiver respectively (generally, it is assumed that both have a unity magnitude, i.e., neither changes the signal's attributes), M the possible number of paths traversed by a transmitted signal to reach a receiver, $A_{q,l}$ the amplitude of the l-th ray of the q-th transmitter, $\delta(t - t_{F_{q,l}})$ the propagation delay between the q-th transmitter and receiver, $f_{d_{q,l}}$ the Doppler shift of the q-th transmitter of the l-th path, $\tilde{n}(t)$ the additive white Gaussian noise (AWGN), ray

$l = 0$ the direct path and $l > 0$ the multipath between a transmitter and receiver, $t_{F_{q,l}} = d_{q,l}/v$, where $d_{q,l}$ is the distance traveled by ray l of the q-th transmitter and v the speed of sound which depends on environmental factors such as temperature, pressure and humidity. Although the effect of pressure and humidity is negligible for the applications considered here, that of the temperature on sound velocity is described below.

Unlike an electromagnetic (EM) signal, the speed of an US signal is directly affected by the air temperature. As the distance between a transmitter and receiver is directly related to the speed of sound, in any UPS, the variability of the speed of sound according to the air temperature needs to be considered, with the relationship between the speed of sound and air temperature given by:

$$v = (331.3 + 0.6T_m) \text{ m/s} \tag{3.4}$$

where T_m is the ambient temperature in °C. This variability needs to be accounted for via calibration before any TOF measurements are taken. Generally, for TOF estimations, the cross-correlation method is used which is described below.

3.4 Frequency Domain Cross-correlation

The mathematical model of cross-correlation in the discrete time domain was presented in Chapter 2, Section 2.3.1.1. However, as it is often simpler in practice to perform the calculation in the frequency domain. Let the time domain transmitted and received signals be $s_T(t)$ and $s_R(t)$ respectively. Now using the Fourier transform, $s_T(t)$ and $s_R(t)$ can be described by a complex function of frequency as follows:

$$S_T(f) = \Im(s_T(t)) = A_T(f)e^{j\theta_T} \tag{3.5}$$

$$S_R(f) = \Im(s_R(t)) = A_R(f)e^{j\theta_R} \tag{3.6}$$

where $\Im$ denotes the Fourier transform operation and, A and θ represents the amplitude and phase of the complex frequency components of each signal respectively. Now, the cross-correlation of the transmitted and received signals in the frequency domain is:

$$\begin{aligned} C(f) &= S_T^*(f)S_R(f) \\ &= |A_T(f)A_R(f)|\, e^{-j\theta_T}e^{j\theta_R} \\ &= |A_T(f)A_R(f)|\, e^{j(\theta_R-\theta_T)} \end{aligned} \tag{3.7}$$

where $*$ denotes the complex conjugate. The inverse Fourier transform of $C(f)$ represents the cross-correlation output as:

$$c(t) = \Im^{-1}(C(f)) = \Im^{-1}(|A_T(f)A_R(f)|\, e^{j(\theta_R-\theta_T)}) \tag{3.8}$$

where $\Im^{-1}$ is the inverse Fourier transform. This cross-correlation provides a signal with a maximum value when the transmitted and received signals are perfectly aligned in time.

The inverse Fourier transform of the exponential function (i.e., equation (3.8)) of a single frequency component is a sine function which gradually becomes a sinc function if the number of frequency components is increased and, finally, a delta function for an infinite number of frequency components. Therefore, it can be said that, by increasing the number of frequency components, i.e., the signal's bandwidth, the output from the cross-correlation ($c(t)$) can be narrowed, with the correlation width (ΔT) inversely proportional to the bandwidth (W) of the signal,

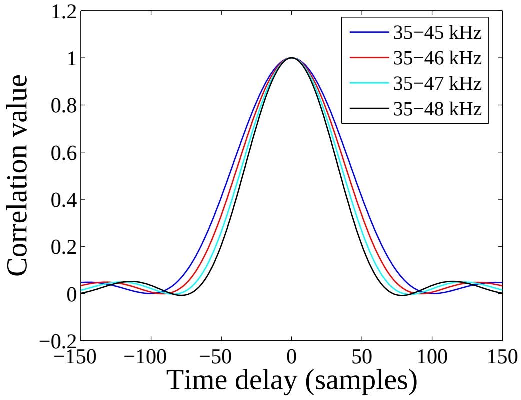

Figure 3.2: Effect of bandwidth on cross-correlation width.

i.e.,

$$\Delta T \propto \frac{1}{W} \tag{3.9}$$

as shown in Figure 3.2.

Therefore, by increasing the bandwidth (W), one can reduce the width of the peak which means that system accuracy is improved because the probability of separating the reflected path or multipath will be increased in time by more than the width of the cross-correlated pulse. The problem here is that increasing the system bandwidth will increase the system cost. Therefore, in the following section, a phase-correlation technique which is able to provide a sharp peak without physically increasing the bandwidth is proposed.

3.5 Phase-correlation Method

According to equation (3.8), the cross-correlation output will be a delta function, i.e., approximately zero everywhere except at the position of time delay if each frequency index of $C(f)$ has a value, i.e., an infinite bandwidth. This could possibly be achieved virtually, without physically increasing the bandwidth, by modifying

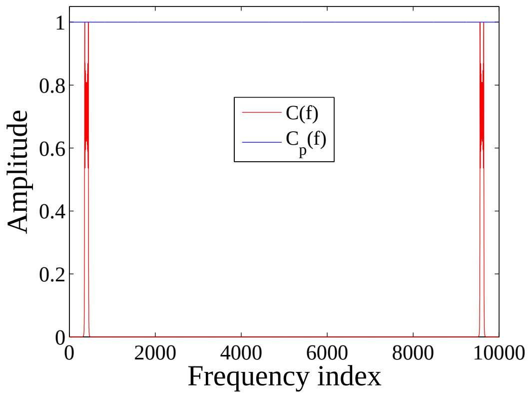

Figure 3.3: Frequency spectrum of $C(f)$ and $C_p(f)$ for [35-45] kHz chirp.

equation (3.8) as:

$$\begin{aligned} C_p(f) &= \frac{|A_T(f)A_R(f)|e^{j(\theta_R-\theta_T)}}{|A_T(f)A_R(f)|} \\ &= e^{j(\theta_R-\theta_T)} \end{aligned} \tag{3.10}$$

This equation means that all the frequency spectrum of $C_p(f)$ has a unity magnitude whereas $C(f)$ has particular values at the transmitted frequency components as shown in Figure 3.3. Therefore, the inverse Fourier transform of $C_p(f)$ given in the following equation is a delta function which produces a peak at the minimum phase difference between the transmitted and received signals as it has a value at all frequency components.

$$c_p(t) = \Im^{-1}(C_p(f)) = \Im^{-1}(e^{j(\theta_R-\theta_T)}) \tag{3.11}$$

Hence, ideally, it can be said that, for any band of a signal, without physically increasing the bandwidth, the output from phase-correlation will be a delta function as all the frequency components of $C_p(f)$ will have unity magnitudes.

In summary, the proposed phase-correlation method is as follows.

1. Calculate the Fourier transform of the transmitted signal, i.e., $S_T(f) = A_T e^{j\theta_T}$.

2. Calculate the Fourier transform of the received signal, i.e., $S_R(f) = A_R e^{j\theta_R}$.

3. Calculate the angle difference between the received and transmitted signals, i.e., $\Delta\theta = (\theta_R - \theta_T)$.

4. Calculate the exponential of $\Delta\theta$, i.e., $C_p(f) = e^{j\Delta\theta}$.

5. Calculate the inverse Fourier transform of $C_p(f)$, i.e., $c_p(t) = \Im^{-1}(C_p(f))$.

6. Find the position of the maximum value of $c_p(t)$ which corresponds to the TOF in the sample domain.

As there are different types of signals competing in the field of UPSs, the following section describes which signal will be useful for the phase-correlation method.

3.5.1 Choice of Signal for Phase-correlation

In the field of UPSs, there are mainly two types of competing signals: single tone sinusoidal and linear chirp.

A single tone sinusoidal signal is used by an UPS because most of the US hardware available is tailored to 40 kHz US waves and is efficient for estimating the TOF when used with an additional radio frequency (RF) signal using the velocity-difference TDOA technique [3, 15, 38, 41, 43, 69–71, 82–84]. However, it performs poorly in a TOF estimation when cross-correlation is used because, in a particular signal length, there will be several cycles which produce very similar peaks adjacent to the main peak when cross-correlated with the received signal. Hence, a false peak may be detected in a noisy environment [94]. Therefore, using a single tone signal along with cross-correlation for TOF estimation is not a good choice.

To improve the accuracy of the cross-correlation technique, a frequency modulated (FM) signal, i.e., a chirp signal, is introduced. It is a sinusoidal wave of constant amplitude which sweeps the desired bandwidth (W) within a certain time period in a linear or nonlinear (e.g., quadratic or logarithmic) manner. Using a linear chirp signal in conjunction with cross-correlation has been demonstrated to provide superior performance in radar and sonar applications[95, 96]. Also, a chirp signal performs well in the field of indoor positioning [16, 49, 54, 82, 171].

The performances of phase-correlation for both signals is tested and, as previously mentioned, its output for any band of signal is a delta function.

To verify this statement, initially, the performance of a sine wave is tested in a noiseless environment, with the output from the phase-correlation shown in Figure 3.4(a) having a sharp spike.

However as, in a real scenario, noise will be added with the received signal which means that over all the frequency spectrum of $C_p(f)$ a random phase will be added, hence the phase of the majority of the frequency components will be random and there will be no defined peak (shown in Figure 3.4(b)).

Therefore, to evaluate the performance of the phase-correlation technique, a chirp signal is also tested in the presence of noise, with the phase-correlation output shown in Figure 3.4(c) in which a sharp peak is visible. The reason for this sharp peak in the presence of noise is that a significant amount of frequency components contributes to phase-correlation whereas a single tone signal has only one frequency component.

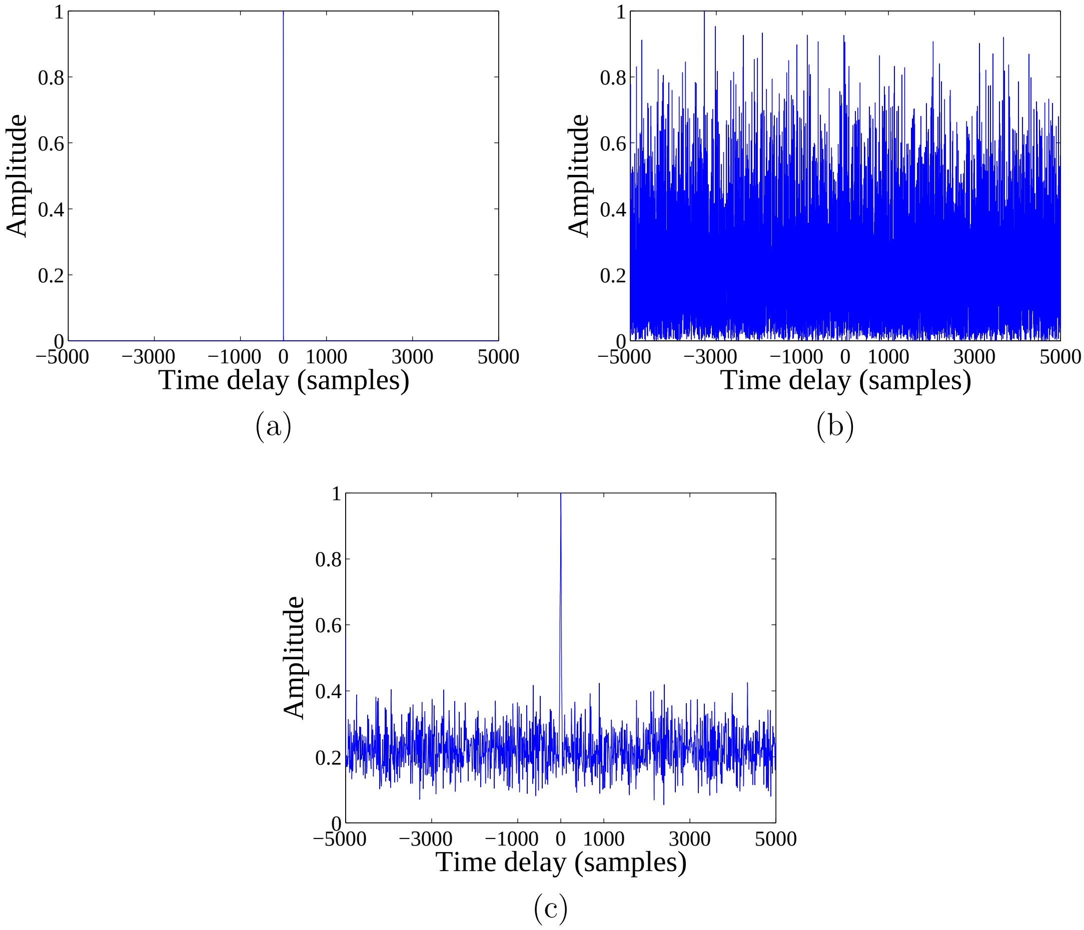

Figure 3.4: Phase-correlation output from simulation: (a) noiseless 40 kHz sine wave; (b) 40 kHz sine wave when the SNR is 15 dB; and (c) [35-45] kHz chirp when the SNR is 15 dB.

So, it can be said that the performance of phase-correlation depends on two important factors: the amount of frequency components contributing to it, i.e., the signal's bandwidth; and the relative amount of noise contributing to the received signal, i.e., the SNR of the received signal. Therefore, two important relationships can be established.

Firstly, if the bandwidth (W) of a signal increases, the SNR of the phase-correlation output ($c_p(t)$) (which can be defined as the ratio of the square of the correlation main peak amplitude to the variance of the correlation noise) increases as shown in Figure 3.5(a). The equation for the correlation SNR ($\mathrm{SNR}_{\mathrm{Corr}}$) is given as:

$$\mathrm{SNR}_{\mathrm{Corr}} = 20 \log \frac{\left|\mathrm{Corr}_{(\text{main peak})}\right|^2}{\mathrm{Var}(\mathrm{Corr}_{\text{noise}})} \tag{3.12}$$

where Var and Corr represent variance and correlation respectively. Generally, except the width of the correlation main peak, all other components are considered as noise.

If the $\mathrm{SNR}_{\mathrm{Corr}}$ of phase-correlation increases, the probability of obtaining accurate peak detection ($P(T_D)$), i.e., the TOF, also increases and vice versa. Mathematically,

$$P(T_D) \propto W \tag{3.13}$$

Secondly, for a fixed bandwidth, if the received signal's SNR (SNR_{s_R}) increases, the $\mathrm{SNR}_{\mathrm{Corr}}$ of the phase-correlation output ($c_p(t)$) also increases (shown in Figure 3.5(b)), hence, the probability of obtaining accurate peak detection ($P(T_D)$), i.e., the TOF, increases and vice versa. Mathematically,

$$P(T_D) \propto \mathrm{SNR}_{s_R} \tag{3.14}$$

How these two factors affect system accuracy is demonstrated in Section 3.6. To visualize how phase-correlation works better than cross-correlation in a close multipath environment an example is demonstrated below.

3.5.2 Understanding Phase-correlation using an Example

The following example demonstrates how the proposed phase-correlation method provides a more accurate TOF than cross-correlation for close multipath reception.

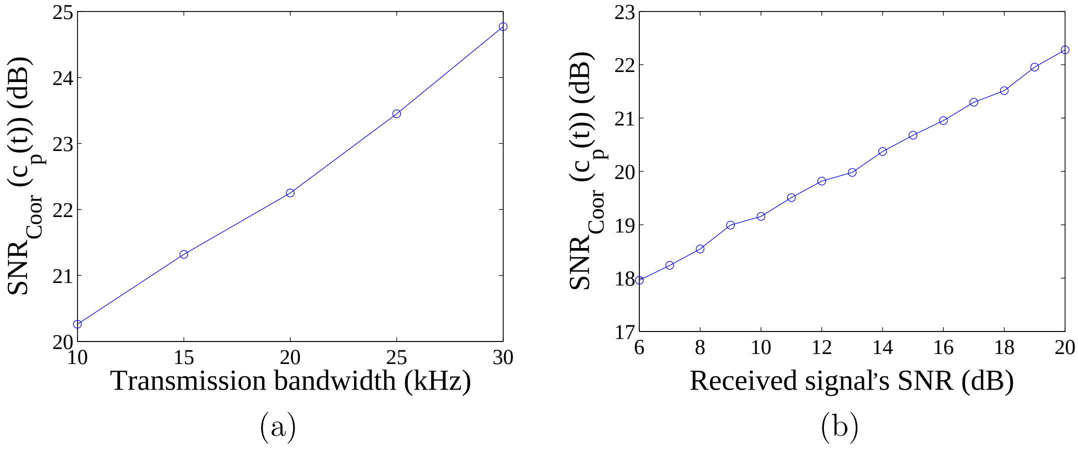

Figure 3.5: SNRs of phase-correlation ($c_p(t)$) when: (a) the signal's bandwidth is varied; and (b) the received signal's SNR is varied.

In it, two cases are considered where a linear chirp [35-45] kHz/10 ms (i.e., the length of the linear chirp is 10 ms and, its initial and final frequencies are 35 kHz and 45 kHz respectively) was used for transmission which was also used during the real experiment and the SNR was 15 dB.

In the first case, the receiver receives the transmitted chirp with sufficient separation between the direct and reflected paths, which are, 1500 samples and 1950 samples which correspond to 51.6 cm and 67.08 cm respectively when the speed of sound is 344 m/s at 21°C, with the corresponding path loss considered using reflection coefficients of 0.9. A reflection coefficient of 0.9 means that 10% of the signal's energy is lost upon reflection which indicates that the multipath effect is more intense at a higher reflection coefficient, and vice-versa. The outputs from the cross- and phase-correlations are shown in Figure 3.6 which indicates that both methods can estimate the direct path, i.e., the TOF, and the reflected path accurately when they are sufficiently separated in time.

In the second case, the receiver receives the transmitted chirp with a small separation in time between the direct and reflected paths, which are, 1500 samples

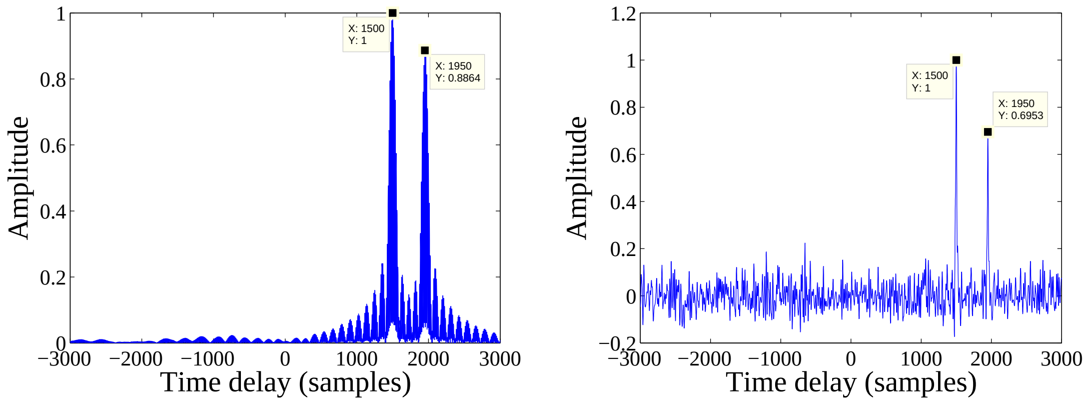

(a) (b)

Figure 3.6: Outputs when direct and reflected paths are well separated in time from: (a) cross-correlation; and (b) phase-correlation.

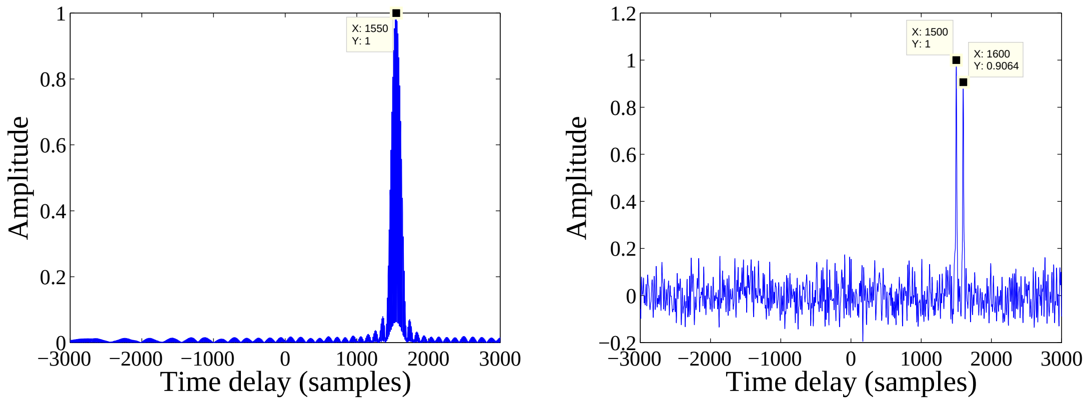

(a) (b)

Figure 3.7: Outputs when direct and reflected paths close in time from: (a) cross-correlation; and (b) phase-correlation.

and 1600 samples which correspond to 51.6 cm and 55.04 cm respectively when the speed of sound and temperature are the same as in case-1. The outputs from the cross- and phase-correlations are shown in Figure 3.7 which indicates that the peak for the reflected path is not visible in the cross-correlation output as in Figure 3.6 which means that the reflected path has a direct effect on the correlation's width and its peak is generated at a false position with an error of 50 samples, i.e., 1.72 cm; but, for phase-correlation, two distinct spikes are visible at exactly the same positions of the direct and reflected paths. Therefore, it can be said that phase-correlation has the capability to detect the direct and reflected paths accurately even when the main and multipath signals are closely separated in time.

3.6 Simulation Results

A customized environment was simulated in Matlab to evaluate the performance of the proposed phase-correlation method for distance measurement. The simulator was designed to build a virtual two-dimensional (2D) rectangular room with (top, left) and (bottom, right) coordinates as: (-5, $d/2$) and (d+5, $-d/2$) respectively, where d is the distance between the transmitter and receiver and is varied from 40 to 60 cm, with the receiver and transmitter positioned at (0, 0) and (d, 0) respectively. In the simulator, a fixed number of reflection points at different positions of the transmitter in the enclosed geometry was generated, as per the described system model. Measurements were taken at different positions inside the room for distances between 40 cm and 60 cm with gaps of 5 cm and each simulation was run for 7 iterations, with its final position taken as the median of the calculated positions.

The simulation was performed in a multipath environment (5 paths) with reflection coefficients of 0.9 to 0.5, and the corresponding signal's attenuation calculated using the formula $A = A_0\, e^{-\gamma d}$, where A_0 is the unattenuated amplitude of the propagating wave at a location, A is the reduced amplitude after the wave has traveled a distance (d) from that initial location and γ is the attenuation coefficient of the traveling wave in the d direction.

To verify equation (3.13), the bandwidth of a chirp signal was varied from 10 kHz to 25 kHz with 5 kHz gaps, the initial frequency was 35 kHz and the received

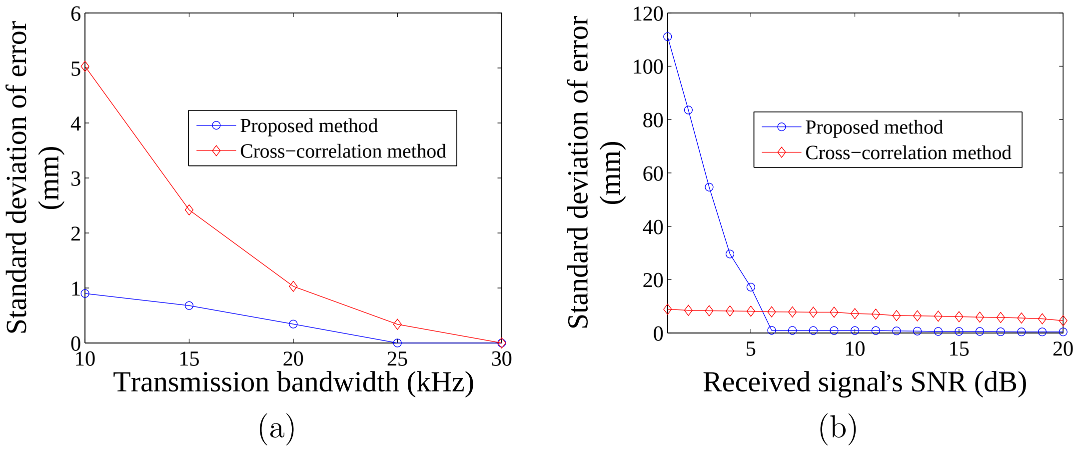

Figure 3.8: Accuracy effected by: (a) transmission bandwidth; and (b) received signal's SNR.

signal's SNR fixed at 6 dB. To verify equation (3.14), the SNR of the received signal was varied from 1 dB to 20 dB with 1 dB gaps for a fixed chirp [35-45] kHz/10 ms. This chirp was used because the transmitter in the experiments can utilize a 10% bandwidth of the center frequency (40 kHz).

The results obtained from this simulation using the proposed and cross-correlation methods are compared in Figure 3.8(a) and Figure 3.8(b) respectively. Figure 3.8(a) shows that the standard deviation of error from the proposed method decreases with increases in the bandwidth for a fixed SNR, which validates equation (3.13). It is also noted that, to reach the same accuracy as the proposed method, cross-correlation requires a significantly larger bandwidth.

Again, Figure 3.8(b) shows that the standard deviation of error from the proposed method increases with decreases in the signal's SNR which validates equation (3.14). It is noted that, the performance of the proposed method abruptly degrades when the received signal's SNR is lower than 6 dB. This is because the phases of the narrowband received signal are highly affected by the noise, and results in no defined peak which means that the proposed method is highly sensitive to the SNR. But, for the cross-correlation, the standard deviation of error is almost constant as cross-correlation of the random noise is theoretically zero.

Therefore, it can be said that phase-correlation has the ability to provide precise results in moderate SNR (> 6 dB) and highly multipath environments, and can be applied in medical applications which require high accuracy. Recently, the phase-correlation method was verified for a broadband chirp signal in [59] which also showed that at low SNR the performance of the phase-correlation is more degraded than the cross-correlation but the performance is better at higher SNR values. [59] also showed that at a low sampling rate the accuracy of the phase-correlation method is higher than the cross-correlation method which reduces the computational cost, though this analysis is not considered here.

3.7 Experimental Procedure

To evaluate the proposed method, a set of experiments were conducted according to the procedures described below. In these experiments, a Piezotite MA40S4S and MA40S4R, which operate in a narrow band of frequencies centered around 40 kHz, were used as transmitters and receivers. To capture and digitize the transmitted and received signals and to measure the room temperature, a Measurement Computing USB-1604 DAQ module with a sampling rate of 1 Msample/s and a digital thermometer were used respectively. The transmitted signal was a linear chirp [35-45] kHz/10 ms.

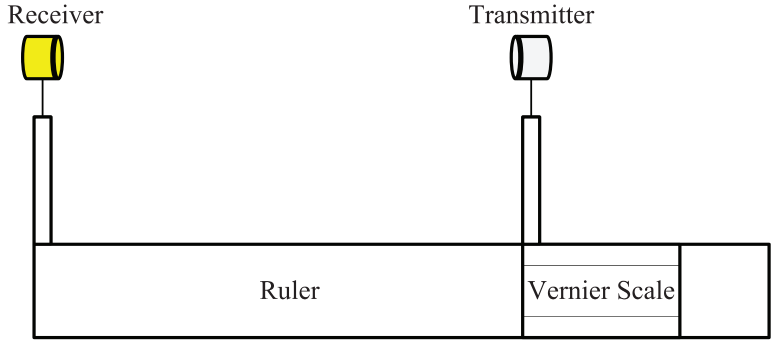

Figure 3.9: Configuration of transmitter and receiver during distance measurement.

3.7.1 Distance Measurement

An experiment was performed to evaluate the proposed phase-correlation-based TOF estimation technique in which the transmitter and receiver were attached to opposite ends of a ruler equipped with a Vernier scale with a precision of 0.05 mm. An illustration of this setup is shown in Figure 3.9. The transmitter's positions were varied between 40 cm and 60 cm at intervals of 1 cm and the corresponding distances calculated by converting the TOFs obtained from the proposed method described in Section 3.5 into distances. To demonstrate the improvement in accuracy obtained by the proposed approach, the distances were also calculated using the cross-correlation technique described in Section 3.4 for comparison.

3.7.2 Positioning

In this experiment, in an active mobile architecture (i.e., the reference points were receivers and the target was the transmitter) a transmitter and an array of five receivers were used in a configuration similar to that illustrated in Figure 3.10. The transmitter was moved to 60 different locations inside a $20 \times 20 \times 20$ mm

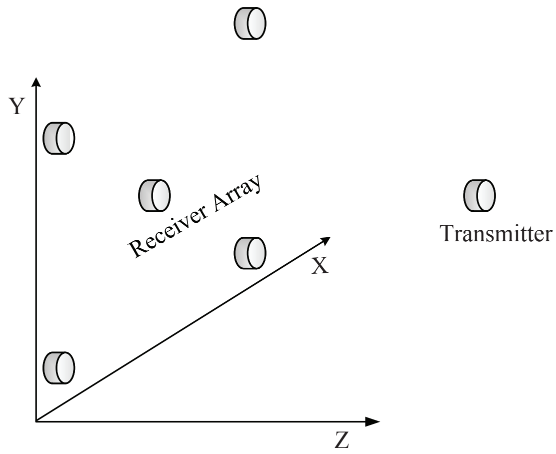

Figure 3.10: Configuration of transmitter and receivers during positioning.

volume, and the true positions were measured using a Vernier scale with a precision of 0.02 mm. For each location of the transmitter the phase-correlation method described in Section 3.5 was used to determine the TOFs of the transmitted signal to each of the five receivers. The position of the transmitter was calculated using the multilateration algorithm described in Chapter 2, Section 2.3.2.1.

To demonstrate the improvement in accuracy provided by the phase-correlation approach, the position of the transmitter was also calculated using the traditional cross-correlation method described in Section 3.4 to measure the TOFs between the transmitter and receivers along with multilateration algorithm.

3.8 Results and Analysis

The results obtained from the above experiments using the proposed and cross-correlation methods are presented and compared in this section.

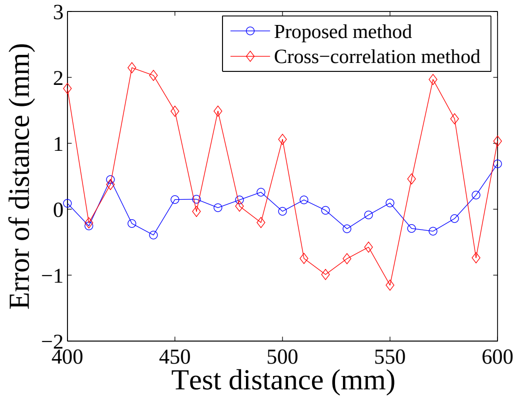

Figure 3.11: Errors in distance measurement obtained from proposed and cross-correlation methods.

3.8.1 Distance Measurement

The errors incurred using the proposed TOF estimation and conventional cross-correlation approaches for distance measurements are shown in Figure 3.11. These plots clearly show the improved precision achieved by the proposed approach, with the standard deviations of errors from it and the cross-correlation method 0.3017 mm and 1.0931 mm respectively.

3.8.2 Positioning

The errors for each of the x, y and z directions in the transmitter's calculated locations using the proposed and traditional cross-correlation approaches are shown in Figure 3.12 and their standard deviations of the errors in each direction in Table 3.1 which demonstrate that the precision obtained using the proposed method is significantly higher than that from the cross-correlation method.

They also indicate that the proposed phase-correlation approach can provide almost sub-millimeter accuracy required for many medical applications. It has

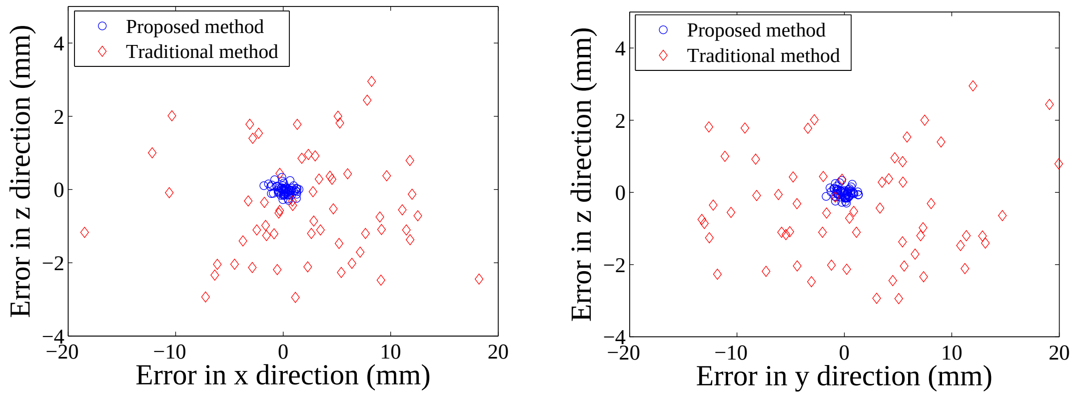

Figure 3.12: Errors in locating transmitter obtained from proposed and traditional methods.

Table 3.1: Standard deviations of errors in transmitter's measured locations (mm).

Methods	Direction		
	x	y	z
Proposed	0.7035	0.6636	0.1298
Cross-correlation	6.7916	8.3894	1.4327

been noticed that for both proposed and traditional approaches the accuracy is higher in x and y directions than z direction. This is because receivers were mounted on a single plane (at $z = 0$ in the proposed coordinate system) and the distances between the receivers were less than the distances between transmitter and receivers which means the surface of the spheres centered at the receivers generated by the multilateration algorithm is almost parallel. This produced larger errors in the position of the intersecting point of the spheres for directions tangential to the surface of the spheres than for directions normal to the surface of the spheres. This phenomenon is known as dilution of precision (DOP).

3.9 Conclusions

In this chapter, to determine the distance between a transmitter and receiver, a new TOF technique using phase-correlation was proposed and then used with the multilateration algorithm to precisely determine the 3D position of a transmitter. The unique features of the proposed approach compared with the cross-correlation technique are that: it has the capability to narrow the correlation peak by virtually rather than physically increasing the signal's bandwidth which not only helps to accurately determine the TOF in an environment in which close multipath reflections occur but can also separate the individual multipath components. It also reduces the system cost as it is not necessary to physically increase the signal's bandwidth. The experimental results showed that the proposed system was able to measure the positions of a transmitter inside a 3D volume with significantly better (almost sub-millimeter) accuracy than the alternative cross-correlation approach. It is worth noting that, although the proposed method achieves almost sub-millimeter accuracy which is a prerequisite for many medical applications, it is highly dependent on the received signal's SNR. In addition, as the phase-correlation technique is a kind of correlation technique, it requires storing both transmitted and received signals which increases the system cost. Most importantly, as all reference points (i.e., receivers) were placed in a single plane, i.e. the $z = 0$ plane, during experiments for simplicity and to determine the receivers coordinates accurately, this configuration suffered from DOP, i.e., created higher errors in the tangential directions of the virtual spheres generated by the multilateration (i.e., in the x and y directions) than normal direction (i.e., in the z direction). The next chapter (Chapter 4) will propose new ways of overcoming these issues to provide improved performance.

Chapter 4

Highly Accurate Ultrasonic Positioning using an OFDM-based Robust Optimization Approach

Ultrasonic positioning systems (UPSs) are used for various types of applications across a wide variety of fields, including robot navigation, device location and pose estimation. In this chapter, the focus is on investigating two major problems in the signalling and positioning phases of existing UPSs and providing corresponding solutions. Firstly, most of the existing UPSs use a single tone or a narrowband chirp signal for positioning which suffer from computational complexity due to the use of correlation technique for time-of-flight (TOF) estimation. In addition, they cannot simultaneously localize multiple transducers due to signal interference. Also, as a moving target introduces Doppler shift into the system, to estimate and compensate this, they use matched filtering techniques which increase the system's cost and complexity. Secondly, it has been noticed that, placing all receivers in a single plane, which is logistically simpler for indoor applications and their distance from the target is larger than the distance between them which is likely to happen, produced larger errors in the position of the intersecting point of the spheres for directions tangential to the surface of the spheres than for directions normal to the surface of the spheres when traditional lateration algorithm was used. In this chapter, firstly, to solve the abovementioned problems of a narrowband signal and correlation-technique, a narrowband orthogonal division multiplexing (OFDM) signal, which can efficiently utilize the entire available frequency spectrum, and a new TOF estimation technique are proposed. Secondly, using the TOF information obtained from this approach, a robust optimization approach for not only overcoming the limitation of the lateration algorithm but also ignoring errors in the distance measurements of the receivers corresponding to one complete cycle of the transmitted signal is proposed. The experimental results show that the proposed system has the precision required for medical applications and its cost and complexity are anticipated to be lower than those of alternative traditional optical systems.

4.1 Introduction

Usually, UPSs use single tone or narrowband chirp signals when a correlation technique is used as the TOF measurement approach. However, these signals suffer from three major problems: 1) although correlation techniques provide better ranging resolution when used with a chirp signal, the complexity of the signal processing required is increased as both the transmitted and received signals need to be stored to perform correlation; 2) it is not possible to simultaneously localize

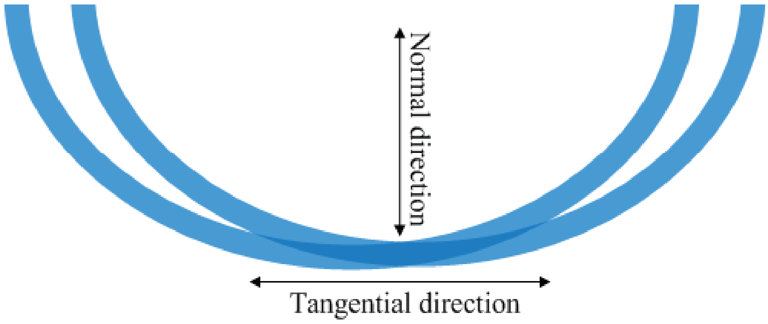

Figure 4.1: Visualization of configuration related errors for the lateration algorithm when positioning targets.

multiple transducers using a narrowband signal because there are always interferences if transmissions occur at the same time (details are provided in the next chapter). This is an important criterion for various medical applications such as gait analysis; and 3) as moving target introduce Doppler shift into the system, to estimate and compensate the Doppler shift, existing narrowband based UPSs use matched filtering techniques. This approach requires a bank of correlators which increases the system cost and complexity (details are provided in the next chapter).

A lateration algorithm is generally used in an UPS to obtain the target's location. For accurate (sub-millimeter) positioning of indoor reference points, it is simpler logistically if they are installed on a fixed plane. However, this configuration means that when lateration is used, the surfaces of the spheres centered at the reference points will be almost parallel when the separation between the reference points and target is larger than the separation between reference points which is likely to happen. This will produce larger errors in the positions of the intersecting points of the spheres for directions tangential to the surfaces of the spheres than for those normal to the surfaces, as shown in Figure 4.1 with the shaded area due to the dilution of precision (DOP) effect. In addition, if the multipath issue is not solved properly at the measurement phase, errors can occur in the TOF of one complete cycle of the transmitted signal. However, lateration does not have the ability to eliminate such types of error from the position estimates.

In this chapter, initially, to solve the abovementioned problems of a narrowband signal and correlation-technique, a narrowband OFDM signal, which can efficiently utilize the entire available frequency spectrum, and a new TOF estimation technique are proposed. Then, using the TOF information obtained from this approach, a steepest descent optimization algorithm is proposed. This optimization algorithm overcomes the limitations of lateration approach and is also able to ignore errors in the distance measurements of receivers corresponding to one complete cycle of the transmitted signal.

The rest of this chapter is organized as follows: Section 4.2 presents an overview of OFDM; in Section 4.3, a new OFDM-based TOF estimation technique is proposed; Section 4.4 presents a new steepest descent optimization approach for positioning; a performance comparison between multilateration and the steepest descent optimization algorithms are given in Section 4.5; Section 4.6.1 describes the experimental procedure for determining the precision of the proposed system; the experimental results are discussed in Section 4.7; and Section 4.8 presents the conclusions drawn from this study.

4.2 Signal Selection

Single tone and chirp signals are the two most commonly used signals in the field of UPSs. As mentioned previously, when a single tone signal is used for positioning, it produces very similar peaks adjacent to the main peak when cross-correlated with the received signal and this may result in a false peak being detected in a noisy and multipath environment. Another problem of the single frequency transmission system is that, in a multipath environment, it may suffer from deep fading. Generally, in indoor environments, numerous reflective objects are present in the neighbourhood of the transmitter and receiver which provide multiple paths that a transmitted signal can traverse. Therefore, a superposition of multiple copies of the transmitted signal, each traversing a different path, is seen by the receiver. A different attenuation, time delay and phase shift from the source to the receiver will be experienced by each signal copy while traveling which results in either constructive or destructive interference, amplifying or attenuating the signal power seen at the receiver. When strong destructive interference occurs, which is frequently referred to as a deep fade, a completely false TOF information may be measured due to the severe drop in the channel signal-to-noise ratio (SNR).

When a chirp signal is used for positioning, though it does not suffer with deep fading, it is not possible to simultaneously position multiple transducers due to the signal interference. For example, if the useful frequency range of an UPS is 35 kHz to 45 kHz and multiple transmitters transmit the same band of signals, at the receiving end they will interfere with each other. This topic is dealt with in more depth in the next chapter. In addition, although using a chirp signal along with the correlation technique is advantageous, the complexity of the signal processing required is increased as both the transmitted and received signals need to be stored to perform correlation.

Hence, to eliminate the abovementioned problems in the signalling phase and to secure a transmission system with a high capacity which can exploit the allocated spectrum more efficiently, a resource management scheme is required. Examples of resource management schemes include: time division multiplexing (TDM), frequency division multiplexing (FDM), OFDM, code division multiplexing (CDM), and space division multiplexing (SDM) based on the principles of sharing time, frequency, code and space respectively. Of these techniques, OFDM has been shown to have a number of advantages and attracted considerable interest [172]. The following section provides an overview of the OFDM technique.

4.2.1 Overview of OFDM

Basically, OFDM is a multicarrier system, in which the available frequency spectrum is divided into many narrowband channels, known as sub-carriers, which are dedicated to a single source. The main benefit of this approach being that multiple transmitters can transmit signals in parallel while maintaining high spectral efficiency.

Conceptually, OFDM is a type of FDM scheme which allows transmitters to transmit information across a communication channel in parallel and offers a more robust alternative to single carrier transmission systems in noisy communications channel that suffer from fading. OFDM offers much more efficient use of the available frequency spectrum than single tone and chirp signals.

The rapid increase in popularity for this scheme is due to the fact that it allows the available channel bandwidth to be used very efficiently. Due to its high spectral efficiency, OFDM has been used for data transfer and positioning in wireless local area networks (WLANs) where data (bits) are modulated with RF sub-carriers and transmitted in parallel [173–182]. Due to the success of multicarrier modulation in the form of OFDM in radio channels it has drawn considerable attention for broadband ultrasonic (US) data transfer in both wired and wireless media [183–186]. Though the OFDM scheme has been used for US data transfer its performance still has not been investigated for UPSs.

By spacing the channels much closer together, OFDM uses the spectrum efficiently. This is achieved by making all the sub-carriers orthogonal to one another, avoiding interference between the closely spaced sub-carriers. These sub-carriers that do not interfere with each other are called orthogonal signals.

The spectrum of each sub-carrier may overlap with each other but remain orthogonal which means that the center frequency of each sub-carrier occurs at a null in the spectrum of all the other sub-carriers. Hence, OFDM transmission allows the carriers to be as close as theoretically possible. Since there is no signal interference between the sub-carriers this results in very high spectral efficiency. These orthogonal frequencies may be transmitted across a single communications channel. If signal orthogonality is maintained properly, at the receiving end they may be recovered without suffering from signal degradation resulting from interference from adjacent sub-carriers. In schemes such as TDM, temporal orthogonality is an inherent feature as only a single source out of a set of possible multiple sources is transmitted per timeslot (details described in next chapter). In non-OFDM systems such as FDM, the orthogonality is maintained by ensuring that the separate sources are spaced far enough apart in the frequency domain to ensure that no interference occurs. However, even though the sub-carriers are as densely packed as possible in OFDM, orthogonality is preserved by ensuring that all the sub-carrier baseband frequencies are integer multiples of the reciprocal of the signal period which is dependent on the sampling rate of the transmitter. This means that, all the sub-carriers have an integer number of cycles per period. In other words, in a particular time interval, each sub-carrier frequency is an integral multiple of a base frequency, and the number of cycles between two adjacent sub-carriers differs by exactly one.

Mathematically, two signals are said to be orthogonal if their dot product is

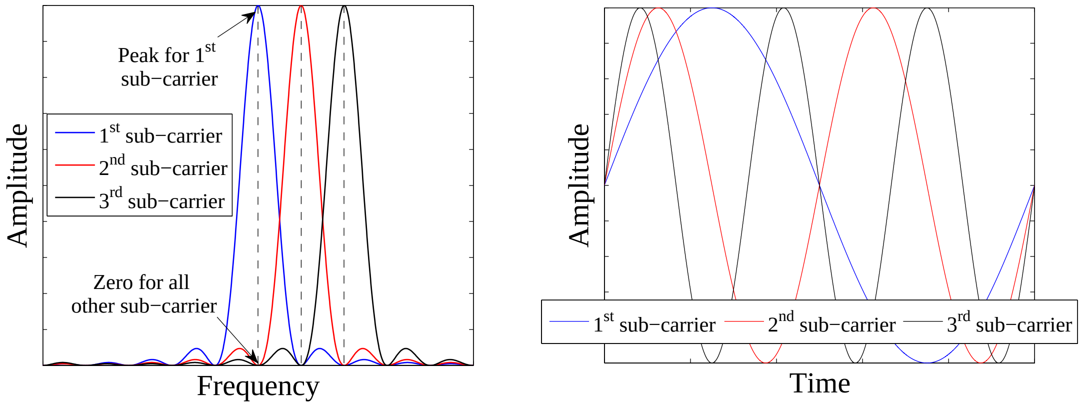

(a) (b)

Figure 4.2: Visulization of three orthogonal sub-carriers of an OFDM signal in: (a) frequency domain; and (b) time domain.

zero which means that if they are multiplied and summed over an interval 0 to τ as described by equation (4.1), then the result is zero. Consider a set of signals $s_T(t)$. Orthogonality exists if:

$$\begin{aligned} \textstyle\int_0^\tau s_{T_p}(t)s^*_{T_q}(t)dt &= k \quad \text{for} \quad p = q \\ &= 0 \quad \text{for} \quad p \neq q \end{aligned} \tag{4.1}$$

where $s_{T_p}(t)s$ and $s_{T_q}(t)$ are the p-th and q-th elements in the set, * denotes the complex conjugate of the signal and $[0, \tau]$ is the signal length. To make the sub-carriers orthogonal the separation between sub-carriers must be $\frac{1}{\tau}$. The sub-carrier's orthogonality can be observed in either the time domain or in the frequency domain. From the frequency domain perspective, the center frequency of each sub-carrier occurs at a null in the spectrum of all the other sub-carriers, i.e., orthogonality in an OFDM system occurs when at the peak of each sub-carrier spectrum, the contribution from all other sub-carries is zero as shown in Figure 4.2(a). From the time domain perspective, each sub-carrier is a sinusoid with an integer number of cycles within the signal period and the number of cycles between two adjacent sub-carriers differs exactly by one as shown in Figure 4.2(b).

From the above discussion three major advantages of using an OFDM signal in the field of UPS are:

1. OFDM is more robust than single carrier transmission systems in a multi-path fading channel environment due to its frequency diversity. That is, the effects of multipath fading can be considered as constant (flat) over an OFDM sub-channel if the sub-channel is sufficiently narrow-banded (i.e., if the number of sub-channels are sufficiently large).

2. OFDM offers much more efficient use of the available spectrum than single tone and chirp based positioning system due to the simultaneous use of multiple frequencies for data transmission. This topic is dealt with in more depth in the next chapter.

3. Channel estimation is easier with the use of pilot carrier(s). For example, by making one of the sub-carriers have a higher magnitude than the others, the frequency shift of the signal from a moving target due to Doppler effect can be calculated. This topic also is dealt with in more depth in the next chapter.

Each sub-carrier of an OFDM signal is represented by $A_T(t)e^{j2\pi ft}$ where f and $A_T(t)$ represent the frequency and amplitude of the sub-carrier respectively. Generally, an OFDM waveform is created in the frequency domain initially and then converted to a real-valued time domain waveform using the inverse fast Fourier transform (IFFT). In order to correctly create the time domain waveforms, the conjugate of the real sub-carrier values (the imaginary frequency components) must be inserted into the fast Fourier transform (FFT) array. Though one of the main reasons of introducing an OFDM signal is for simultaneous multiple transducers positioning, in this chapter, initially the performance of the OFDM signal for single transducer is tested in active mobile architecture (i.e., the reference points were receivers and the target was the transmitter) and a new TOF estimation technique is proposed using the OFDM signal. The following section describes the generation of a narrowband OFDM signal in the digital frequency domain.

4.2.2 Fast Fourier Transform (FFT) Implementation of an OFDM Signal

If the sampling frequency of a discrete signal is F_s and its length is N samples, the frequency resolution is given by:

$$r_s = \frac{F_s}{N} \tag{4.2}$$

Letting the lower carrier frequency of the desired OFDM signal be f_l and the upper carrier frequency be f_u, to maintain orthogonality, the sub-carrier gap must be at minimum r_s. Now the frequency domain OFDM signal is given by:

$$S_T[n] = \begin{cases} A[n]e^{j\theta[n]} & \text{where } \ n = (\frac{f_l}{r_s} + 1) + l \\ A[n]e^{-j\theta[n]} & \text{where } \ n = (N + 1 - \frac{f_l}{r_s}) - l \\ 0 & \text{elsewhere} \end{cases} \tag{4.3}$$

for $l = 0, 1, \ldots, \frac{f_u - f_l}{r_s}$. In this equation A and θ indicate the amplitude and phase of each carrier respectively, and n represents the sample points in the frequency domain. The IFFT of $S_T[n]$ represents the corresponding time domain signal:

$$s_T[k] = \frac{1}{N}\sum_{n=1}^{N} S_T[n]e^{-\frac{2\pi ikn}{N}}, \qquad 0 \leq n \leq N-1 \tag{4.4}$$

where k represents the sampled points in the time domain. A conceptual block diagram of the designed narrowband OFDM signal is shown in Figure 4.3 where each branch corresponds to a sub-carrier.

In summary, the design process of the narrowband OFDM signal for a single transducer positioning is given below.

Algorithm 1: Pseudo code of the narrowband OFDM signal for a single transducer positioning

- Set $f_l,\ f_u\ N,\ F_s,\ A,\ \theta$
- Set $S_T(n) = \text{zeros}(1, N)$
- Calculate r_s
- **for** $l = 0 : \frac{f_u - f_l}{r_s}$ **do**

  Calculate

  $S_T(n)$

  end for
- Calculate $s_T(k)$

To visualize the design process of a narrowband OFDM signal, consider the following example. If an UPS has a sampling rate (F_s) of 1 Msample/s, the lower and upper carrier frequencies (f_l and f_u) are 35 kHz and 45 kHz respectively and they have constant amplitudes (A) and phases (θ), then for a signal length of (N)

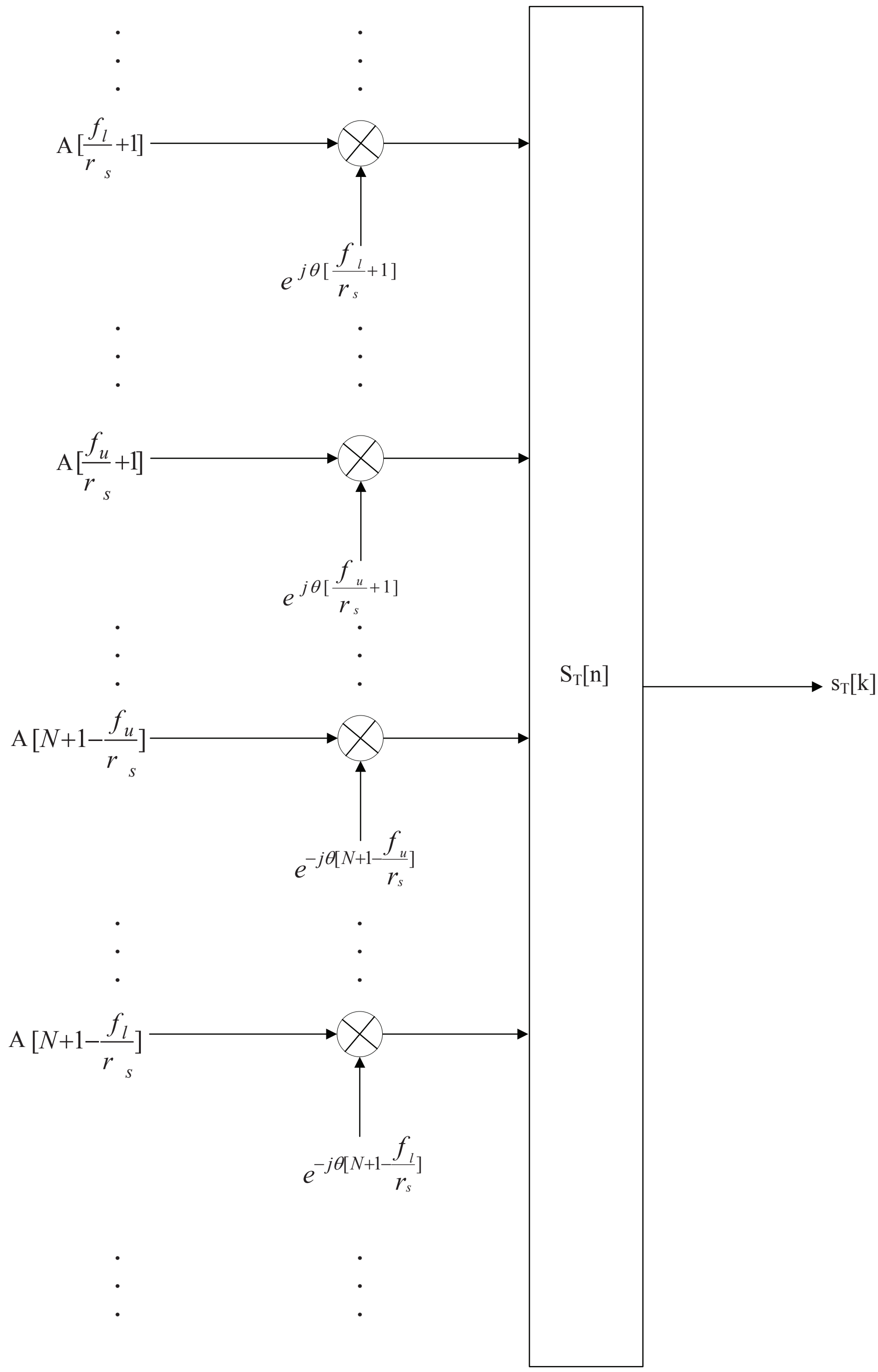

Figure 4.3: Conceptual block diagram of the OFDM signal.

1000 samples in the frequency domain, the frequency resolution (r_s) according to equation (4.2) will be:

$$r_s = \frac{F_s}{N} = \frac{1 \text{ Msample/s}}{1000 \text{ sample}} = 1000 \text{ Hz}$$

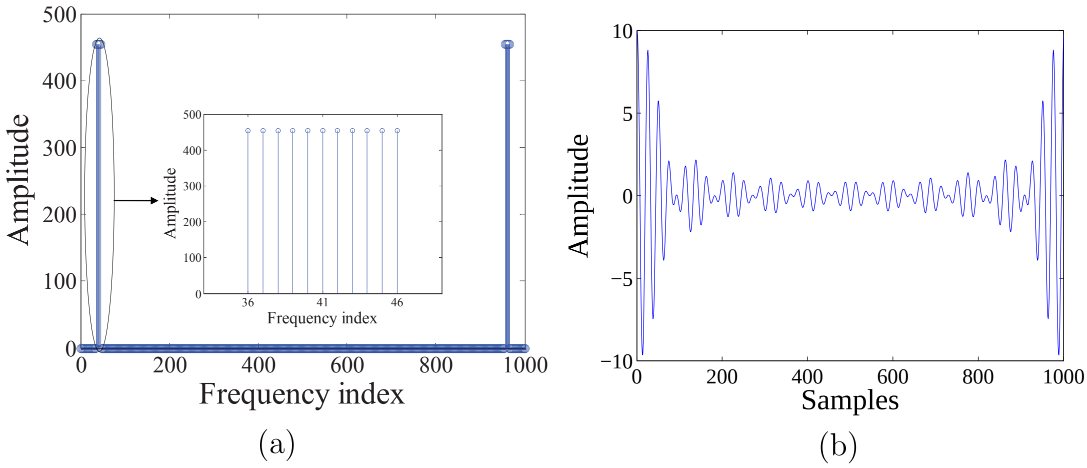

Figure 4.4: Visulization of a narrowband OFDM signal of length 1000 samples in: (a) frequency domain; and (b) time domain.

and its corresponding frequency and time domain signals according to equations (4.3) and (4.4) are shown in Figure 4.4(a) and 4.4(b) respectively. The frequency resolution r_s means each frequency index represents r_s Hz in the Fourier domain. For example frequency index 36 means $36 \times 1000 = 36000$ Hz if the index started with 0, but if the index started with 1 as in Figure 4.4(a), the index 36 means $(36\text{-}1) \times 1000 = 35000$ Hz.

It should be noted that, if all the frequency components have equal amplitudes and zero phases, the resultant OFDM signal will be a narrowband approximation of an impulse which would have the highest amplitude at the start as shown in Figure 4.4(b). Now, utilizing this property and by removing the transducer effect from the received signal, in the following section a new OFDM-based TOF technique is proposed.

4.3 OFDM-based TOF Estimation Technique

The active element of an US transducer is constructed from a piezoelectric material which changes electrical energy into mechanical energy and creates sound when a voltage is applied to it. The amount of vibration and sound generated from the transducer depends not only on this voltage but also on the resonant properties of the transducer. Every material has a natural propensity to vibrate at a particular frequency which is called its resonant frequency, with that of piezo-electric transducers causing a non-linear phase frequency response which limits the overall performance of a positioning system. Therefore, an equalization technique is required to achieve an overall linear phase response of the transducer.

The frequency response of transducers can be modelled by placing the transmitter and a receiver face to face so that the length of the wireless channel between the transmitted and received signals is effectively zero. Now the inverse frequency response of the transducers (H_{tx}) which is called an equalizer or frequency response compensator is given by:

$$H_{tx} = \left(\frac{S_T}{S_{R_p}} \right) \tag{4.5}$$

where S_T and S_{R_p} represent the transmitted and received signals in the frequency domain respectively.

Now using this equalizer, a new OFDM-based TOF technique which eliminates the transducers effect and significantly reduces noise from the received signal (s_R) is proposed.

To estimate the TOF, initially, the start of the transmission of the OFDM signal is recorded and then the start of that pulse in the received signal is estimated by applying a threshold-based approach. Let the estimated starting point of the received OFDM signal be n_i samples. A pulse ($s_{R_{th}}$) is then cropped to the same length of the transmitted signal from the few samples (n_{off}) before the roughly estimated position so that the start of the OFDM signal is always present in the cropped signal, as shown in equation (4.6).

$$s_{R_{th}} = s_R(n), \qquad n_s \leq n \leq n_s + N \tag{4.6}$$

where $n_s = n_i - n_{off}$ and N is the duration of an original OFDM pulse in samples.

To eliminate the transducer effects and reduce the noise, equalization is performed using the pre-calculated H_{tx}:

$$s_{R_{eq}} = \Im^{-1}\Bigg(S_{R_{th}} H_{tx}\Bigg) \tag{4.7}$$

where $s_{R_{eq}}$ is the equalized received signal in the time domain and $S_{R_{th}}$ is the cropped received signal in the frequency domain. This equalized received signal will be almost the same as the transmitted signal as the transducer effect is removed and there is very little noise because the equalized received signal has only those noise components that were added to the transmitted frequencies.

As the equalized received pulse has a similar shape to the transmitted OFDM pulse, which has its highest amplitude at its start, the final TOF is calculated by finding the position of the first maximum peak (n_f) of the equalized received signal, with the start of the OFDM signal represented as:

$$n_r = n_s + n_f \tag{4.8}$$

Now, if the start of the transmitted signal is recorded as n_t, the TOF (n_F) between the transmitted and received signals is:

$$n_F = n_r - n_t \tag{4.9}$$

In summary, the proposed OFDM-based TOF estimation technique is described as follows:

1. Calculate the transducer response H_{tx} by placing the transmitter and receiver face to face so that the wireless channel length between transmitter and receiver is effectively zero.

2. Record the starting sample (n_t) of the transmitted signal.

3. Roughly estimate the start (n_i) of the received signal (s_R) by applying a threshold detection approach.

4. Crop the received signal $(s_{R_{th}})$ by a few samples (n_s) before the roughly estimated position.

5. Find the equalized received signal $(s_{R_{eq}})$ using equation (4.7).

6. Find the position (n_f) of the first peak of $s_{R_{th}}$.

7. Calculate the start of s_R as $n_r = n_s + n_f$.

8. Estimate the TOF as $n_F = n_r - n_t$.

Now, using this TOF information, in the following section, a new steepest descent optimization positioning algorithm is proposed to solve the previously mentioned problem of the lateration algorithm.

4.4 Transducer Localization using Steepest Descent Optimization

For this step in the process, five reference points are considered and the ideal positions of their centers (in cm) are given in the following matrix.

$$\mathbf{P} = \begin{bmatrix} -30 & -30 & 0 \\ 0 & 0 & 0 \\ 30 & -30 & 0 \\ -30 & 30 & 0 \\ 30 & 30 & 0 \end{bmatrix}$$

The reference points are mounted in a single plane (at $z = 0$ in the proposed coordinate system) and their positions relative to the transducers which are to be localized are illustrated in Figure 4.5. In practice, these ideal positions are slightly modified after calibration to account for any inaccuracies in the mounting process.

The purpose of the proposed optimization approach is to determine the relative positions of the reference points and target transducer which best correspond to the distances measured by the TOF of the US signal. To fulfil this objective, it is initially assumed that the transducer which is to be localized is placed at the same position as reference point R_2, i.e., (0,0,0). Then, to estimate the positions of the reference points with respect to the transducer, a steepest descent optimization approach is used to determine the translation in the z direction and rotations around the x and y axes of the reference plane. This places the five reference points at positions which best correspond to their measured distances from the transducer. Figure 4.5 illustrates the positions of the reference points (in yellow)

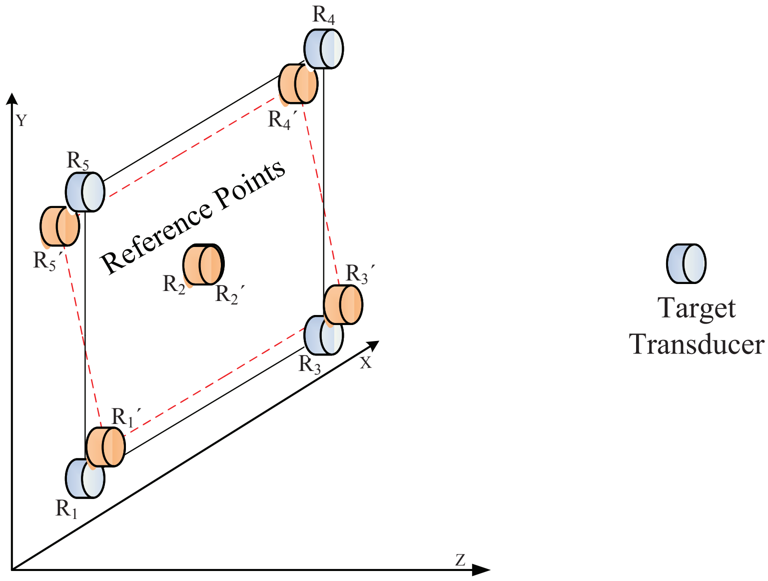

Figure 4.5: Deviation of receiver plane.

after the reference plane's rotation around its x axis. This optimization problem corresponds to finding the matrix ($\mathbf{M}$) which minimizes the error, $\mathbf{M} \ni \; min \; (E)$ where,

$$E = \sum_{r=1}^{5} (\| \mathbf{M}\mathbf{p}_r^{(0)} \| - d_r)^2 \tag{4.10}$$

where $\mathbf{p}_r^{(0)} = [x_r^{(0)} \quad y_r^{(0)} \quad z_r^{(0)} 1]^T$ is the initial position of reference point r in homogeneous coordinates, d_r is the distance from the transducer (which to be localized) to reference point r estimated from the TOF and $\mathbf{M}$ a specific three-dimensional (3D) rigid-body transformation consisting of rotations around the x and y axes (R_x and R_y respectively) followed by a translation in the z direction (T_z).

These parameters define the transformation matrix $\mathbf{M}$ as:

$$\mathbf{M} = \mathbf{TR} \tag{4.11}$$

where $\mathbf{T}$ is the translation matrix given by:

$$\mathbf{T} = \begin{bmatrix} 1 & 0 & 0 & 0 \\ 0 & 1 & 0 & 0 \\ 0 & 0 & 1 & T_z \\ 0 & 0 & 0 & 1 \end{bmatrix}$$

and the rotation matrix around the x and y axes ($\mathbf{R}$) is given by:

$$\mathbf{R} = \begin{bmatrix} \cos(R_y) & 0 & -\sin(R_y) & 0 \\ -\sin(R_x)\sin(R_y) & \cos(R_x) & -\sin(R_x)\cos(R_y) & 0 \\ \cos(R_x)\sin(R_y) & \sin(R_x) & \cos(R_x)\cos(R_y) & 0 \\ 0 & 0 & 0 & 1 \end{bmatrix}$$

Then, the steepest descent optimization approach is required to find the optimum values of T_z, R_x and R_y.

For iteration n of the optimization, the new positions of the reference points are given by:

$$\mathbf{p}_r^{(n)} = [x_r^{(n)} \quad y_r^{(n)} \quad z_r^{(n)} \quad 1]^T = \mathbf{M}^{(n)}\mathbf{p}_r^{(0)} \tag{4.12}$$

where the values of the transformation parameters are given by:

$$\mathbf{m}^{(n+1)} = \mathbf{m}^{(n)} - \alpha\nabla\mathbf{E} \tag{4.13}$$

where α is a constant step size,

$$\mathbf{m} = [T_z \quad R_x \quad R_y]^T \tag{4.14}$$

and

$$\nabla\mathbf{E} = [\frac{\partial E}{\partial T_z} \quad \frac{\partial E}{\partial R_x} \quad \frac{\partial E}{\partial R_y}]^T \tag{4.15}$$

The elements of $\nabla\mathbf{E}$ are defined as:

$$\frac{\partial E}{\partial T_z} = 2\sum_{r=1}^{5} \frac{(\|\mathbf{p}_r^{(n)}\| - d_r)}{\|\mathbf{p}_r^{(n)}\|}(T_z^{(n)} + \cos(R_x^{(n)})\sin(R_y^{(n)})x_r^{(0)} + \sin(R_x^{(n)})y_r^{(0)} + \cos(R_x^{(n)})\cos(R_y^{(n)})z_r^{(0)}) \tag{4.16}$$

$$\frac{\partial E}{\partial R_x} = 2\sum_{r=1}^{5} \frac{(\|\mathbf{p}_r^{(n)}\| - d_r)}{\|\mathbf{p}_r^{(n)}\|}(-\sin(R_x^{(n)})\sin(R_y^{(n)})T_z^{(n)}x_r^{(0)} + \cos(R_x^{(n)})T_z^{(n)}y_r^{(0)} - \cos(R_y^{(n)})\sin(R_x^{(n)})T_z^{(n)}z_r^{(0)}) \tag{4.17}$$

$$\frac{\partial E}{\partial R_y} = 2\sum_{r=1}^{5} \frac{(\|\mathbf{p}_r^{(n)}\| - d_r)}{\|\mathbf{p}_r^{(n)}\|}(\cos(R_x^{(n)})\cos(R_y^{(n)})T_z^{(n)}x_r^{(0)} - \cos(R_x^{(n)})\sin(R_y^{(n)})T_z^{(n)}z_r^{(0)}) \tag{4.18}$$

If $e_r = 2(\|\mathbf{p}_r^{(n)}\| - d_r)$ and it is assumed that R_x and R_y are small, these expressions can be simplified to give:

$$\frac{\partial E}{\partial T_z} \approx \sum_{r=1}^{5} \frac{1}{\|\mathbf{p}_r^{(n)}\|} e_r z_r^{(n)} \tag{4.19}$$

$$\frac{\partial E}{\partial R_x} \approx \sum_{r=1}^{5} \frac{T_z^{(n)}}{\|\mathbf{p}_r^{(n)}\|} e_r y_r^{(0)} \tag{4.20}$$

$$\frac{\partial E}{\partial R_y} \approx \sum_{r=1}^{5} \frac{T_z^{(n)}}{\|\mathbf{p}_r^{(n)}\|} e_r x_r^{(0)} \tag{4.21}$$

Then, to minimize the effect of the outliers in the e_r terms that are proportional to one complete cycle of the transmitted signal, the summation is replaced by a median operation and the step-size (α) adjusted accordingly.

Once the optimization converges to a solution (usually within 10 iterations), the position of the transducer is calculated with respect to the initial position of the reference plane using the inverse of the optimum value of $\mathbf{M}$:

$$\mathbf{p}_t = \mathbf{M}^{-1} \begin{bmatrix} 0 & 0 & 0 & 1 \end{bmatrix}^T \tag{4.22}$$

Using this approach, the transducer's positions can be calculated.

In summary, the proposed steepest descent positioning algorithm is implemented as follows and requires iterations of steps 1 to 3 until the optimization converges to a solution.

- **Step 1:** initialize 1) the reference point's coordinates ($\mathbf{p}_r^{(0)}$), 2) the distance (d_r) from the transducer (which to be localized) to reference point r estimated using the proposed TOF technique and 3) the translation in the z direction (T_z), and rotations around the x and y axes (R_x and R_y respectively).
- **Step 2:** calculate the 3D rigid-body transformation matrix ($\mathbf{M}$) using equation (4.11) and the error (E) using equation (4.10).
- **Step 3:** if E from step 2 has not converged to a solution, update the transformation parameters (T_z, R_x, R_y) using equation (4.13) and then go back to step 2; else calculate the transducer's position using equation (4.22).

The flowchart of the proposed positioning algorithm is shown in Figure 4.6.

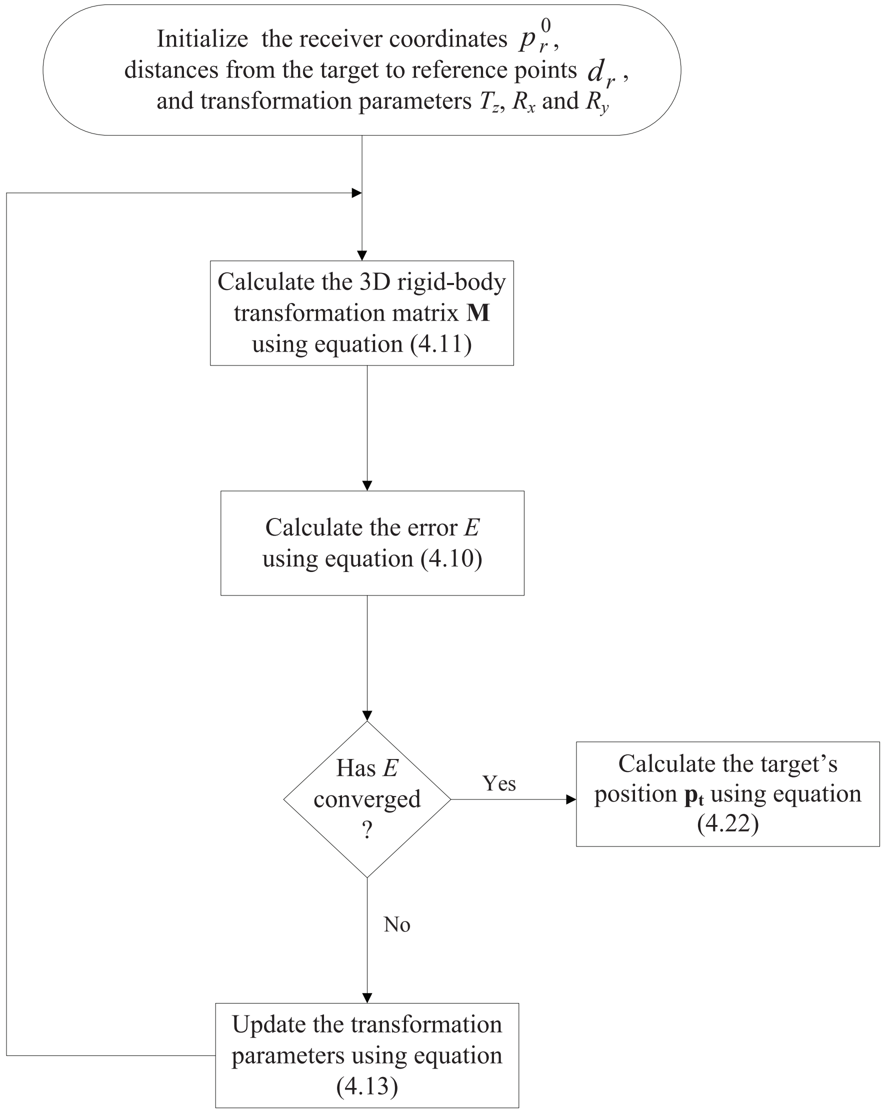

Figure 4.6: Flowchart of proposed steepest descent algorithm for 3D positioning.

4.5 Performance Comparison between the Multilateration and Steepest Decent Optimization Algorithms

To provide a comparison between the traditional multilateration algorithm and the proposed steepest descent optimization algorithm, a Matlab simulation was performed. In this simulation, using an active mobile architecture, a transmitter and

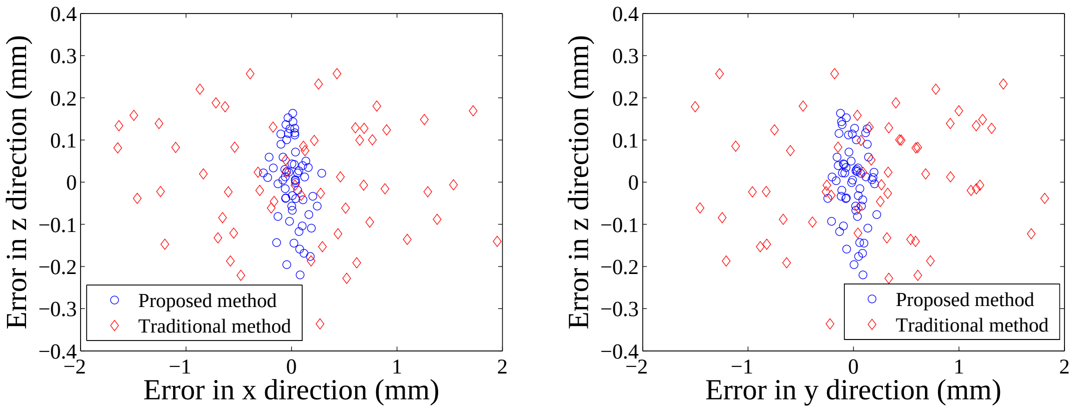

Figure 4.7: Errors in locating the transmitter for the proposed and traditional methods.

an array of five receivers were used in a configuration similar to that illustrated in Figure 4.5, i.e., the receivers were placed on a single plane and the distance between the transmitter and receiver was larger than the distance between reference points. In this simulation, errors in the distance between transmitter and receivers were introduced which is common in practical situations due to multipath and environmental uncertainty. The position of the transmitter was calculated for 60 trials using both traditional multilateration and the proposed steepest decent optimization algorithms. The localization results obtained from the proposed approach and the traditional multilateration method are shown in Figure 4.7. From these results it can be seen that, due to the problem of DOP, for the multilateration approach, the errors in the x and y directions, i.e., the tangential direction of the spheres generated by the multilateration algorithm, are higher than the errors in the z direction, i.e., the normal direction of the spheres. On the other hand, the proposed steepest decent optimization method does not suffer with such types of errors during positioning of the target as it determines the translation in the z direction and rotations around the x and y axes of the receiver plane which places the receivers at positions which best correspond to their measured distances from the target.

4.6 Experimental Procedure

To evaluate the proposed method, a set of experiments was conducted using the same devices as in Chapter 3 (Piezotite MA40S4S and MA40S4R as transmitter and receiver, a Measurement Computing USB-1606 data acquisition (DAQ) module as a capturing device and a digital thermometer for measuring the room temperature) according to the procedures described below.

4.6.1 Distance Measurement

To evaluate the proposed OFDM-based TOF estimation technique described in Section 4.3 an experiment was performed using the same procedure described in Chapter 3, Section 3.7 where a [35-45] kHz/10 ms OFDM signal was transmitted. To demonstrate the improvement in accuracy provided by the proposed approach, the distances were also calculated using a traditional chirp signal ([35-45] kHz/10 ms) along with cross-correlation.

4.6.2 Positioning

To evaluate the proposed steepest descent optimization algorithm described in Section 4.4 to estimate the 3D positions of a transmitter along with the proposed OFDM-based TOF estimation technique, an experiment was conducted using an active mobile architecture (i.e., reference points were receivers and target was transmitter) according to the same procedure described in Chapter 3, Section 3.7.2 where a [35-45] kHz/10 ms OFDM signal was used for transmission. To demonstrate the improvement in accuracy provided by the proposed approach, the positions of the transmitter were also calculated by the traditional cross-correlation-based multilateration algorithm using a [35-45] kHz/10 ms chirp signal.

4.7 Results and Analysis

The results obtained from the above experiments are discussed below.

4.7.1 Distance Measurement

To visualize the proposed TOF technique described in Section 4.3, a test case (from the first experiment) when the true delay between the transmitter and receiver was 60 cm (which corresponded to 1744 samples when the speed of sound was 344 m/s at 21° and sampling rate of 1 Msample/s) was analysed. In this case, Figure 4.8(a) shows the transmitted OFDM signal with a length of 10000 samples (i.e., 10 ms), which consisted of 101 frequency components from a frequency range of 35 kHz to 45 kHz, with the start of the transmitted pulse recorded at $n_t = 2008$ samples. The shape of the received OFDM signal shown in Figure 4.8(b) was not the same as that of the transmitted signal because of the transducer and noise effects. The threshold selected was one-fifth of the maximum strength of the received pulse and calculated as 0.35. Comparing the received signal with the threshold, the possible start of the OFDM signal was found at 3857 samples, as indicated by n_i in Figure 4.8(b). Due to uncertainty, a point in the received signal was selected at 500 samples (n_{off}) before n_i, as indicated by n_s in Figure 4.8(b), and then cropped

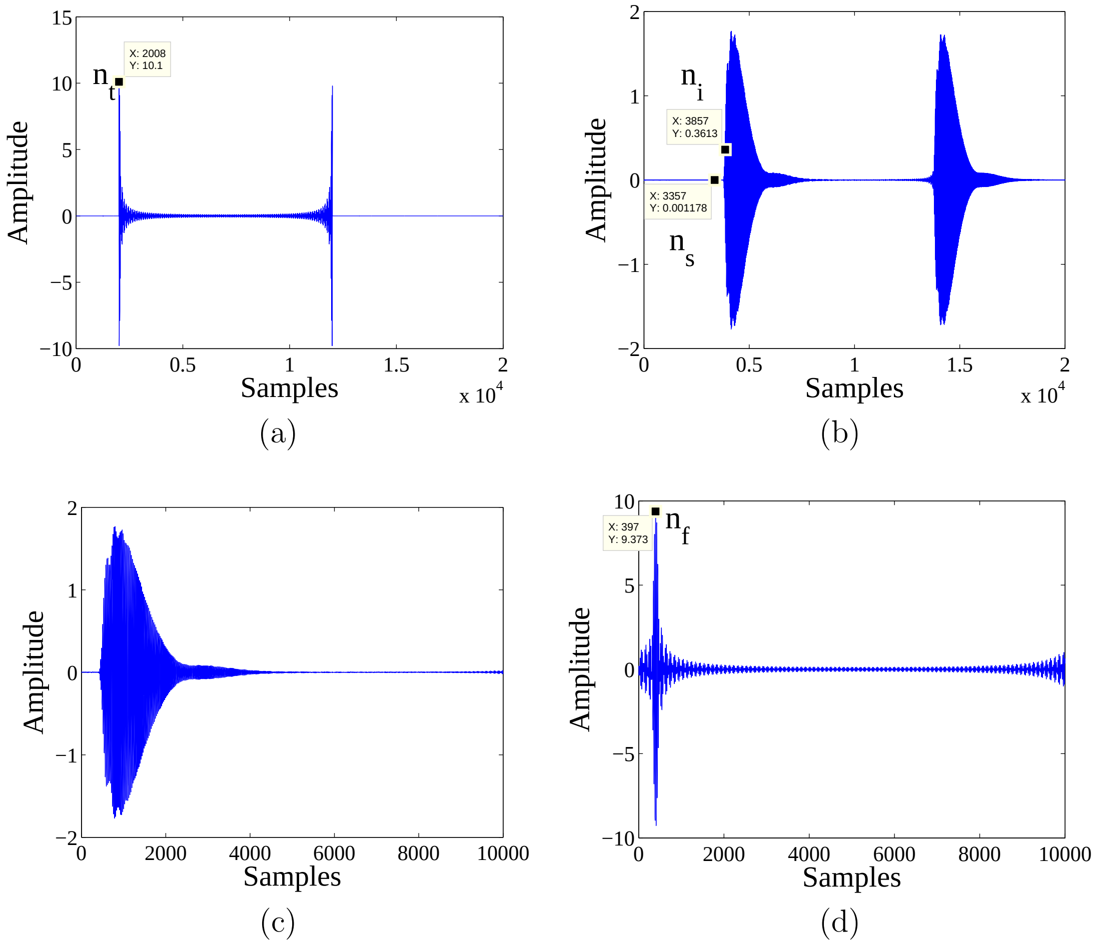

Figure 4.8: Steps in the OFDM-based TOF estimation method: (a) transmitted signal; (b) received signal; (c) cropped received signal; and (d) equalized received signal.

to the same length as the transmitted signal (Figure 4.8(c)). This cropped signal was then equalized using equation (4.7). Finally, the position of the first maximum peak of the equalized received signal was searched and found to be 397 samples, as indicated in Figure 4.8(d) by n_f. From the above analysis, it can be said that:

$$n_t = 2008 \text{ samples}$$
$$n_i = 3857 \text{ samples}$$
$$n_{off} = 500 \text{ samples}$$
$$n_s = n_i - n_{off} = 3857 - 500 = 3357 \text{ samples}$$
$$n_f = 397 \text{ samples}$$
$$n_r = n_f + n_s = 397 + 3357 = 3754 \text{ samples}$$

Therefore, the estimated TOF was calculated as:

$$n_F = n_r - n_t = 3754 - 2008 = 1746 \text{ samples}$$

The estimated TOF agreed with the distance traveled by the transmitted OFDM signal to the receiver, that is, 1746×1e-6×344×100 = 60.0624 cm, while the actual distance was 60 cm which indicated an error of 0.6240 mm. The proposed TOF estimation technique was also evaluated numerically for underwater depth estimation in [187].

The above procedure was applied to calculate the distance to the transmitter from the receiver, which was varied from 40 to 60 cm at 1 cm intervals. The errors when using the proposed TOF estimation technique and conventional cross-correlation approach for a chirp signal are shown in Figure 4.9.

These plots clearly show the improved precision achieved by the proposed OFDM-based TOF estimation approach. The standard deviation of error of the proposed and chirp-based cross-correlation systems were 0.2319 mm and 1.1074 mm respectively.

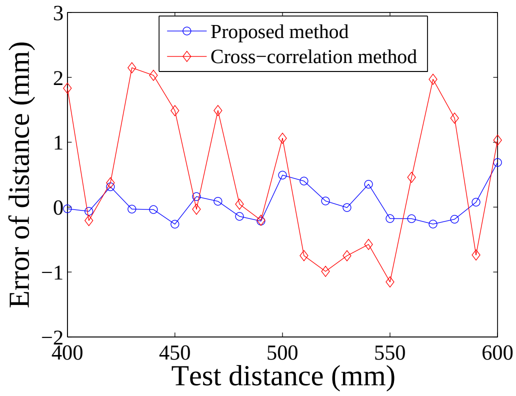

Figure 4.9: Errors in distance measurement obtained from proposed and cross-correlation methods.

In summary, the OFDM-based TOF estimation technique has the following advantages over the traditional chirp-based cross-correlation approach.

1. As it is a threshold-based approach, no correlation is required and, therefore, complexity is reduced.
2. There is no need to store both the transmitted and received signals in memory as the estimation process is based on only a received signal.
3. It has a good noise cancelation property as the frequency components other than those present in an OFDM signal are forcefully set to zero during equalization.

Along with these advantages, the OFDM signal has the following two major benefits.

1. It can simultaneously transmit more than one OFDM signal using a fixed bandwidth without signal interference which allows the simultaneous positioning of multiple transducers (as detailed in Chapter 5).

Table 4.1: Convergence of transformation parameters (cm).

Iteration n	Error E	Translation in z direction (T_z)	Rotation in x direction (R_x)	Rotation in y direction (R_y)
1	41.6533	40.6759	-1.1276	-0.1155
2	20.6689	61.2048	-1.8476	-0.1890
3	3.5507	64.8426	-2.1829	-0.2227
4	0.3423	65.2201	-2.3574	-0.2400
5	0.0784	65.2201	-2.4632	-0.2641
6	0.0442	65.2201	-2.5161	-0.2769
7	0.0272	65.2207	-2.5497	-0.2836
8	0.0171	65.2240	-2.5692	-0.2839
9	0.0114	65.2262	-2.5771	-0.2826
10	0.0096	65.2269	-2.5807	-0.2820

2. One of the frequencies of an OFDM signal can be taken as a pilot carrier and its strength can be considerably increased to estimate the Doppler shift (as detailed in Chapter 5).

4.7.2 Positioning

To realize the convergence of the proposed steepest descent optimization algorithm, the results for the transformation parameters (T_z, R_x, and R_y) obtained at each iteration for positioning the transmitter (from the second experiment) are shown in Table 4.1. Using these results, the final transformation matrix ($\mathbf{M}$) and corresponding location of the transmitter were obtained (in cm) as:

$$\mathbf{M} = \begin{bmatrix} 0.9991 & 0.0001 & -0.0431 & 0 \\ 0 & 1.0000 & 0.0028 & 0 \\ 0.0431 & -0.0028 & 0.9991 & 65.2131 \\ 0 & 0 & 0 & 1.0000 \end{bmatrix}$$

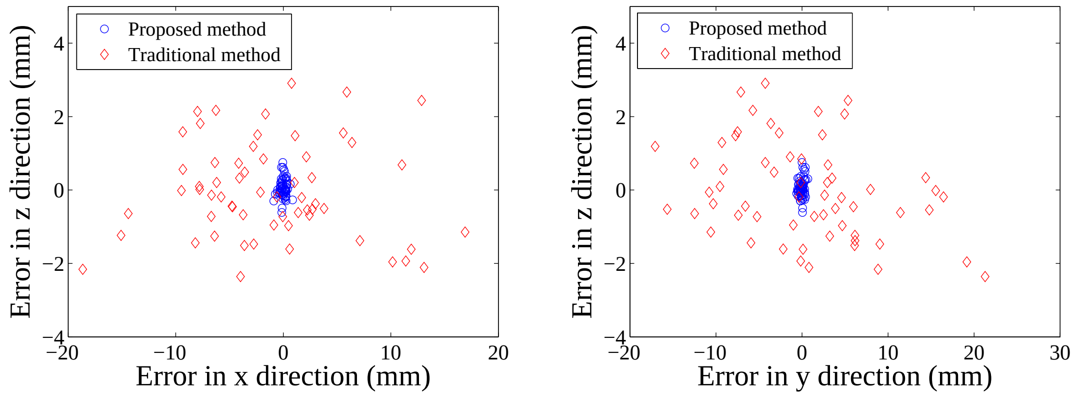

Figure 4.10: Errors in locating the transmitter obtained from the proposed and traditional methods.

$$\mathbf{p_t} = \begin{bmatrix} -2.8120 & 0.1834 & -65.1522 \end{bmatrix}$$

Using this process, the transmitter's location was calculated for other positions. The errors for each of the x, y and z directions in the transmitter's calculated locations using the proposed and traditional approaches are shown in Figure 4.10. These plots clearly show the improved precision achieved by the proposed method.

The standard deviations of the errors in each direction for the proposed and traditional methods are given in Table 4.2 which demonstrate that the accuracy obtained using the proposed method is significantly higher than that of the traditional approach. These results also demonstrate that the proposed steepest decent algorithm does not suffer with configuration related error like the multilateration algorithm (described earlier) as it determine the position of the transmitter using the translation in the z direction and rotations around the x and y axes of the receiver plane. In addition, they also show that the proposed approach using an OFDM signal provides the sub-millimeter accuracy required for many medical applications.

Table 4.2: Standard deviations of errors in transmitter's measured locations (mm).

Methods	Direction		
	x	y	z
Proposed	0.3035	0.2824	0.2602
Traditional	7.2078	8.5492	1.3093

In summary, the abovementioned steepest descent optimization algorithm has the following advantages for positioning over existing trilateration and multilateration algorithms.

1. Unlike the lateration algorithm, it does not suffer from DOP.
2. In the case of a narrowband ultrasonic (US) signal, errors can occur in the TOF of one complete cycle of the transmitted signal due to the effects of multi-path echoes and noise if they are not compensated properly in measurement phase. The lateration algorithm cannot eliminate these errors from position estimates whereas the proposed algorithm can.

4.8 Conclusions

In this chapter, initially, to determine the distance between a transmitter and receiver, a new TOF technique using an OFDM signal was proposed. Then, using this distance information, a steepest descent optimization algorithm for precisely determining the 3D position of a transmitter was introduced. The unique features of this proposed OFDM-based TOF technique compared with the existing chirp-based correlation technique are: it is computationally efficient; has efficient memory use and good de-noising properties; and provides higher accuracy. Furthermore, OFDM signals allow the simultaneous positioning of multiple transmitters without signal interference and, using OFDM, the Doppler shift can be easily calculated by introducing a pilot carrier (both of which are described in the next chapter). Again, the unique features of the proposed steepest descent optimization algorithm over the traditional lateration algorithms are: it does not suffer from DOP errors; and is able to ignore the errors in the distance measurements of the receivers corresponding to one complete cycle of the transmitted signal. The experimental results showed that the proposed system is able to measure the positions of a transmitter inside a 3D volume with significantly better accuracy than the alternative trilateration approach.

In the next chapter, to solve two major problems of the single tone or narrow-band chirp signals (i.e., simultaneous multiple transducer positioning and a highly computationally complex Doppler shift estimation and compensation process), the introduced OFDM-based steepest descent optimization algorithm is initially extended to handle multiple transducer positioning. Then, it is further extended for tracking a moving transmitter in a complex pendulum model with compensation of the Doppler shift associated with its movement.

Chapter 5

Toward a Highly Accurate UPS for Gait Analysis

Techniques that could be used to examine human motion accurately are useful in various applications; one of them is gait analysis. Gait analysis systems are widely used in different applications in almost all major fields of human movement for both clinical and research purposes. Traditionally, they use optical motion capture systems (MCSs) whereby movements are obtained from cameras which track multiple optical markers placed at specific limb positions on a subject. Although they have been able to provide sub-millimeter accuracy, their costs are prohibitive for many users and they require a very complex setup. In addition, they are responsive to changes in lighting and shadow. In the previous chapter, an orthogonal frequency division multiplexing (OFDM)-based steepest descent optimization algorithm was developed. In this chapter, with gait analysis in mind, this algorithm is extended from single transducer positioning to simultaneous multiple transducers positioning. Then, a Doppler shift estimation and compensation technique for tracking a moving transducer in a complex pendulum model, which has the velocity required for gait analysis, is proposed. The proposed methods for simultaneous multiple transducers positioning and tracking a single transducer are evaluated experimentally. The tracking results of various pendulum trajectories of the transducer are compared with a commercially available optical MCS, Vicon, and it is shown that the proposed system has the same order of precision but incurs less cost and complexity than the Vicon MCS.

5.1 Introduction

In almost all substantial fields of human movement, gait analysis has been used in a wide variety of applications for both clinical and research purposes. In the clinical decision-making processes, such as diagnoses of disorders, and future treatment plans in physical medicine and rehabilitation, it plays an important role. Traditionally, gait analysis systems use an optical MCS which use one or more cameras to capture the displacement of reflective markers placed at specific limb positions [38, 188]. Although these systems have been able to provide sub-millimeter accuracy, their cost makes them out of reach for many users and they require a very complex setup. In addition, they are responsive to changes in lighting and shadow [18, 19]. Therefore, with the aim of overcoming these limitations, UPSs have drawn considerable attention [21–39].

In the past, several ultrasonic positioning and tracking systems have been developed which use either an active (i.e., the reference points are receivers and the target is the transmitter) or passive mobile architecture (i.e., the reference points are transmitter and the target is the receiver). However, due to signal interference, all UPSs have difficulty simultaneously locating multiple *transducers*[1] in three-dimensional (3D) space when they use narrowband transducers. Although they attempt to overcome this using time division multiplexing (TDM) techniques, this leads to a slower update rate as only one transmitter is allowed to send at a time which limits the number of location updates possible in a given time interval [21, 189] (this phenomenon with its limitations is described in depth in Section 5.2). Therefore, this is not an efficient solution for gait analysis applications for which simultaneous multiple transducers positioning is a prerequisite. Some methods for overcoming the multiple transducer access problem have been proposed using broadband transducers [16, 19, 28, 30, 46, 190–192] that are more expensive than narrowband transducers.

In general, all these systems obtain more precise location information when a transducer is stationary as when it is in motion, there is a frequency shift of the transmitted ultrasonic (US) signal known as the Doppler effect which results in an inaccurate estimation of the time-of-flight (TOF) and, thus, the transducer's position. Therefore, for high-precision tracking, estimating and compensating for this effect is a prerequisite. Generally, most existing systems, e.g., [16, 47, 51, 58, 97–101] use a bank of correlators to estimate and compensate the Doppler shift, which results in higher system cost and complexity (this phenomenon with its limitations is described in depth in Section 5.4.1).

In the previous chapter, a steepest descent optimization approach for precise 3D positioning using an OFDM signal was proposed. This algorithm offered advantages over the traditional lateration algorithm by compensating errors in distance measurements of the receivers corresponding to one complete cycle of the

[1]For an active mobile architecture the tracking or locating transducer(s) is the transmitter(s) and for a passive mobile architecture it is the receiver(s).

transmitted signal and overcoming the configuration related problem of the lateration algorithm. In addition, the introduced OFDM-based TOF approach provided higher accuracy than the traditional chirp-based cross-correlation approach with less complexity. Along with these advantages, it was mentioned that the OFDM signals have the capability to locate multiple transducers simultaneously and, easily estimate and compensate the Doppler shift.

In this chapter, with gait analysis in mind, the work discussed in the previous chapter is extended to simultaneous multiple transducer positioning and then, a Doppler shift estimation and compensation technique for tracking a moving transducer in a complex pendulum model is proposed. The proposed methods for simultaneous multiple transducers positioning and tracking are evaluated experimentally and the tracking results of various pendulum trajectories of a transducer are compared with a commercially available optical MCS, Vicon, and it is shown that the proposed system has the same order of precision but incurs less cost and complexity than the Vicon MCS.

The rest of this chapter is organized as follows: Section 5.2 describes the limitations of existing narrowband-based UPSs for multiple transducer positioning followed by an efficient solution for it; the performance of the proposed system evaluated through a Matlab simulation is presented in Section 5.3; Section 5.4, describes the limitations of existing narrowband US signals for Doppler shift estimation and then presents a new Doppler shift detection and compensation technique; Section 5.5 describes the experimental procedure for determining the accuracy of the proposed systems for multiple transducer positioning, which is followed by a description of an experiment involving tracking a transmitter in a complex pendulum model with the proposed and Vicon systems; the experimental results are discussed in Section 5.6; and Section 5.7 presents the conclusions drawn from this study.

5.2 Multiple Transducer Positioning

Gait analysis deals with the simultaneous positioning of multiple markers in an optical-based system. When an UPS is used for gait analysis, it must have the capability to deal with multiple transducers which can be achieved by a resource management system. However, when existing UPSs use narrowband signals for multiple transducer positioning in either active or passive mobile architecture, they suffer from the following problem.

5.2.1 Limitations of Narrowband US Signal in Multiple Transducer Positioning

All narrowband-based UPSs, transmit either a single tone or narrowband chirp signal for multiple transducer positioning either in active or in passive mobile architecture and, when multiple transmitters transmit the same signal, these signals interfere with each other at the receiving end. In a general sense, there is a simple solution to this multiple access problem of narrowband-based UPSs, as described below.

The solution is to share the whole available bandwidth among the multiple transmitters at different time slots, that is, transmit the same pulse from collocated transmitters at different times, i.e., one after another with a proper interval to avoid signal interference at the receiving end. This approach is known as the TDM technique. The major problem of this approach is its slower update rate, that is, as only one transmitter is allowed to send at a time, the number of location updates possible in a given time interval is limited. Within this longer update time, the transducers (transmitter for the active mobile case and receiver for the passive mobile case) may move significantly from their previous positions.

Therefore, as a solution to eliminate the abovementioned problem of both architectures, in the following section, an option using the OFDM signal is proposed.

5.2.2 Proposed Solution for Multiple Transducer Positioning

In Section 4.2.1, Chapter 4, an OFDM signal for single transducer positioning in an active mobile architecture was introduced. This approach took advantages of the OFDM equalization technique for noise reduction, transducer effect elimination and also reduced the computational complexity of the correlation-based positioning system. The main advantage of the OFDM signal is that all sub-carriers are orthogonal and dedicated to a single source unlike in frequency division multiplexing (FDM). By using this orthogonal property, simultaneous multiple transducer positioning is possible in an OFDM-based system while maintaining orthogonality. The following section presents pictorial and mathematical representations of the OFDM technique for simultaneous multiple transducer positioning.

5.2.2.1 OFDM signal for multiple transducer positioning

The OFDM based multiple transducer positioning system works in a three stage process. In the first stage, all the available orthogonal frequency components are placed serially as shown in Figure 5.1 where there are nine orthogonal frequency components ($f_1, f_2, \cdots, f_9$). Although only nine sub-carriers are illustrated, the number of sub-carriers may be higher depending on the bandwidth. For example, the total number of sub-carriers in the OFDM based single transducer positioning system proposed in the previous chapter was 101.

The second stage involves converting all the frequency components into a number of shorter parallel sub-sets. In active and passive mobile architectures, the number of sub-sets is equal to the number of transducers to be localized and the number of transducers to be used as reference points respectively. For example, continuing on from the example shown in Figure 5.1, suppose it is required to localize three transducers in an active mobile architecture or three transducers are to be used as reference points in a passive mobile architecture. This means that the number of sub-sets will be three in both cases where each of which contains three frequency components (shown in the Figure 5.1).

In the final stage, using all the frequency components contained in each sub-sets, an OFDM signal is generated for each transmitter (indicated by the dash circle in Figure 5.1). Though all the OFDM signals are transmitted in parallel from the individual transmitter, the receivers received these signals without any interference as they use different subcarriers, i.e., non-overlapping frequency components.

The number of sub-sets is equal to the number of transducers to be localized in an active mobile architecture and number of transducers to be used as reference points in a passive mobile architecture. Therefore, a passive mobile architecture offers better scalability because, when using only three reference points (minimum), it would be able to calculate any desired number of transducers within the operating environment as the wireless channel is not dependent on the number of devices to be localized.

This phenomenon can also be described mathematically as described below.

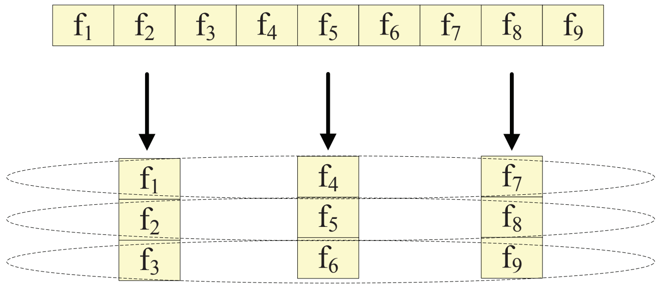

Figure 5.1: Frequency allocation in an OFDM system for positioning in active and passive mobile architectures.

5.2.2.2 Mathematical model of OFDM signals for multiple transducer positioning

In Section 4.2.2, Chapter 4, the mathematical model of an OFDM signal for single transducer positioning was presented. In this section, this model is modified for multiple transducer positioning, for both active and passive mobile architectures, by introducing a frequency separation between two successive sub-carriers while maintaining orthogonality. This design process explains how orthogonal frequency components are distributed to the transmitters utilizing the available bandwidth. Recalling equation (4.3), if the sampling frequency of a signal is F_s and its length is N samples, the frequency resolution is $r_s = \frac{F_s}{N}$. Letting the lower carrier of the desired OFDM signal be f_l and the upper carrier f_u, i.e., a bandwidth of $W = f_u - f_l$. As the frequency resolution is r_s, the available orthogonal frequency components are:

$$f = \{f_l, f_l + r_s, f_l + 2r_s, \cdots, f_u\} \tag{5.1}$$

Now, if a represents the number of transmitters, the frequency domain OFDM signal distributed to the transmitters is given by:

$$X_{a,i,c}[n_{a,i,c}] = \begin{cases} A[n_{a,i,c}]e^{j\theta[n_{a,i,c}]} & \text{where } n_{a,i,c} = \frac{f_l}{r_s} + \frac{\Delta f(i-1)}{ar_s} + \frac{\Delta f(c-1)}{r_s} \\ A[n_{a,i,c}]e^{-j\theta[n_{a,i,c}]} & \text{where } n_{a,i,c} = N + 1 - \left(\frac{f_l}{r_s} + \frac{\Delta f(i-1)}{ar_s} + \frac{\Delta f(c-1)}{r_s}\right) \\ 0 & \text{elsewhere} \end{cases} \tag{5.2}$$

where c is the number of frequency components present in each OFDM signal. The value of Δf is given by:

$$\Delta f = ar_s \tag{5.3}$$

For each a, i is given as:

$$i = 1, 2, \cdots, a \tag{5.4}$$

and the value of c is given as:

$$c = 1, 2, \cdots, \frac{W}{\Delta f} \tag{5.5}$$

For the active mobile case, equation (5.3) states that, for a fixed frequency resolution, the more transmitters to be localized, the greater the frequency separation (Δf) between adjacent sub-carriers needed. However, according to equation (5.5), there are fewer frequency components which means that when the OFDM signal becomes a single tone signal, the introduced OFDM based TOF estimation in Chapter 4, Section 4.3 will not work because the proposed method requires at least two frequency components to produce the largest peak at the beginning of the OFDM signal. Although, using a single frequency component, one could use cross-correlation for TOF estimation, but this will not only increase the computational complexity but also the overall error of the system. For example, if an active mobile architecture based system uses [35-45] kHz/10 ms OFDM signal for transmission, it can localize a maximum of 50 transducers using the proposed OFDM-based TOF estimation technique (with higher accuracy and lower complexity) and 101 transducers using the traditional cross-correlation based TOF estimation technique (with lower accuracy and higher computational complexity). On the contrary, a passive mobile architecture would be able to localize any desired number of transducers as the wireless channel is not dependent on the number of transducers to be localized in this approach.

In summary, the signal design process for multiple transducers positioning can be explained through the pseudo-code:

Algorithm 2: Pseudo code of the narrowband OFDM signals for multiple transducers positioning

- Set,f_l, f_u, N
- Calculate r_s
- Calculate Δf
- **for** $a = 1 : \frac{\Delta f}{r_s}$ **do**

    for $i = 1 : a$ **do**

        for $c = 1 : \frac{W}{\Delta f}$ **do**

        Calculate $n_{a,i,c}$

        end for

    end for

end for

To demonstrate the performance of the proposed method for simultaneous multiple transducer positioning, a Matlab simulation was performed which is described below.

5.3 Simulation Results

A customized environment was simulated in Matlab to evaluate the performance of the proposed UPS. In this simulator, in a virtual 3D rectangular room, five reference points were considered and 50 transducers were introduced with the aim of localizing these using both passive and active mobile architectures. The true positions of the target transducers were known. The location of the five reference points were as follows:

$$\mathbf{P} = \begin{bmatrix} -30 & -30 & 0 \\ 0 & 0 & 0 \\ 30 & -30 & 0 \\ -30 & 30 & 0 \\ 30 & 30 & 0 \end{bmatrix}$$

The simulation was performed in a noisy multipath environment (5 paths at random positions) with reflection coefficients of 0.9 to 0.5, and the corresponding attenuation of the signal was calculated using the formula described in Chapter 3, Section 3.6. In both active and passive cases, [35-35] kHz/10 ms OFDM signals were used where frequency components were allocated to the reference points in the passive mobile architecture and to the transducers to be localized in the active mobile architecture according to the procedure described in Section 5.2.2.2. The position of the target transducers were calculated in both mobile architectures using the steepest decent optimization algorithm described in Chapter 4,

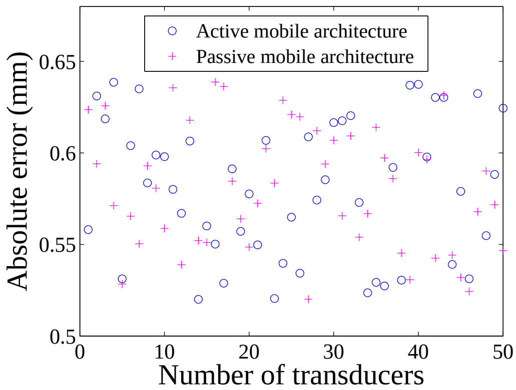

Figure 5.2: Absolute location errors of the proposed method in both active and passive mobile architectures.

Section 4.4 using the TOF information calculated using the procedure described in Section 4.3, Chapter 4. The absolute location errors (calculated using the Euclidean distance between true and estimated positions) of the target transducers in both architectures is shown in Figure 5.2 which shows that the accuracy for both architectures is almost the same. But it is important to note that, in an active mobile architecture it was not possible to localize more than 50 transducers as frequency components were limited whereas in a passive mobile architecture it was possible to localize any desired number of transducers within the operating environment as the wireless channel did not depend on the target transducers.

This section describes how a narrowband-based UPS can utilize the whole effective bandwidth for multiple transducer positioning. The method is also valid for broadband UPSs. This proposed method is then extended to tracking in the following section to provide the required functionality for a gait analysis system.

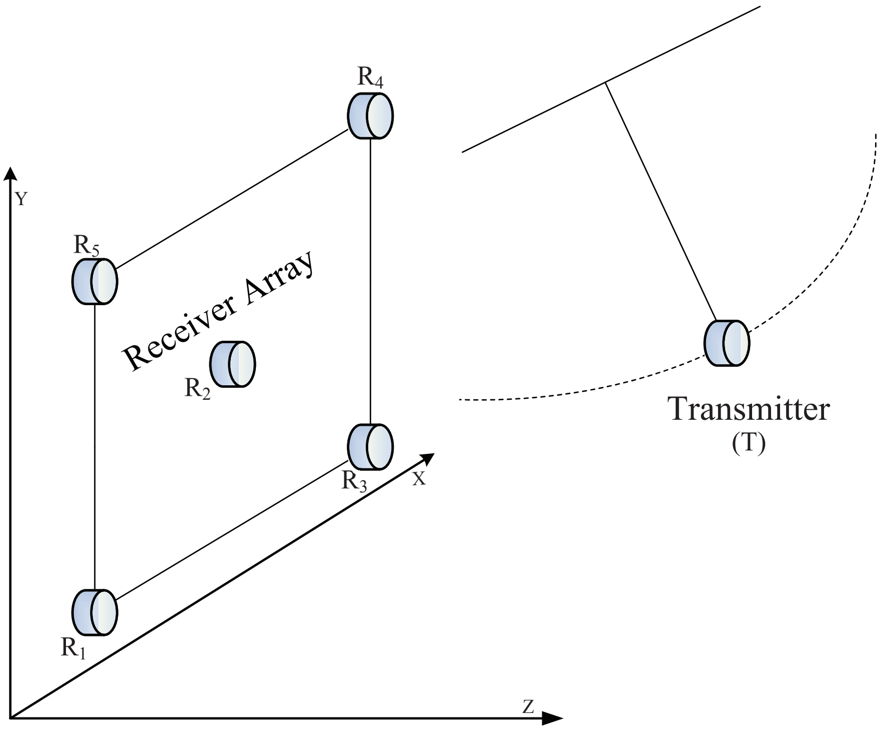

Figure 5.3: Tracking of a transmitter in a complex pendulum model.

5.4 Ultrasonic Tracking

To represent the operation of a tracking system, consider Figure 5.3 in which, in an active mobile architecture, a single transmitter (T) is moving with velocity v_T in an area deployed with R_i receivers, where $i = 1, 2, \cdots, 5$, and we are interested in tracking it. Let T transmit an OFDM signal with the frequency f_T (which contains multiple orthogonal frequency components, i.e., multiple sub-carriers) measured by receiver R_i. As T moves within the coverage area of R_i, it is observed that f_T is Doppler-shifted by Δf_{ds_i} due to the movement associated with T. The Doppler shift is the apparent frequency difference between the frequency at which the signal leaves the transmitter (T) and that at which it arrives at a receivers (R_i) with its amount dependent on the relative motion between them. Now, the apparent frequency due to the Doppler shift at R_i is given by:

$$f_{r_i} = f_T + \Delta f_{ds_i} \tag{5.6}$$

Due to this frequency shift, there will be an error at each calculated position of T. After estimating the Doppler shift on the received signal and then compensating, the final position of T can be easily calculated using the proposed steepest decent optimization algorithm described in Chapter 4, Section 4.4. Once the correct position of T is known, the velocity of T (v_T) can be calculated by knowing the system update rate (i.e., how many positions of T are calculated per second) given by:

$$v_T = \frac{d_T}{t_u} \tag{5.7}$$

where d_T represents the distance between two consecutive positions of T and t_u the update rate.

Therefore, to calculate the accurate position of T and its velocity (v_T), it is necessary to estimate the Doppler shift at R_i and then compensate. The following section describes how the existing narrowband-based UPSs suffer when estimating the Doppler shift and then a solution for estimating and compensating the Doppler shift using a narrowband OFDM signal is proposed.

5.4.1 Limitations of a Narrowband Signal for Doppler Shift Estimation

Of course, all positioning systems work better with static rather than dynamic positioning of an object. In a dynamic case, due to the Doppler shift, the performance of a system is dramatically degraded. The more the Doppler shift the

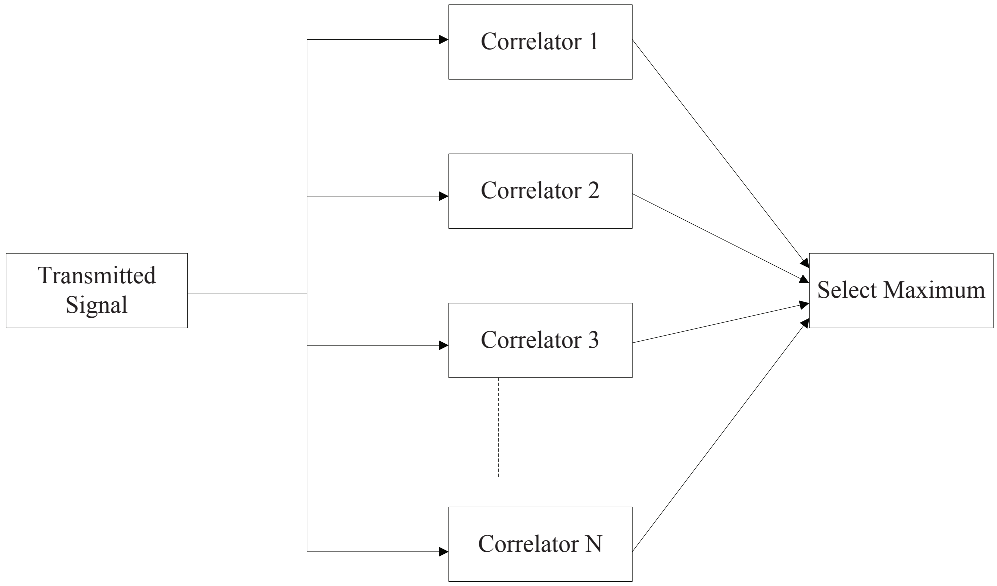

Figure 5.4: Matched filter-based Doppler shift estimation technique.

lower the system performance. For dynamic object positioning, most of the existing systems e.g., [16, 47, 51, 58, 97–101] use a matched filtering technique where a bank of correlators are created by shifting the frequency of the transmitted signal to different values and then each signal is cross-correlated with the received signal. The branch at which the maximum correlation peak is obtained represents the Doppler shift. This approach is illustrated in Figure 5.4. The disadvantage of this type of method is that it requires a large number of correlators which not only increases computational complexity but the system cost. Therefore, in the following section, a method for estimating the Doppler shift using a narrowband OFDM signal which does not require any matched filter and also does not need to transmit a separate signal as does the broadband positioning system [51] is proposed. As an OFDM signal is sensitive to frequency shifting [172, 193–195], it is necessary to know how it is affected before performing the proposed Doppler shift estimation and compensation technique.

5.4.2 Effect of Doppler Shift on an OFDM Signal

In the previous chapter it was mentioned that OFDM transmission allows the sub-carriers to be as close as theoretically possible as the spectrum of each sub-carrier spectrum overlaps with, but remains orthogonal to, the others. This means that, all the other sub-carriers spectra are zero at the maximum of each sub-carrier spectrum and all the sub-carriers have an integer number of cycles per period when considered from a frequency domain and time domain perspective (shown in Chapter 4, Figure 4.2(a) and Figure 4.2(b)) respectively. However, with a small change in sub-carrier frequency due to the Doppler shift, the orthogonality of an OFDM signal is lost. This results in a non-zero spectral value of the sub-carriers at the maximum of each sub-carrier spectrum and the corresponding sinusoid of each sub-carrier no longer have an integer number of cycles within a particular time interval when considered from the frequency domain and time domain perspective (shown in Figure 5.5(b) and Figure 5.5(b)) respectively. Due to this non-orthogonal characteristic of the OFDM signal, inter sub-carrier interference (ICI) occurs. Therefore, the performance of the system is reduced which is demonstrated in Section 5.4.4 with numerical results. To improve the performance of the system and retain the orthogonality of the received OFDM signal, it is necessary to estimate the Doppler shift and then compensate. In the following section, a Doppler shift estimation and compensation technique is proposed.

5.4.3 Doppler Shift Estimation and Compensation Technique

In this section, a new Doppler shift estimation and compensation technique is proposed. In it, unlike in the matched filter-based Doppler shift estimation method

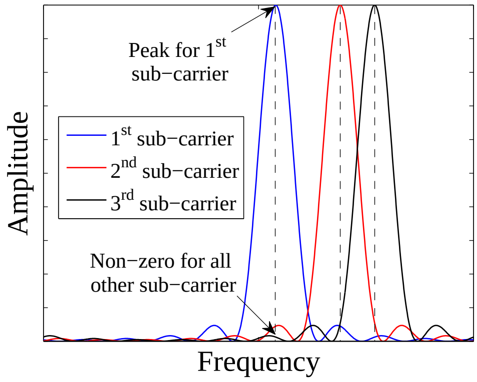

(a)

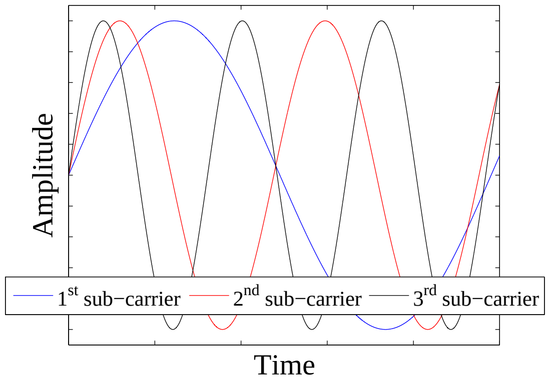

(b)

Figure 5.5: Visulization of three non-orthogonal sub-carriers of an OFDM signal in: (a) frequency domain; and (b) time domain.

described in Section 5.4.1, the Doppler shift is estimated by introducing a pilot carrier, with a significantly increased amplitude compared with those of the other sub-carriers, in the OFDM signal described in Section 5.2.2.2. Then, the Doppler shift is compensated in the received signal to retrieve the orthogonality of the OFDM signal which facilitates channel equalization and noise cancelation. The procedure for estimating and compensating the Doppler shift is described below.

Initially, in the designed OFDM signal described in Section 5.2.2.2, one of the operating frequencies is taken as the pilot carrier (f_p) in equation (5.2) (i.e., $f_p \epsilon [f_l, f_u]$) that has a higher amplitude than the other sub-carriers and is transmitted from transmitter T (in Figure 5.3). When T is moved from its initial position, a Doppler shift is introduced in the received signal, resulting in the position of the pilot carrier being shifted from that location during transmission.

To estimate the Doppler shift introduced in the received signal due to the movement of T, the received signal is padded with zeros so that the frequency resolution becomes 1 Hz, whereby each frequency index in the frequency domain signal represents the corresponding frequency; for example, frequency index 40000 represents 40000 Hz.

Now, if the frequency of the pilot carrier of the transmitted signal is f_p Hz and, in the received signal, it is changed to f_{ds} Hz due to the Doppler shift, the Doppler shift is given by:

$$\Delta f_{ds} = f_{ds} - f_p \tag{5.8}$$

Using this information, a new replica of the received signal is generated in the frequency domain as:

$$f_{r_{\text{new}}} = f_r - \left(\frac{f_r}{f_{ds}}\right) \Delta f_{ds} \tag{5.9}$$

where f_r is the frequency of the original received signal. This signal is converted to a time domain signal for individual received signal and the procedure described in Section 4.3, Chapter 4 is applied to estimate the TOF. Now, using the TOF information of each received signal, the position of T is calculated using the procedure described in Section 4.4, Chapter 4 at each update rate and velocity using equation (5.7).

To visualize the proposed Doppler shift estimation and compensation technique an example is demonstrated below.

5.4.4 Understanding of the OFDM-based Doppler shift Estimation and Compensation Technique using an Example

To maintain consistency with the experimental data, initially, a [35-45] kHz/10 ms OFDM signal with a pilot carrier and a separation of 200 Hz was transmitted at a sampling rate of 1 Msample/s. The frequency of the pilot carrier was chosen as 40 kHz. This sub-carrier is given a power of three times those of the other sub-carriers as shown in Figure 5.6(a). The transmitted OFDM signal was then received by a receiver with a 100 Hz Doppler shift. The aim is to estimate this Doppler shift and then compensate.

The length of the received signal was increased to 1000000 samples (the same as the sampling frequency) by being padded with zeros and the frequency resolution becomes 1 Hz, as shown in Figure 5.6(b) in which it is seen that the pilot carrier's frequency in the received signal shifted to 40.1 kHz (f_{ds}) (which was 40 kHz (f_p) during transmission). Therefore, the Doppler shift was calculated by taking the pilot's carrier frequency difference between the transmitted and received signals as:

$$\Delta f_{ds} = f_{ds} - f_p = 40100 - 40000 = 100 \text{ Hz}$$

Now, to compensate for this Doppler shift, a new replica of the received signal was generated according to equation (5.9). The frequency spectrum of the Doppler shift compensated received signal is shown in Figure 5.6(c) which shows that the frequencies line up with those of the transmitted signal.

To demonstrate the improvement in the signal after compensating the Doppler shift, a Doppler shift versus Doppler shifted received signal's correlation signal-to-noise-ratio (SNR) plot is shown in Figure 5.7. This Figure indicates that the correlation SNR decreased when the Doppler shift increased and, when the Doppler shift was compensated, the correlation SNR was constant at the same level as when the Doppler shift was 0 Hz.

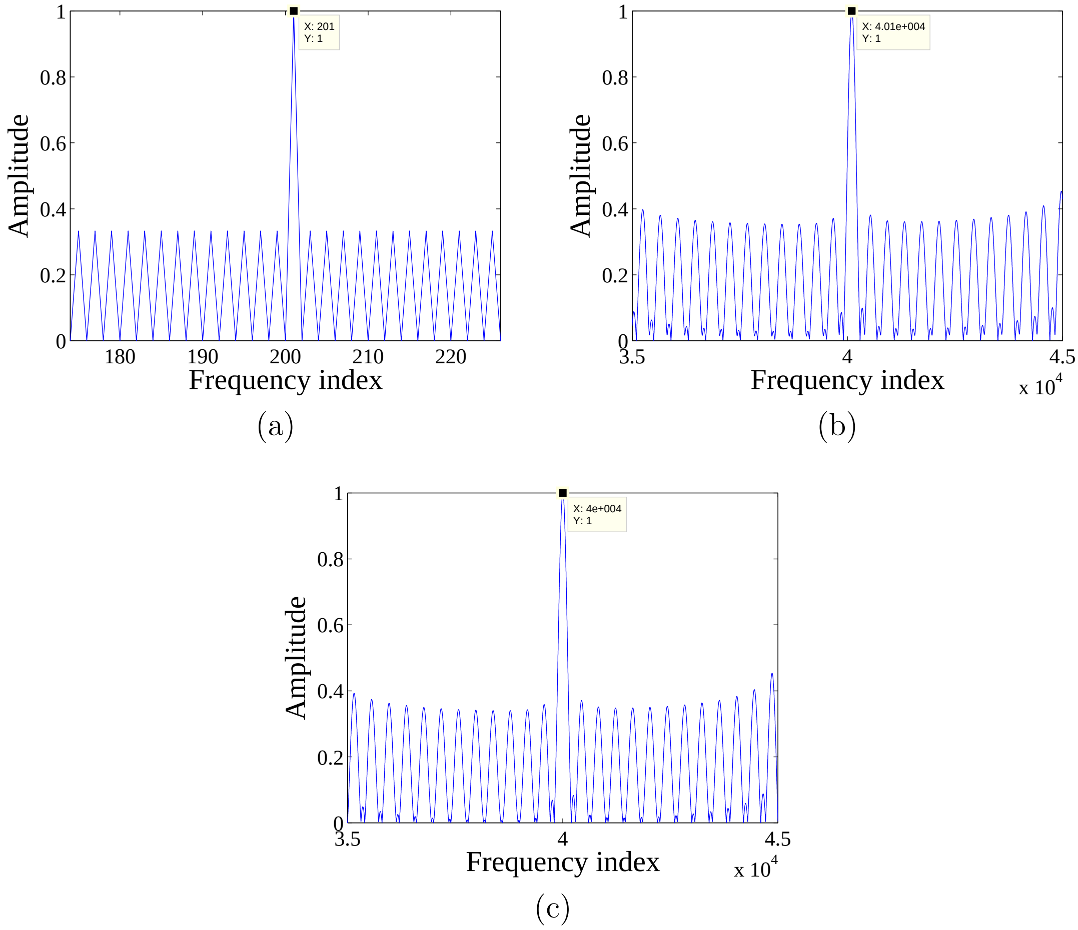

Figure 5.6: Visualization of proposed Doppler shift estimation and compensation technique: (a) frequency spectrum of transmitted signal which indicates the amplitude of a particular sub-carrier (pilot carrier) three times higher than other sub-carriers; (b) frequency spectrum of the received signal after Doppler shift; and (c) frequency spectrum of the received signal after compensating for the Doppler shift.

5.5 Experimental Procedure

To evaluate the proposed method for gait analysis, a set of experiments was conducted using the same devices as those used for the experiments in Chapter 3 and a Vicon optical MCS, according to the procedures described below.

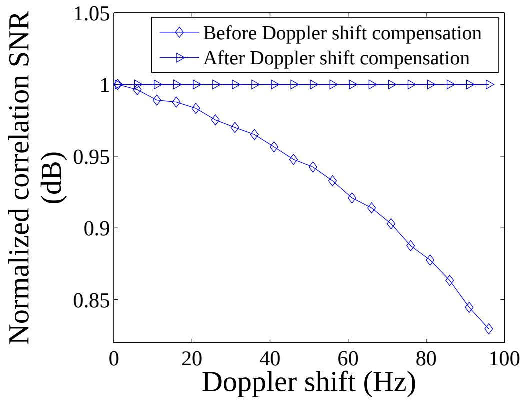

Figure 5.7: Effect of Doppler shift on signal's SNR.

5.5.1 Positioning of Multiple Transducers

To evaluate the proposed OFDM-based multiple transducer positioning system described in Section 5.2.2, two separate experiments were conducted for both active and passive mobile architectures where the number of transducers to be localized and number of reference points was five. The configuration of the experimental setup was as shown in Figure 4.5, Chapter 4 except the number of transducers to be localized were five instead one. The target transducers were separated by a fixed offset and moved at 20 different locations inside a 20×20×20 mm volume, and the true positions were measured using a Vernier scale with a precision of 0.02 mm. In both cases, [35-45] kHz/ 10 ms OFDM signals were used where frequency components were allocated to the reference points in a passive mobile architecture and to the transducers which to be localized in an active mobile architecture according to the procedure described in Section 5.2.2.

To demonstrate the improvement in accuracy provided by the proposed approach, the positions of the target transducers were also calculated by the traditional cross-correlation-based multilateration algorithm for both architectures using [35-45] kHz/10 ms chirp signal through TDM technique, i.e., chirp signals were transmitted at different times from the transmitters to avoid the signal interference which reduces the positioning update rate.

5.5.2 Test Protocol for Tracking

Once, the experiments for positioning multiple transducers were completed, a set of experiments was performed to track a moving transducer in an active mobile architecture to prove that the proposed system could be used for gait analysis. Though the tracking could also be performed using a passive mobile architecture, the active mobile architecture was chosen to provide a fair comparison with the traditional approach. In a passive architecture the traditional approach needs to use the TDM technique even for tracking a single transducer whereas for an active architecture it does not. For tracking, a physical pendulum was used to test the accuracy of the proposed US system when compared with the Vicon system. A pendulum was chosen due to the predictable behaviour of the pendulum swing and its similarity to the motion of body parts especially during gait analysis. As the Vicon system offers sub-millimeter accuracy, the results obtained from the Vicon system were considered to be a suitable ground truth. In the following section a brief description of the Vicon system is given.

5.5.2.1 Brief overview of the Vicon system

The Vicon system consists of a number of cameras, with a near-infrared (NIR) strobe light, which is reflected from the markers placed on the tracking object, attached to each. To track the individual positions of the markers, image processing is performed at each camera. The Vicon system uses a form of triangulation algorithm to determine the exact locations of the markers attached to the object.

The Vicon system used for this experiment consists of 10 Bonita cameras, each of which has a resolution of one megapixel (1024×1024 pixels) with a 82.7°×66.85° field of view. An Ethernet hub supplies power and exchanges data using a single gigabit Ethernet cable to each camera and a laptop or PC is connected to the hub to communicate with the cameras through TCP/IP. To extract the camera data within the capture volume, a software package called "Tracker" is installed on the computer. The extracted data provides information regarding the position of the tracked object and then user code is written to log, display or transmit it as desired.

Calibration

The calibration process in the Vicon system provides the capture volume to the system, enabling "Tracker" to determine the positions, orientations and lens properties of all the cameras in the system, and produce 3D data. Throughout this process, a calibration parameters file containing the calibration settings and image threshold data specified for each camera is created by "Tracker" which is used when data from these cameras is processed. A calibration object of known geometry with five active markers, called a wand, is supplied by the Vicon system and allows calibration when moved through the capture volume in random trajectories until an adequate number of frames (1000 frames by default) has been observed by each camera. This process is completely automated and requires only a few minutes, apart from the time required to move the wand.

After completing the camera calibration process, it is necessary to determine the origin of the capture volume and its orientation (x, y and z axes) using "Tracker" so that the tracking object is displayed in the right way in "Tracker's" work space. In the experimental case, the origin was set by placing the wand flat on the ground in roughly the center of the indoor test facility and aligning it parallel to the camera-mounting truss structure.

Software Development Kit

The information contained in the Vicon DataStream is generally accessed by the Vicon DataStream Software Development Kit (SDK) and the function calls within the SDK allow users to connect to and request data from the Vicon DataStream. The SDK is delivered as shared libraries (dynamic-link libraries (DLLs)) on Windows. These libraries and supporting files are required to be copied alongside the client executable for running.

The object must be defined in “Tracker” in order to access the state data and its motion data must be captured as a rigid, asymmetrical arrangement of at least 3 markers which are selected using the mouse in “Tracker’s” graphical user interface. The object is specified with a name which user code can reference in an SDK function call when the object’s position is requested. The position data generally provides floating-point numbers with 64-bit precision.

Camera Mounting

An important consideration in the Vicon system is the mechanical stability of the cameras as a small shift in position can have a big impact on system accuracy. In the experiment, a robust tri-truss structure was used to support the cameras which is capable of carrying much greater loads than required (up to several hundred kg point load), but assures low deflections. This structure consisted of a span of aluminium triangular truss elements to which the cameras were fitted using aluminium clamps. Figure 5.8 shows a Bonita 10 camera clamped to the truss structure.

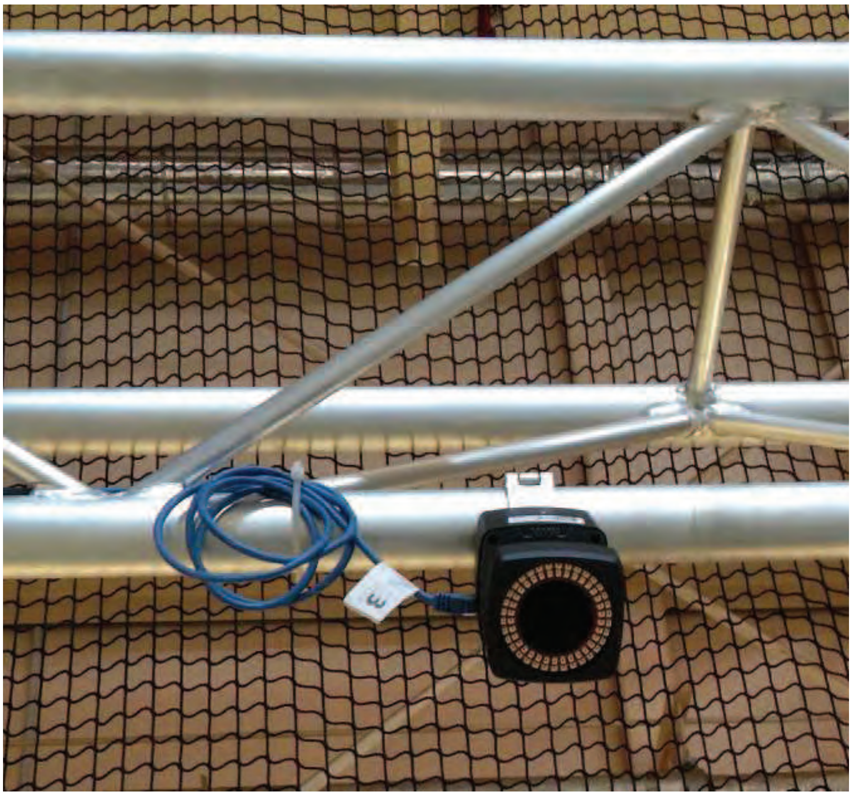

Figure 5.8: Bonita 10 camera clamped to the truss structure.

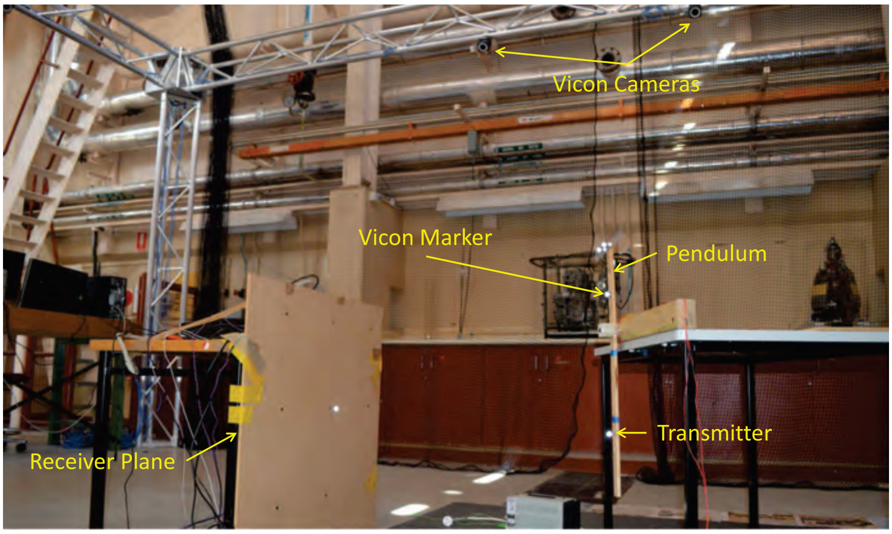

Figure 5.9: Experimental setup for both the Vicon and US systems.

5.5.2.2 Experimental procedure and data collection

The experimental setup for the Vicon and proposed systems is shown in Figure 5.9. A pendulum assembly was placed in the center of the Vicon's field of view so that the markers on it could be viewed by a sufficient number of cameras. Although at least 3 markers are required for the Vicon system to define an object, in this experiment 4 markers (each of 12 mm diameter) placed on the pendulum assembly in an "L" shape were used, one of which was the desired tracking point (the bottom marker in Figure 5.9) which was attached to the wooden pendulum approximately 33 cm from the base which was attached securely to a table. Then, the pendulum's bottom point was manually pulled away from the vertical to approximately 90° and gently released so that the pendulum swung in a vertical plane. Data was captured by the Vicon system from just before the pendulum started moving at a frame rate of 100 Hz using the procedure previously described.

In the US setup shown in Figure 5.9, a transmitter was placed at a known offset from the bottom Vicon marker and 5 receivers (although 9 receivers are visible in Figure 5.9, only the central and corner receivers were used) were placed on a plane approximately 100 cm from the pendulum assembly and a [35-45] kHz/10 ms OFDM signal with a sub-carrier separation of 200 Hz was used for transmission. During the Vicon system's data capture, the transmitter continuously transmitted the OFDM signals with a separation of 10 ms between two successive signal bursts. All the devices (i.e., transmitter, receiver, DAQ and thermometer) used in this experiment were the same as those used for the experiments in Chapter 3, Section 3.7.

5.5.2.3 Data processing

Although the data was simultaneously captured for both the US and Vicon systems, it was not possible to place the tracking marker at exactly the same position as the transmitter during experimentation as it would have blocked transmission of the US signal. Hence, it was placed at a known offset from the transmitter which was then compensated for during later processing. As the Vicon system provided coordinates with respect to its origin (calculated using the wand) and the US system with respect to the location of the central receiver (R_2), a method for transforming the former to the latter was required. To accurately achieve this transformation, an additional marker was placed at a known offset from the position of R_2 and its coordinates were also calculated using the Vicon system (Figure 5.9). Of course, during the positioning of the additional marker it was confirmed that the receivers (used by the US system) were completely parallel to the Vicon's coordinate plane. The known offset was compensated for during later processing. Now, if the tracked marker's coordinates after compensation are $((x_{v1}, y_{v1}, z_{v1}), ..., (x_{vn}, y_{vn}, z_{vn}))$ and the coordinates, after compensation, of the marker placed beside R_2 are (x_v, y_v, z_v), the transformed Vicon coordinates will be $((x_{v1} - x_v, y_{v1} - y_v, z_{v1} - z_v)..., (x_{vn} - x_v, y_{vn} - y_v, z_{vn} - z_v))$. The markers' height is also compensated for during this transformation. As the Vicon system and the US system might start sampling at different times, and they sample at every 10 ms and 20 ms respectively, a method for synchronizing the two sets of data was required. To achieve this, multiple data were captured for both systems simultaneously and checked manually for the sample when the pendulum began moving. The set of data where both systems captured data closest to the time when the pendulum movement began was chosen for analysis.

In the case of US positioning, the OFDM-based TOF estimation technique described in Section 4.3, Chapter 4 was used to estimate the distances from the moving transmitter to the receivers after compensating the Doppler shift using the procedure described in Section 5.4.3. The steepest descent optimization algorithm described in Section 4.4, Chapter 4 was used to estimate the 3D positions of the transmitter.

As already stated in Section 5.2.2, the simultaneous positioning of multiple stationary transmitters with sub-millimeter accuracy is possible (results shown in Section 5.6.1) using the orthogonal nature of an OFDM signal, hence, the proposed system will be able to simultaneously track multiple transmitters once they are connected to the system. However, in this implementation, the tracking is confined to a single transmitter.

To demonstrate the improvement in accuracy provided by the proposed approach, tracking of the transmitter was also conducted using the traditional chirp-based cross-correlation method using the multilateration algorithm.

5.6 Results and Analysis

The results obtained from the above experiments using the proposed methods, the Vicon system and the traditional method are discussed and compared.

5.6.1 Multiple Transducer Positioning

After completing the experiments in both active and passive mobile architectures for multiple transducer positioning, the position of each transducer was calculated for the both proposed and traditional methods. The combined errors of the x, y and z directions in the calculated locations of all transducers using the proposed and traditional approaches in both architectures are shown in Figure 5.10 and Figure 5.11 respectively and the standard deviations of these errors in each direction are shown in Table 5.1.

Table 5.1: Standard deviations of errors in the measured locations of the transducers in both active and passive mobile architectures (mm).

Number of Transducer	Architecture											
	Active						Passive					
	Proposed			Traditional			Proposed			Traditional		
	x	y	z	x	y	z	x	y	z	x	y	z
1	0.3117	0.3240	0.3145	9.8011	9.7268	1.5510	0.3245	0.3195	0.3176	9.8011	9.7268	1.5510
2	0.3420	0.3085	0.3042	9.7159	9.6940	1.5894	0.3183	0.3164	0.3206	9.7159	9.6940	1.5894
3	0.3260	0.3045	0.3293	9.6434	9.9123	1.5851	0.3142	0.3156	0.3276	9.6434	9.9123	1.5851
4	0.3350	0.3325	0.3321	9.3386	9.9555	1.5323	0.3203	0.3141	0.3245	9.3386	9.9555	1.5323
5	0.3261	0.3329	0.3084	9.8633	9.9687	1.5429	0.3165	0.3273	0.3240	9.8633	9.9687	1.5429

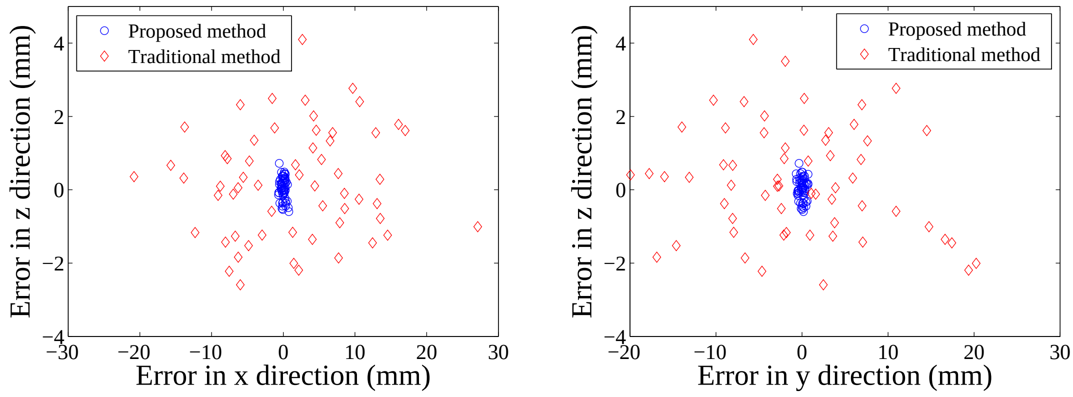

Figure 5.10: Errors in location of the transducers from the proposed and traditional methods in an active mobile architecture.

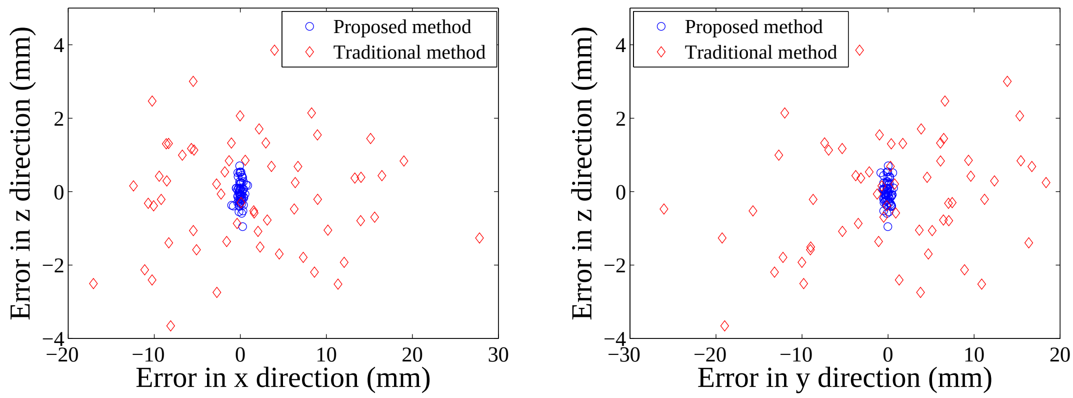

Figure 5.11: Errors in location of the transducers from the proposed and traditional methods in a passive mobile architecture.

These results show that the precision obtained using the proposed method was significantly higher and provided the sub-millimeter accuracy required for many medical applications. It should be noted that the calculated location errors for the traditional TDM-based technique for both active and passive mobile architectures are almost the same. This is because the targets were static and thus there was no impact on the system performance by the motion of the targets. However, for the positioning of moving targets, the system performance for both architectures will be different [69] (as discussed in Chapter 2, Section 2.2). The proposed method did not suffer from the lower positioning update rate like the TDM-based traditional method. It is also important to note that, the scalability of the passive mobile architecture was not bounded by the frequency components like the active mobile architecture.

In summary, the OFDM-based technique for multiple transducer positioning has the following advantages along with those provided by the OFDM-based TOF estimation technique over the traditional chirp-based cross-correlation technique and the steepest descent optimization approach over the traditional lateration algorithm.

1. Multiple transducers can be simultaneously localized without the update rate being affected as it is in the traditional TDM technique.

2. Without introducing broadband transducers, the proposed method provides an efficient solution to the problem of simultaneously locating multiple transducer using the orthogonal property of an OFDM signal.

5.6.2 Tracking

Two different experiments were conducted to evaluate the proposed method for tracking in the active mobile architecture. In the first, the pendulum assembly was placed approximately parallel to the receiver plane and, in the second, at an angle of $\approx 45^\circ$ to the receiver plane. Although the data were captured for a number of pendulum cycles, the results presented here are for only a single cycle, with the trajectories obtained using the proposed method and the Vicon system shown in Figure 5.12.

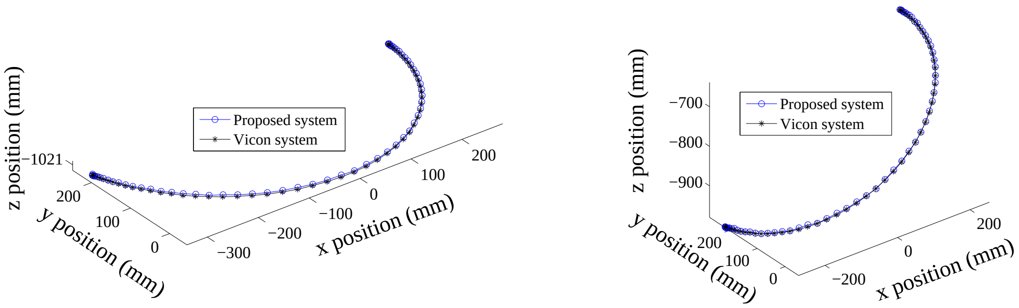

Figure 5.12: Pendulum tracks estimated by proposed method when transmitter placed: (a) almost parallel to the receiver plane; and (b) at angle of ≈ 45° to the receiver plane.

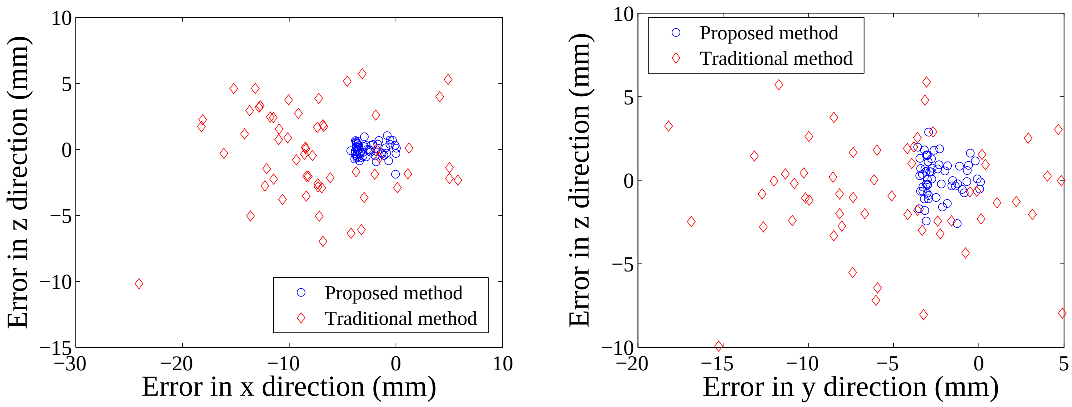

Figure 5.13: Errors in locations of the transmitter using the proposed and traditional methods when the transmitter was placed approximately parallel to the receiver plane.

The errors in the calculated locations of the transmitter in each x, y and z direction for both experiments when using the proposed and traditional methods are shown in Figure 5.13 and Figure 5.14 respectively. These plots clearly show the improved precision achieved by the proposed steepest descent optimization algorithm after compensating for the Doppler effect.

To demonstrate the performance of the proposed Doppler effect compensation, Figure 5.15 shows the absolute location errors (calculated using the Euclidean distance between true and estimated positions) with respect to the velocity of the

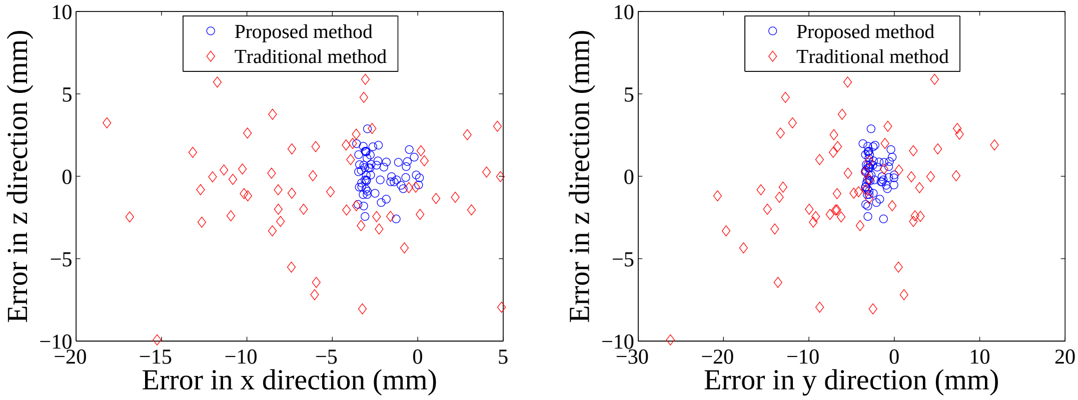

Figure 5.14: Errors in locations of the transmitter using the proposed and traditional methods when the transmitter was placed at an angle of ≈ 45 ° to the receiver plane.

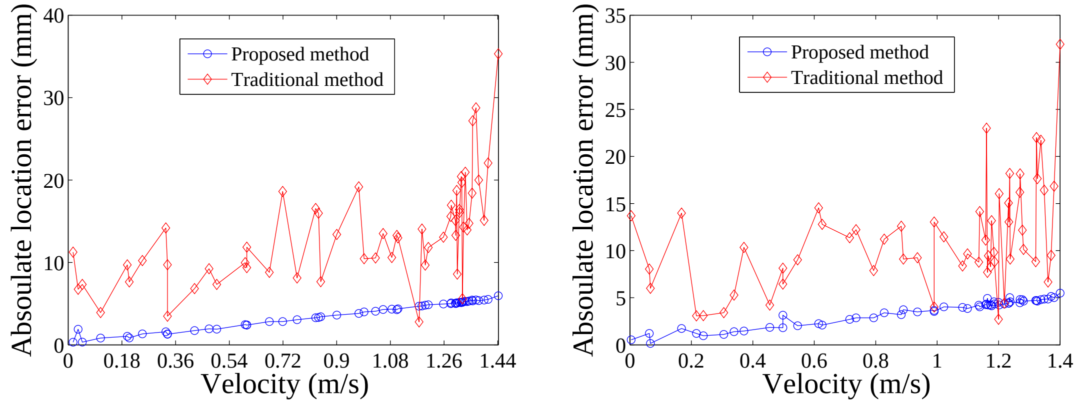

Figure 5.15: Absolute location errors with respect to transmitter velocity calculated by the proposed and traditional approaches when the transmitter was placed: (a) approximately parallel to the receiver plane; and (b) at an angle of ≈ 45 ° to the receiver plane.

transmitter from the two experiments using both the proposed and traditional methods. These plots show significantly larger location errors for the traditional method than for the proposed method.

The standard deviation of errors in each direction and the mean absolute error obtained from the proposed and traditional methods are given in Tables 5.2 and 5.3 respectively. These results show that the proposed method obtained significantly

Table 5.2: Standard deviation of errors in measured locations of the transmitter (mm).

Experiment	Methods	Direction		
		x	y	z
1	Proposed	1.2774	1.2728	0.5292
	Traditional	6.2269	8.1983	3.3796
2	Proposed	1.0665	1.0562	1.1380
	Traditional	5.5861	7.7550	3.2696

Table 5.3: Mean absolute errors in measured locations of the transmitter (mm).

Experiment	Mean Absolute Error	
	Proposed Method	Traditional Method
1	3.7636	13.4518
2	3.5426	11.2870

higher accuracy than the traditional approach.

In summary, the above proposed tracking method has the following advantages over existing systems.

1. Without using a matched filter, it can estimate the Doppler shift which reduces computational complexity and system cost.
2. It is anticipated that, for gait analysis, this system can be used instead of the traditional and expensive optical MCS which would not only reduce a system's cost but also its complexity.

5.7 Conclusions

In this chapter, it was proposed to use OFDM signals to achieve simultaneous multiple transducer positioning which offers the unique features of: efficiently utilizing the bandwidth; without affecting on the update rate; and reduced system costs as a broadband transducer is not required for simultaneous multiple transducer positioning. Also, as distinct from the traditional Doppler shift estimation and compensation technique, the proposed tracking algorithm does not require a matched filter to estimate the Doppler shift.

The experimental results showed that, the proposed system is able to measure the 3D locations of multiple transducers with sub-millimeter accuracy and the 3D trajectory of a moving transmitter with millimeter accuracy which is significantly better than that of the alternative traditional approach.

The accuracy of the proposed system is compared with that of the Vicon system, and it was shown that the proposed system has the same order of precision but incurs less cost and complexity than the Vicon MCS.

Moreover, the proposed system can also be used in larger scale indoor positioning applications where location information needs to be stored centrally (e.g., in office environment and research labs) using an active mobile architecture and for those applications where user privacy is an issue (e.g., in museums, supermarkets, or government buildings) using a passive mobile architecture.

Chapter 6

Conclusions and Future Work

Location sensing provides endless opportunities for a wide range of indoor applications. Motivated by the promise of ultrasound in delivering high positioning accuracy with lower cost, this dissertation presented different ultrasonic (US) location sensing techniques. This chapter summarizes the contributions made in this dissertation and also outlines some possible future research directions.

6.1 Contributions

In Chapter 3, a new technique to calculate time-of-flight (TOF) using phase-correlation was introduced. The proposed scheme demonstrates a method for narrowing the correlation peak by increasing the signal's bandwidth virtually rather than physically. This feature of the proposed technique helps to accurately determine the TOF in environments where close multipath echoes occur. The other attributes of the proposed technique are: it can separate the individual multipath components as the correlation peak is narrow; and reduces the system cost as it does not need to increase the signal's bandwidth physically to improve the accuracy of the system. The proposed method was evaluated in an indoor environment and experimental results showed that the proposed method provides superior performance, in terms of accuracy and system cost, when compared with the state of art, i.e., cross-correlation.

In Chapter 4, two new techniques, one for the measurement phase and another for the positioning phase were proposed. In the measurement phase, an orthogonal frequency division multiplexing (OFDM)-based TOF technique was introduced that not only provides higher accuracy compared to the existing chirp-based cross-correlation technique but also has the following desirable attributes: computational efficiency; does not need to store both transmitted and received signals and; good de-noising properties. Then, in the positioning phase, a steepest descent optimization algorithm was proposed which has the following advantages over the traditional lateration algorithm : i) overcoming the error introduced by the lateration algorithm when reference points are positioned on a single plane and the separation between them is less than the separation between reference points and target and; ii) compensation for errors in distance measurements of the receivers corresponding to one complete cycle of the transmitted signal if they are not compensated for properly in the measurement phase. The proposed approach was tested in an indoor environment and its performance was compared with the traditional cross-correlation-based multilateration method which uses a narrow-band chirp signal. The experimental results showed that the proposed approach achieved higher accuracy (sub-millimeter) than the traditional approach.

In Chapter 5, utilizing the orthogonal nature of the OFDM signal, the proposed steepest decent optimization algorithm was extended from single transducer positioning to simultaneous multiple transducer positioning. Then, the proposed

OFDM-based steepest descent optimization algorithm was further extended for tracking a moving transducer in a complex pendulum model where Doppler shift associated with the movement of the transducer was estimated by introducing a pilot carrier in the OFDM signal, and then compensated. Unlike the traditional time division multiplexing (TDM)-based multiple transducer positioning approach which reduces system update rate or the broadband-based approach that increases system cost, the proposed approach neither used TDM technique nor a broadband transducer, thus neither impacts on system update rate nor increases the cost of the system. Also, as distinct from the traditional matched filter based Doppler shift estimation technique, the proposed tracking system does not require any matched filter to estimate the Doppler shift. The experimental results showed that the proposed system was able to calculate the three-dimensional (3D) locations of multiple transducers with sub-millimeter accuracy and the 3D trajectory of a moving transducer with millimeter accuracy which is significantly better than that of the alternative traditional cross-correlation-based multilateration method which uses single tone or chirp signal. The experimental results of various pendulum trajectories obtained using the proposed method were compared with that obtained using a Vicon system and it was shown that proposed system has the same order of precision but incurs less cost and complexity than the Vicon MCS.

6.2 Future Research Directions

As a continuation of the current research, the following suggestions for the use of the OFDM-based steepest decent optimization algorithm in different applications are provided.

6.2.1 Underwater Positioning

Generally, most of the underwater positioning systems use lateration algorithm to estimate the location of target(s) [196]. However, in an underwater based positioning system, when reference points are installed on a single plane (which is logistically simple and provides accurate coordinate information of the reference points) and the separation between them is less than the separation between them and the target(s) (which is likely to happen) the surface of the spheres centered at the reference points (generated by the lateration algorithm) is almost parallel which produces larger errors in the position of the intersecting point of the spheres for directions tangential to the surface of the spheres than for directions normal to the surface of the spheres.

Future work in this research area would be to apply the steepest decent optimization algorithm for underwater localization to eliminate this kind of problem as it is already shown that the proposed steepest decent optimization algorithm has that ability. Moreover, if an OFDM signal(s) is used for underwater localization, the same benefits can be obtained as for indoor environments, i.e., TOF estimation with lower cost and complexity than cross-correlation techniques, simultaneous multiple target positioning without using broadband transducers and Doppler shift estimation for moving target positioning without using matched filtering technique. Toward this aim, an experiment was conducted to see the performance of the proposed OFDM based TOF estimation technique where TOF was estimated by finding the highest peak of the received signal. Experimental results (given in Appendix B) showed that the proposed system is able to detect the peak at the start of the received signal after equalization was performed.

6.2.2 Tracking Multiple Targets

In this current research, although the performance of the OFDM-based steepest optimization algorithm was evaluated for multiple transducer positioning, the tracking performance was confined to a single transducer. Future work for this approach could involve tracking multiple transducers which could be used for different applications such as, in the entertainment industry, to create life-like models, in robotic science to produce human-like actions in robots, in an office environment and industry, to track multiple targets.

Appendix A

Indoor Positioning Systems

A.1 Existing Ultrasonic Positioning Systems (UPSs)

Active Bat: This was one of the first UPSs established by AT&T Research [70, 71] (1999) (Figure A.1(a)) and, using an active mobile architecture, it consists of a group of mobile or fixed wireless transmitters (called bats) and ceiling-mounted receivers. Synchronization between the bats and receivers is achieved by sending RF pulses to them and, in response to the request of a RF pulse, a bat transmits an US pulse to the receivers which calculate their distances from the bat using the (velocity-difference) TDOA technique. From these measurements, the base station calculates the positions of the bats utilizing the multilateration algorithm. This system achieved a precision of 7 cm in a strongly controlled and centralized structural design.

Cricket: This is an US-based system which provides user-centric location support for ubiquitous applications and was developed at Massachusetts Institute of

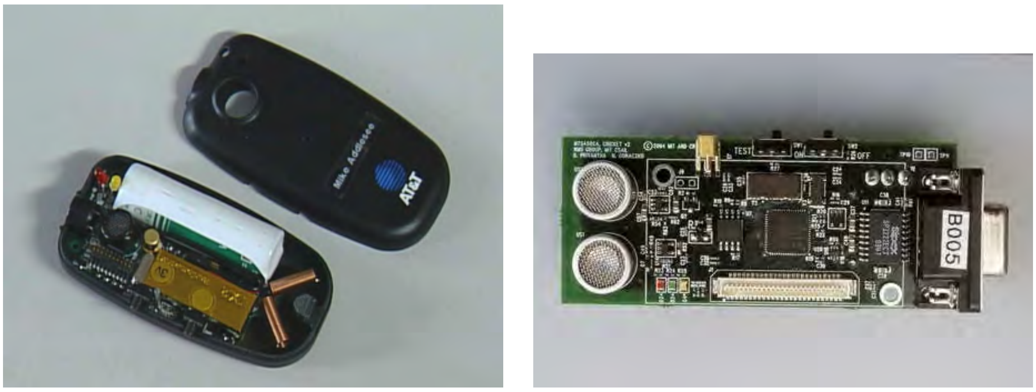

(a) (b)

Figure A.1: UPSs: (a) Active Bat [1]; and (b) Cricket [2].

Technology in 2000 [41] (Figure A.1(b)). Using a passive mobile architecture, this indoor system consists of a set of beacons in the ceiling and receivers attached to the devices that require location. An RF signal is used to send the beacons' location information to the receivers and US pulses measure the distances between the receivers and nearby beacons which are used to find the positions of the receivers using the trilateration algorithm. This system has a reported precision of 10 cm and provides advantages in terms of scalability and privacy as it uses a passive mobile architecture but has the disadvantages that it lacks centralized management or monitoring and has a low coverage range due to the unidirectionality of its US transducers.

Low-cost indoor positioning system: Using a passive mobile architecture Randell and Muller described a system [82] which allows wearable and mobile computers to autonomously compute their position. This system uses 4 US transducers, located at the corners of a square on the ceiling wired to a controller and a MD (receiver). The controller transmits a radio trigger followed by an US pulse from each of the 4 transmitters consecutively. The mobile receiver unit, synchronized by the radio trigger, calculates the TOF, from which it estimates its position with 3D accuracies between 10 and 25 cm.

Cricket Compass: This system [42] was among the first to be capable of taking AOA measurements of sensor motes (crickets). Its operational architecture is the same as that of Cricket [41], except that a compass device is attached to the target (receiver) to deduce its orientation using the AOA information of the US pulses, with orientation accuracy of 5°.

Smith's system: To track a MD, a combination of active and passive mobile location architectures was proposed in [69] using a Kalman filter (KF) and extended KF (EKF), with a method developed to transition between the passive and active modes of the MD. Until the KF's confidence is in a bad state, the MD (listener) does not transmit any information. It then becomes an active transmitter and generates simultaneous RF and US pulses, with the RF message having no information other than a randomly generated nonce which helps to hide the MD's identity. Whenever a beacon hears an RF message produced by a MD and its corresponding US pulse, it waits for a short random period of time and then broadcasts the nonce (set by the mobile) together with the distance estimate. After receiving this information from nearby beacons, the MD can accurately calculate its position, since the simultaneity condition holds for these distance samples, and then use this position estimate to reset its KF. The median error with passive, active and hybrid architectures at a speed of 1.43 m/s was reported as 22 cm, 4.7 cm and 14.9 cm respectively.

Ad-hoc localization system (AHLoS): This system, which was developed by A. Savvides, C. Han and Mani B. Strivastava at the University of California's Networked and Embedded Systems Lab in 2001 (Figure A.2) [15], enables sensor nodes to determine their locations using a set of distributed iterative algorithms which drive an ad-hoc network of sensor nodes, a small percentage of which are aware of their locations through either a manual configuration or using a GPS. Medusa

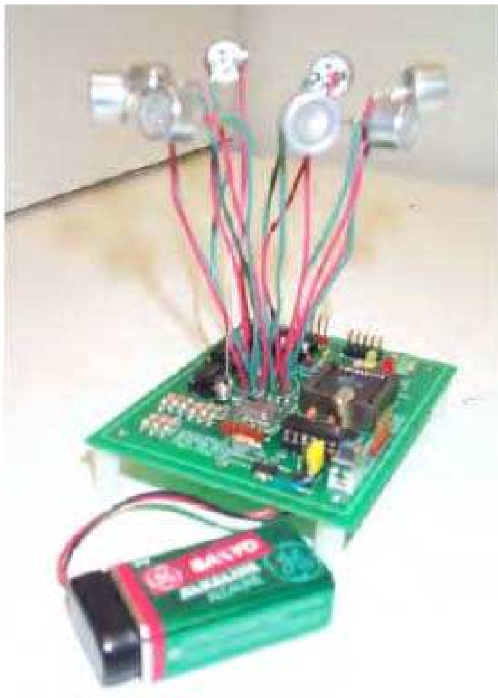

Figure A.2: ALHoS: Medusa MK-2 sensor mote with omnidirectional US transmit/receive unit [3].

motes are used by this system, which features an omnidirectional US transceiver unit to overcome the narrow directionality problem of US transducers, and the nodes with known locations are called beacon nodes and those with unknown locations are called unknown nodes. Using the (velocity-difference) TDOA between the RF and US pulses, the inter-nodal separation distance is obtained. In AHLoS, if an unknown node is within a one-hop distance from at least three beacon nodes, it calculates its position through an iterative multilateration algorithm, otherwise it considers the location information over multiple hops in a collaborative multilateration scheme. When 50 Medusa nodes (10% are initially configured as beacons) were installed on a square grid with a side of 15 m, the system's positioning error was within 20 cm and its ranging precision was 2 cm for node separations of less than 3 m.

iBadge: This is a wearable system built for a Smart Kindergarten [3] which has numerous functional units, including a localization unit, to obtain a precise spatial position. While its performance and working principle are the same as those of AHLoS, it can estimate the target's badge position in the presence of an obstacle to its nearby badge by utilizing a collaborative multilateration process based on a distributed KF [119].

Huitema's system: This is an US motion analysis system which is capable of measuring temporal and spatial gait parameters while subjects walk on the floor [23]. It uses two US receivers, one attached to each shoe of the subject and a transmitter placed stationary on the floor. The transmitter transmits 8 consecutive pulses at intervals of 25 ms. The propagation delays for both receivers are measured using a bit counter that reaches its full range in 25 ms and begins counting the moment a burst is transmitted. When the transmitted burst is received by the US receivers, its output is stored and instantly converted to an analog output signal. Then, an input signal processor eliminates most noise from the input signal using a low-pass filter and testing of the minimum pulse strength. From their evaluation, at velocities of 0.85 m/s, 1.35 m/s and 1.91 m/s, the maximum toe-off errors were found to be 60 ms, 25 ms and 25 ms, and the heel-strike errors were 55 ms, 35 ms and 25 ms respectively.

Distributed object locating system for physical space internetworking (DOLPHIN): This system [43] is similar to the Cricket system [41, 42], except that it needs only a few pre-configured reference nodes to locate all the other nodes in the system using a hop-by-hop location mechanism. It consists of two types of nodes: a reference node (fixed at a known position) and a normal node (the position of which is to be determined), with a one-chip CPU feature pulse counter to measure the TDOA of the US pulse. The reference node simultaneously transmits RF and US signals to the normal node and, using the (velocity-difference) TDOA between these signals, the distance between the reference and normal nodes are obtained. Finally, using the multilateration algorithm, the 3D position of the normal node is calculated, with the reported position estimation accuracy of this system being approximately 15 cm.

Whitehouse's system: This US ranging system was developed to minimize the prediction gap (the difference between a real-world localization error and that predicted by simulation) (Figure A.3) [4, 197]. It uses 8 US transducers adapted at different angles, 4 for transmission and 4 for reception. Although the circuitry is analogous to that of the Medusa system, it has an additional switchable circuit so that a single transducer can act as a transceiver while the nodes measuring the TOF use the same principle as that of Cricket [41]. Rather than using narrowband US transducers, the center frequency of which is at 40 kHz (used in both Cricket and ALHos), the center frequency of the transducers used in this system was reduced to 25 kHz which improves range resolution. This system reaches up to a 12 m range with less than a 5 cm standard deviation of error when the transducers are face to face. To overcome the unidirectionality effect of the US transducer, it uses a metal cone (Figure A.3) to spread and collect the acoustic energy uniformly in the plane of the other sensor nodes. With this arrangement, this system achieves around a 5 m range with a 90% precision of less than 6.5 cm.

WALRUS: The concepts proposed in [41, 71, 198] were combined to produce this low-cost, private, indoor, room-level positioning system [199] which utilizes US beacons to determine the locations of MDs. It uses ordinary audio hardware (desktop speakers and PDA/laptop microphones) to transmit and receive US signals and 802.11 communications as the information-bearing channel.

The WALRUS system consists of two main components: a server-side beacon module (transmitter) and mobile client software (receiver). The former runs as a desktop PC with attached speakers (to produce sounds of around 21 kHz) and

Figure A.3: Whitehouse's US ranging platform [4] (surrounding white area contains MICA2 dot and battery, and supports reflective cone above US transducer protruding from top).

supplies US signals to a MD and periodically broadcasts 802.11 datagram packets (which contain the room information) simultaneously with a short audio signal at 21 KHz. The mobile client software listens for the 802.11 datagram packets and corresponding US pulses. Although it can hear multiple 802.11 packets as the RF signals travel through walls, it can pick up the desired ones using the US pulses if the speakers are in the same room. Its resolution is restricted to room level.

BUZZ: This is an indoor positioning system presented in [200] which positions mobile computers using narrowband US signals, and involves the design and implementation of two novel systems, the synchronous and asynchronous BUZZ, each of which has a particular application. Positions are calculated through the use of transmission patterns, with the timing information communicated from the infrastructure to wearable receiving devices.

Synchronous BUZZ was an improvement proposed in [82] that eliminated the radio signal from the design which offers advantages in terms of clock synchronization, size and weight of the receiver. A central control unit connected to the beacons by wires is used to provide synchronization and, for positioning, an EKF and four beacon measurements are required. However, it has the limitation of the MD having to be placed in a particular location at start up. It calculates a 3D position with 4 cm precision 50% of the time and 10 cm precision 95% of the time, and its update rate is 33 Hz.

Asynchronous BUZZ is a wireless system like Cricket [41] but, as it does not use RF signals, it has advantages over Cricket in terms of system cost, power consumption and beacon sizes. Control of the transmission signal is decentralized and it is designed for low-precision applications. Its positioning error was within 50 cm.

Sonitor: This is a real-time indoor tracking and location technology produced by Sonitor Technologies Inc. [201]. As it does not require LOS transmission between the detectors and the targets to be tracked it is able to track hidden objects. In Sonitor, US tags which transmit the unique identification of each person or device are attached to people or equipment for tracking by wireless detectors located in various rooms or an open indoor area. The transmitted signals are detected by the detectors which forward this information to a centrally positioned calculation and management system that stores the tags' locations and associated times through an existing wired or wireless local area network (LAN). To protect the US signals against interference and effectively detect the received signals, a digital signal-processing algorithm is patented in Sonitor. Also, an energy-efficient technique is proposed by the Sonitor UPS which extends battery life by up to 5 years and 600,000 transmissions. However, this system cannot provide the absolute position of a target and several detectors are required to be fixed in each part of the

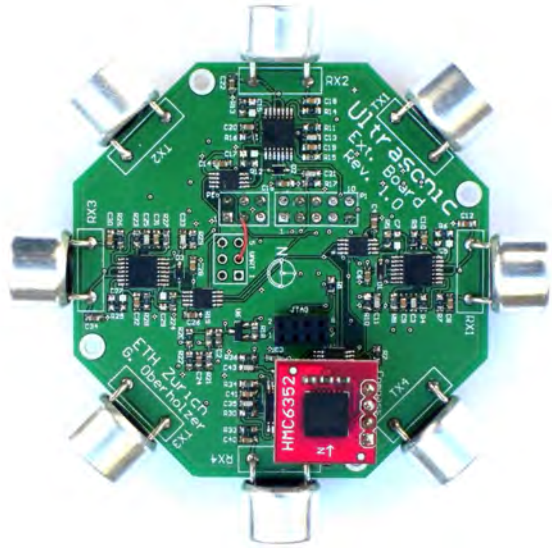

Figure A.4: Spider Bat: top view of US board with attached digital compass [5].

tracking area, while its precision is limited to room level.

Spider Bat: This US-based ranging system (2011) (Figure A.4) was designed to augment existing low-cost, low-power sensing devices with distance and angle information in [5]. It consists of four independently controllable US transmitters and receivers, a microcontroller to control the transmission operation and process the received signal, and a digital compass which provides the absolute rotations of the nodes. The innovation of this system is its capability to measure the absolute angles between sensor nodes which was not available in earlier systems [41, 119].

The sender transmits a radio packet followed by an US pulse node to initiate a single measurement while nearby nodes listen for incoming US waves. The (velocity-difference) TDOA is used for range estimation. The standard deviation of error of this system is 5.39 mm at the maximum distance of 14 cm and its mean angular error is less than 5° for short distances. Its localization inaccuracy is 15.5 cm (minimized to 5.7 cm by applying the least squares method) for a worst-case scenario in an indoor environment and 61.2 cm for an outdoor environment.

Sato's system: This is an US motion capture system described in [32] and, using an active mobile architecture it consists of 5 US transmitters attached to the user's body and 4 US receivers acting as reference points. To avoid signal interference at the receiving end, each transmitter transmits a signal at a different time, i.e., it uses the TDM technique which reduces the system update rate. In the measurement phase, it uses a phase-based technique called the extended phase accordance method and, in the positioning phase, a multilateration algorithm. The accuracy achieved by this system was 4-5 cm.

Interacting multiple model (IMM) system: This is a TDOA-based UPS presented in [84]. The IMM estimator runs an EKF to track a mobile station (MS) for a LOS case and a robust EKF (REKF) for a non-LOS (NLOS) one. The results from the EKF and REKF estimators are combined by calculating the probabilities of each estimator to obtain high positioning accuracy. A 2D isotropic transmitter with a beam width of 360° and eight US transducers with 45° angles of aperture are used to transmit an US signal.

A number of receivers at fixed positions and connected via a wireless LAN (WLAN) for time synchronization are used to receive the US signal. The positioning update rate of this system is more than 3 Hz and its precision is in the cm range (3.4 cm in theory).

Kim's system: This system adopted a hybrid algorithm (HA) using an US signal to find the posture of a mobile robot in a static environment [83]. The system architecture of this system is shown in Figure A.5. A group of US transmitters is used at a known position on the ceiling and an array of three receivers placed on top of the robot. All the transmitters and robot are fitted with RF modules to calculate the TOF data between them, with all the receiver modules on the robot connected to an RF module via a controller area network (CAN). To calculate the

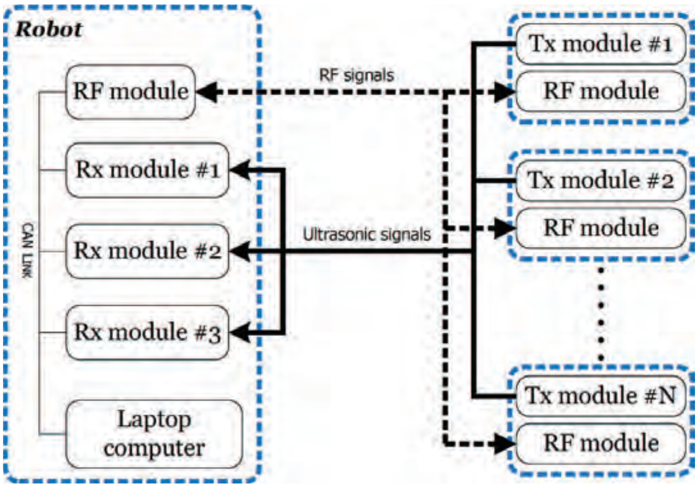

Figure A.5: System architecture of Kim's system [6].

distances between the receiver modules on the robot and US transmitter modules, the robot consecutively activates each transmitter module by a command message from one of its RF modules at a sampling instant. A transmitter module consists of a microcontroller, US transmitter, RF transceiver and temperature sensor. After receiving an activation message, it (the transmitter module) answers with a radio message, which includes its identification (ID) number, position and temperature information, and simultaneously transmits a modulated US signal. The RF module measures the time difference between the arrivals of the RF and US signals using the (velocity-difference) TDOA, and the HA uses direct and indirect methods for self-localization. The direct method uses the US distance measurement directly without additional processes whereas the indirect method uses ranges, ranges and bearing differences, and ranges and angles of departure extracted from the US distance measurements between a transmitter and three receivers. Several experiments were conducted with different numbers of transmitters and orientations and the results showed that the mean errors of positioning and orientation of this system are 2.1 cm and 0.82° respectively.

More recently, the same authors presented a dynamic US hybrid localization algorithm in [6] that combines a dynamic distance estimation method for moving robots and the US hybrid localization algorithm to estimate the pose of a robot utilizing an EKF. Several experiments were conducted for several trajectories and, each time, as expected, the positioning and orientation errors were higher than those for the static one.

Qi's system: This system measures 3D foot trajectories using a wearable wireless US sensor network in an active mobile architecture [38]. It consists of a narrowband US transmitter (mobile), 4 receivers (anchors) with known fixed positions and an RF module. To calculate the distance between the transmitter and receivers, it utilizes the (velocity-difference) TDOA technique. It applies pre-filtering in the range measurements to reduce the errors in tracking and localization, and then the pre-localization algorithm using the Newton-Gauss (NG) method filtered by an EKF. The experimental results showed that the proposed system had sufficient accuracy with a net root mean square error of 4.2 cm for 3D displacement, especially for foot clearance.

Hazas's system: This is the first broadband US location system proposed for achieving fine-grained location estimates [190, 191]. It provides advantages over narrowband systems in terms of signal interferences, data rates and noise sensitivity by using the direct sequence code division multiple access (DSCDMA) method. To generate the transmitted signal, a 50 kHz carrier wave is modulated by 51-bit-long Gold codes using binary phase shift keying (BPSK) and two types of positioning systems are proposed. The first is polled and centralized, which uses an active mobile architecture and has an accuracy of approximately 2 cm while the second is privacy-oriented, uses a passive mobile architecture and can be synchronous or asynchronous. The synchronous system utilizes the conventional multilateration algorithm along with cross-correlation to estimate the receiver's position whereas the asynchronous system uses direct-sequence pseudo-range measurements, and their system accuracies are 4.9 cm and 26.6 cm respectively.

Frequency hopped spread spectrum (FHSS): This positioning system was developed in [192] and uses broadband US signal. This system uses a set of fixed nodes at well-known locations called base stations (BSs) and MDs whose positions and orientations are to be determined. The TOF and AOA are calculated by the MD using a circular array of transducers utilizing US and RF signals, with both direct sequence spread spectrum (DSSS) and FHSS signals used to provide a comparison of accuracy and robustness. The authors conclude that, using FHSS is more beneficial than DSSS, because only noise and multipath in the same band of frequencies affects the accuracy due to its variable carrier frequency. The experimental results show better accuracy for FHSS than DSS. FHSS provides a 3D estimation accuracy of less than 1.5 cm for 95% of cases

Reference-free UPS: This system, which was developed in [46], utilizes broadband transducers and a FHSS technique. It does not require any reference signal for time synchronization between a transmitter and receiver and incorporates a new technique called the hybrid AOA-TOF which is an improvement over the conventional AOA technique. For TOF measurement, it uses the cross-correlation technique and its reported 3D precision is approximately 9.5 cm.

CDMA: This system is employed in an UPS in [19] for fine-grained location estimates. It uses four transmitters attached to the ceiling, with four distinct Gold codes generated and assigned to each of them. For location estimation, two methods are proposed. The first obtains the mean of four location estimates using the trilateration technique and, in the second, a single robust position estimate is obtained using only three distances while the least reliable fourth distance measurement is not considered. On the ground plane, the results show a 2 cm precision

99% of the time and 95% of the time when the MD is higher than the ground plane and near the ceiling respectively. However, all the experiments were conducted in a noise-free environment whereas, in a real indoor environment, the accuracy would be less and the hardware's complexity greater.

Álvarez's system: This system [202] presents the design of a Doppler-tolerant receiver for a broadband US local positioning system architecture based on the emission of Kasami codes and was implemented in an FPGA architecture. Five receivers, each containing a bank of seven filters, each of which is matched to a different frequency-shifted version of the Kasami codes to be detected, are used. A Doppler resolution of 0.67 m/s was considered for the design of the matched filter, with an interpolation factor added between two consecutive samples of each received signal to obtain the desired resolution. Firstly, a set of test signals were synthetically generated to simulate the different positions and velocities of the receiver to analyse its performance. The simulated results showed that the sensor is capable of detecting the signals coming from all beacons moving at velocities of up to 3 m/s in a horizontal plane. Secondly, a set of real signals obtained by a prototype was used.

Aloui's system: This is a scene analysis-based localization system which adopts the TOAs of signals from a transmitter to receiver as a fingerprint and computes the target position through a local linear estimator [203]. As it uses the scene analysis algorithm, in the off-line phase, a set of positions, called fingerprint positions (or sampling locations), in the target environment are selected and a position-dependent signal parameter extracted at each position to define the positions signature (also called a fingerprint). Then, using these fingerprints, a database is built. During the on-line phase, the target signature is calculated and compared with the signatures in the previously built database to estimate its position. This system was evaluated in both active and passive mobile architectures and the accuracies obtained were 2.7 cm for 93% of measurements and 8.5 cm with 87% precision respectively. However, as it suffered from the fundamental problem of the scene analysis algorithm which is that the fingerprint map is non-stationary, there were variations in the measured signals between the on- and off-line phases at the same location.

A.2 Existing Audible Sound-based Positioning Systems

CALAMARI: This ad-hoc localization system (2002), which was developed at the University of California [7] (Figure A.6), uses a mixture of acoustic TOF and RF RSS for ranging. It uses macro-calibration (through a parameter estimation method) to adjust the (sensor) network as a system, instead of each node separately with respect to the infrastructure (as in GPS, Cricket) or alongside every other node (as in ALHoS). It is capable of perfectly scaling a network's dimensions by means of a simple, accurate ad-hoc multilateration key.

This system consists of a sounder, microphone and tone detector with a central frequency of 4.5 kHz. Ranging errors are significantly reduced, from $\approx 30\%$ of the actual range attained without calibration to $\approx 10\%$ with macro-calibration. The precision of this system is not sufficient for applications in which high precision is required as its accuracy is restricted to the node level.

Kown's system: This is an acoustic localization system developed by F. Kown et al. [204] in 2005 to improve the ranging solutions of previous work, and expanded

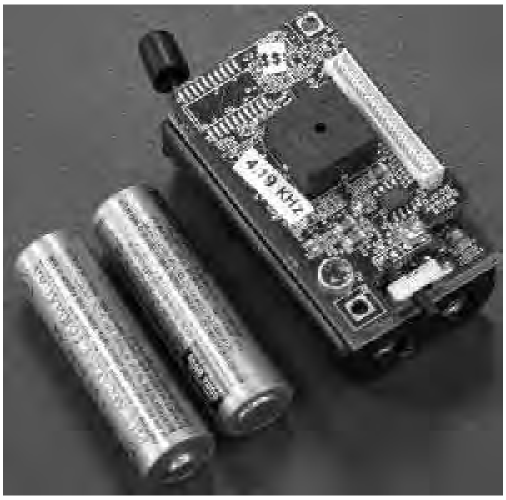

Figure A.6: CALAMARI - Sensorboard Mica/MICA mounted on mote [7].

the practical measurement range threefold (20-30 m) using the MICA2 platform. The transmitting mote is augmented with the MTS310 sensor board with an inexpensive, off-the-shelf piezoelectric buzzer unit which provides output power of 105 dB compared with the 88 dB of the original buzzer, and the results improve the SNR. The maximum range attained by the system was 22 m in 10-15 cm tall grass and over 35 m on a pavement with an accuracy of 11 m.

Kushwaha's system: This location system was based on the MICA2 platform [8, 205] (Figure A.7). Its transmitting part is composed of MICA2 motes equipped with a digital signal processor running at 50 MHz and a peripheral speaker while the receiving part has a custom-designed acoustic sensor board with two self-regulating analog input channels furnished with inexpensive electret microphones and a DSP for operating a signal-processing algorithm. This approach employs the message time-stamping primitives introduced in [206] to synchronize the source and sensor nodes. The maximum reported detection range using cross-correlation of this system was 30 m with a ranging error deviation of 15-20 cm.

Acoustic embedded networked sensing box (ENSBox): This is a platform

(a)

(b)

Figure A.7: Kushwaha's system [8]: (a) MICA2 mote; and (b) Acoustic sensor board.

for prototyping rapidly deployable distributed acoustic sensing systems, particularly the distributed source localization developed by MIT/UCLA [207, 208]. ENSBox incorporates a Linux operating ARM processor with key facilities essential for source localization, that is, a sensor array, network services, time synchronization and self-calibration of the array's position and orientation. It also has a high-precision self-calibration feature which eliminates the need to manually survey the arrays' positions and orientations. After temperature compensation, the precision of this system was 5 times better than those of other audible acoustic systems, such as Sallai [209], Kwon [204] and Kushwaha [205], when cross-correlation is used. The average 2D position error of this system was 5 cm and average orientation error over a partially obstructed 80×50 m outdoor area was 1.5°.

Beep: This 3D indoor positioning system was developed with an active mobile architecture using audible sound technology [9, 210] (Figure A.8). A roaming device, which is to be tracked, sends audible sounds to pre-installed acoustic sensors (S_i) with known positions. These sensors are connected to the central server through a wireless connection. They receive the audible sounds transmitted from the tracked device and then forward these data to the central server through a

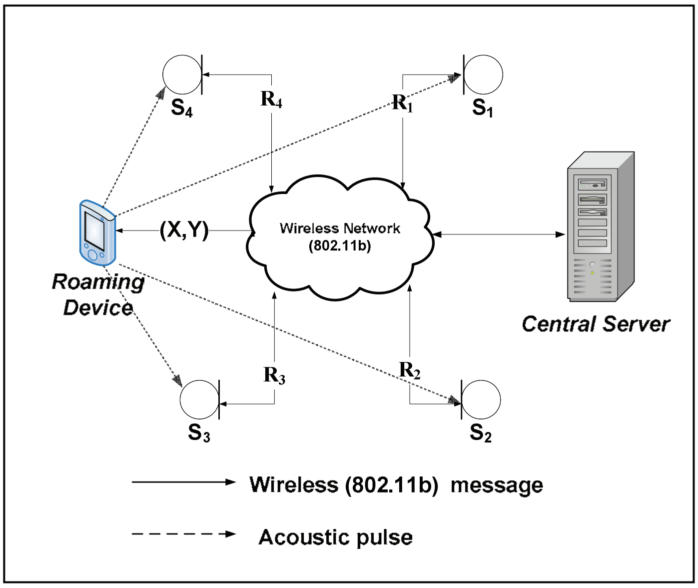

Figure A.8: System architecture of Beep [9].

WLAN. In this system, the triangulation location technique is used with a standard 3D multilateration algorithm based on the TOA measured by the sensors using cross-correlation and, finally, the roaming device can acquire its location information from the central server via the WLAN. The positioning accuracy of this system was 0.4 m in 90% of cases and, in terms of the privacy issue, facilitates users to stop sending audible sounds if they do not want the system to know their locations.

Whisper: At the University of North Carolina at Chapel Hill, Vallidis and Bishop proposed this broadband acoustic body tracking system in 2002 [211]. It transmits pseudo-random audio signals from small speakers to small microphones and then calculates the distances between the speakers and microphones using a correlation technique. To reduce the computational expense of correlation calculations, it uses a KF. As it uses broadband acoustic signals, it has several advantages compared with a narrowband acoustic system, such as being robust to environmental noise, distributing the energy to minimize the audible sound to a whisper and having a high update rate. However, its disadvantages include human-audible background noise and high computational costs due to its use of the KF.

A.3 Existing RFID-based Positioning Systems

SpotON: This is one of the first indoor ad-hoc location systems developed to locate mobile objects with (active) RFID tags using the RF RSS lateration technique [212]. In this system, tags are attached to the objects to be localized. Tags transmit radio packet beacons of a calibrated power at randomized intervals (to reduce packet collisions and maximize fairness and aggregated throughput). Any tag hearing a radio beacon measures the RSSI subject to its receiver-specific calibration model to calculate its distance from a transmitting tag. It utilizes the compactness of tags and correlation of several measurements to reach sub-millimeter positioning accuracy. Although it suffers from a variety of problems, such as a large tag cluster size, its requirement for environmental profiling to enhance accuracy and its sensitivity to errors caused by radio irregularities, for an early system, its potential is admirable.

Location ID based on dynamic active RFID calibration (LANDMARC): This is a RFID-based indoor positioning system proposed in [138] in which an RFID active tag is pre-programmed with a unique ID to be identified by the RFID readers, each of which has 8 different power levels, with level 1 providing the shortest and level 8 the longest range. A number of RFID readers are installed to define a certain range based on power levels in which they can detect RFID tags. The accuracy of the system depends on the number of readers and their placements and power levels. LANDMARC improves accuracy by employing extra fixed location reference tags, which become the reference points in the system, rather than placing more RF readers for location calibration. In this approach, a reader not only uses the power-level information to determine the range, as do all the other previously proposed RFID-based positioning system, it also uses the RSSI from each reference tag to a reader. This helps to compensate environmental dynamics (e.g., dynamic human movement) that contribute to variations in the detected range as the reference tags are subject to the same effect in the environment. This system uses the RF RSS k-NN technique to locate mobile targets with active RFID tags and reports a maximum distance error of less than 2 m and a 50th percentile error of $\approx$ 1 m.

WhereNet: This positioning system [213] was developed by Zebra Technology to offer various pieces of equipment to support indoor and outdoor real-time positioning. It uses the 2.4 GHz band, as do the IEEE 802.11 and Bluetooth systems, but has a dedicated standard protocol (ANSI 371.1) optimized for a low-power spread-spectrum location approach. Tags are attached to the target which transmits long-range spread-spectrum radio beacons with unique IDs to the antennas mounted on the ceiling in fixed positions. Then, the signal received by an antenna is forwarded to the local processor which performs the location calculation. This system can track many tags simultaneously and achieves an error range of around 2 m to 3 m.

A.4 Existing Wireless Local Area Network (WLAN)-based Positioning Systems

RADAR: This is a RF-based indoor positioning and tracking system developed by Microsoft research [106]. It uses the RF signal strength to measure the distance between a transmitter and receiver which is then used to locate a user through triangulation. A database of RF signals is generated at a set of fixed receivers for known transmitter locations during the off-line phase. Then, during the on-line phase, the RSS of a transmitter is measured at a fixed set of receivers and compared with the signal strength stored in the database to determine the best fit for the present transmitter's location. This system estimates a user's location with an accuracy of less than 3 m.

COMPASS: Using existing WLAN infrastructures, this system [163] not only provides users' positioning information via a probabilistic-based scene analysis algorithm but also their orientations using low-cost digital compasses. In the case of moving target positioning, this system showed an accuracy of 1.65 m for an area of 312 $\times$ 312 m on a floor inside a building. However, only single-user tracking is considered and, for tracking multiple targets, the system's performance would be degraded in terms of accuracy and scalability.

Hour: This is a RF-based scene analysis and mapping technique using a WLAN and RSS [214–216]. It uses the probabilistic method discussed earlier to attain high location accuracy and clustering techniques to minimize the computational cost. In this approach, the location with the highest likelihood is selected in order to minimize the distance error. It presents better location estimates than the RADAR system with an accuracy of within 2.1 m for more than 90% of cases. Its location estimation could be improved by increasing the number of samples at each sampling location which would provide better estimations of the means and standard deviations of Gaussian distributions.

Ekahau: This indoor positioning system [164] uses existing indoor WLAN infrastructures to continually monitor the motions of Wi-Fi devices and tags utilizing the trilateration technique and RSSI for distance estimation. It presents 2D location information which can be used by location-aware services and applications, and is composed of three parts: a site survey, Wi-Fi location tags and positioning engines. The site survey relies on software tools which provide site calibration before real-time position evaluations and define the network coverage area, SNR, data rate, SS and overlapping of the WLAN in terms of users. The Wi-Fi location tags, which transmit RF signals, can be fixed to any tracked object to enable real-time positioning. The APs in the system measure the RSSI of the transmitted RF signals and forward them to the positioning engine via WLAN. The positioning engine is a software tool which offers real-time positioning to any device, such as a laptop, PDA, etc., using WLAN technology. The positioning accuracy of this system is 1 m if there are three or more overlapping APs that can be used to locate objects.

A.5 Existing Radio Interferometric Localization Systems (RILS)

Maróti's system: RILS is the first interferometry-based localization system proposed in [165] which uses the MICA2 wireless sensor available in the wireless sensor network (WSN). In this approach, the interference signal is generated by a pair of transmitting nodes and its envelope phase is measured by the receiving nodes in a time-synchronized manner at a particular time instant which is repeated on 11 different radio channels in the range from 400 MHz to 430 MHz. Using a WSN communication infrastructure, all the measured phase values are sent to a PC which then works out the $q - ranges$ for the same pair of transmitters and all probable combinations of the receivers with valid phase measurements as the number of contributing receivers is limited by the communication range. Then, the entire process is repeated with different combinations of transmitters to obtain a large number of $q - ranges$ which is then used as input to a genetic algorithm

(GA) to find the relative coordinates of the sensor nodes. This system was capable of localizing the nodes with a mean error of less than 5 cm for an 18×18 m outdoor area in a 16-node experiment.

Kusỳ's positioning system: This system is an enhanced version of [165] proposed in [217] in which it was shown that the ranging performance of [165] is considerably degraded under the $q-range$ ambiguity effect caused by a particular choice of wavelengths and the multi-path effects that lead to a phase shift. In this system, both problems are solved using an interleaved and iterative localization algorithm in which the search space of the $q - range$ estimates in the subsequent localization phase is constrained in order to iteratively distil the ranges. Experimental results show that the range can be accurately measured with RILS and the system has about 4 times the communication range of Maróti's system (170 m) with an accuracy level of a few centimeters.

Kusỳ's tracking system: In [218], the same authors as above extended their method from static node localization to tracking by utilizing the Doppler shift. A Doppler shift measurement is performed via the beat signal described earlier, with the initial position of a tracking node measured by a GA. Once the initial positions are available, the mobile nodes send a request message to one of the reference nodes to transmit a signal which has a slightly different frequency to that transmitted by the mobile node. The rest of the reference nodes measure frequency changes in the interference signal caused by movements of the mobile node which are then fed into an EKF running on a PC to keep an up-to-date model of the node's location. For measurements with eight anchor nodes and a single mobile node in a 50×30 m field, the experimental results show a location, speed and heading accuracy of 1.3-2.2 m, 0.1-0.4 m/s and 7°-18° respectively, from the best- to worst-case tracking scenarios.

Lédeczi and Chang's systems: All the above systems [165, 217, 218] use complex non-linear optimization in the sensor fusion phase which degrades system performance. As the workload of the fusion phase can be considerably reduced by specializing certain nodes in the system, Lédeczi, et al. [219] and Chang et al. [220] proposed employing physically rotating anchor nodes in WSNs for node self-localization. Rather than having the tracked node and anchor node transmitting the interfering carrier signals, two anchor nodes are used for transmission, where one has specialized hardware (spinning antenna) and the other does not. Both nodes transmit at slightly different frequencies to generate the interference signal. Due to the spinning of the antenna (either the physical rotation of a single antenna or its imitation using an antenna array), the target nodes observe a Doppler shift in the receiver which they then use to determine their bearings from the anchor nodes. Using the bearing estimates and anchor location information, the target node location is calculated by the triangulation algorithm. The experimental results in [220] show an average bearing estimation accuracy of 3° leading to a positioning accuracy of about 40 cm in an 8×10 m indoor garage whereas slightly better accuracy was reported in [219].

A.6 Existing Bluetooth-based Positioning Systems

Topaz: Bluetooth technology is used in this location system [221] which is able to provide location coordinates in 2D with an error range of 2 m and, as this accuracy is insufficient in a multi-obstacle indoor environment, includes an IR-based positioning system to provide room-level accuracy. This system consists of wireless tags, APs, and Bluetooth and location servers. The wireless tags are located by numerous Bluetooth and IR-enabled APs fixed in different places, with one Bluetooth server (containing 32 APs) responsible for performing Bluetooth functions, such as managing APs and forwarding the raw RSSI to a location server that calculates the locations of tags. Via the LAN, the location and Bluetooth servers, and location clients are connected. The batteries used in the tags need to be charged once a week whereas other positioning systems support longer battery lives. The update rate of this system is around 10-30 sec.

Antti's and Hallberg's systems: A Bluetooth Local Positioning Application (BLPA), which uses RSSI for distance estimation and EKF using the acquired distance information for 3D positioning was presented in [222]. This system had a reported accuracy of 3.76 m. A similar approach was reported in [223].

A.7 Existing Ultra Wideband (UWB)-based Positioning Systems

Ubisense: This is a commercial location platform that provides a new real-time positioning system based on UWB technology [224]. It uses an active mobile architecture in which the tags transmit UWB signals to networked receivers and are located using the triangulation algorithm with AOA and TDOA information. Ubisense provides location information by creating sensor cells, with each requiring at least four sensors or readers. Throughout buildings or collections of buildings, an unlimited number of readers can be networked together in a manner similar to cellular phone networks. The accuracy offered by Ubisense is approximately tens of centimeters.

Siemens local positioning radar (LPR): This is another example of a UWB-based positioning system [225] which uses the RTT principle between a transponder unit and measuring units (base stations), and the frequency-modulated continuous wave (FMCW) radar principle. Basically, it is used for industrial applications, such as crane and forklift positioning, where a LOS environment is available.

A.8 Existing IR-based Positioning Systems

HiBall: An optoelectronic head tracking system for high precision object tracking in virtual reality applications was proposed in [226]. This system employs ceiling mounted panels of infrared LEDs, which take turns flashing rapidly and successively, and several head-mounted cameras with geometry known to the system. The head mounted cameras measure the position of the flashing LEDs and the final position of the camera is calculated using the geometrical knowledge of these cameras with accuracies less than a millimeter in highly controlled environments. However, this system suffers from, not only requiring a large number of LED panels to cover an entire building, but also expensive camera hardware, high computation costs and interference from ambient light.

Cartesian optoelectronic dynamic anthropometer (CODA): This system was manufactured by Charnwood Dynamics Ltd. [227] in 2006. The CODA mpx30 motion tracking system is composed of a camera that has an array of three sensors and small IR LEDs that are pulsed sequentially. It can identify up to 28 targets in real time with an 800 Hz sampling rate. To minimize patient encumbrance it uses tiny battery packs, each of which has a unique ID so that the system can always recognize the markers. To track bilateral movements such as human gait, a second mpx30 system is required which increases the cost significantly.

The next generation product of Charnwood Dynamics is the Codamotion system which uses lightweight sensor that can be set up at a new location in a matter of minutes. In this sytem, up to six sensor units can be used simultaneously and placed around a capture volume to provide additional sets of eyes and maximum redundancy of viewpoint which enables the tracking of 360° movements and is hence applicable for animation and sport science.

Qualisys: This system [228] uses a custom-designed camera, which is called a motion capture unit (MCU), that has a lens surrounded by IR LEDs and passive markers attached to the subject illuminated by the camera lens during operation. This system can localize 150 targets in 2D in real time. This system comes in two versions, the MCU 240 which operates between 1 and 240 Hz and the MCU1000 which operates between 1 and 1000 Hz. To provide a complete coverage of any complex 3D movement including gait analysis, the Qualisys system uses a ring-type topology where up to 32 MCUs can be connected. The spatial resolution of this system is equal to 1/60,000 of the field of view.

Vicon: The name of this system is derived from video-converter and it is a product of Vicon Motion Capture. This system [229] generally consists of 6-12 cameras placed at known positions and coupled together which rapidly and simultaneously capture a series of images of the object to be tracked. Spheres covered with reflective tape, known as markers, are attached to different points of the tracked object. This system facilitates the focusing on specific aspects (e.g., to study walking, more markers can be positioned on the lower body while, to study drumming, more can be positioned on the hand). From all the captured images, each marker's coordinates can be easily identified as they have highly illuminated pixels in comparison with those in the background, and they are stored in a data station. Finally, the positions of the markers are linked and the triangulation algorithm used to estimate the 3D paths or trajectories that each marker follows throughout the capture time. At least three of the cameras must view a marker to perform triangulation and, to obtain continuous trajectories, interpolation is used to fill the gaps. Although the accuracy of this system is high (sub-millimeter), it is expensive (approximately $200,000) and requires a complex setup. More details of the Vicon system are already provided in Chapter 5, Section 5.5.2.1.

A.9 Existing Vision-based Positioning Systems

Easy Living: This is an example of a vision-based location technique designed by a Microsoft research group [230]. It uses two stereo cameras mounted on the ceiling in such a way that every portion of the room is covered by at least one camera. To cover the measured area and provide updated vision of the raw data to be used in location estimations, two real-time 3D cameras are used. Depth and color pixels are exploited in the modeling of the background to reduce the effect of changes in the background and then the PCs connected to the stereo cameras process the captured images. The entry of a person into a room is identified by this system defining a 'person creation zone' which is usually next to the room's entrance. If a person enters that zone, the stereo unit generates the vision instance of the person, tracks his/her motion and saves the tracking history to provide accurate location estimations. Although the tracked person is not require to carrying any device, this system requires considerable processing power due to complex image processing and suffers in accuracy due to the dynamically changing environment interfering with the vision data. In addition, the system cost is high as it uses 3D cameras.

Appendix B

OFDM-based TOF Estimation for Underwater Communication

To observe the performance of the proposed orthogonal frequency division multiplexing (OFDM)-based time-of-flight (TOF) estimation technique, an experiment was conducted in Lake Burley Griffin, ACT, Australia. In this experiment, a transmitter (A SRD CT/13 [231]) which operates in a wide band of frequencies centered around 13 kHz and a hydrophone (B& K 8104 [232]), which has an approximately flat frequency response over the frequency range 2 kHz to 70 kHz were used. To capture and digitize the transmitted and received signals a UA-101 audio capture device with a sampling rate of 96 ksps was used in the experiments [233]. The transmitted signal was an OFDM signal [5-15] kHz/1 ms. Both transmitter and hydrophone were separated by a fixed unknown offset and were placed at approximately 7.5 m (half of the total lake depth) away from the water surface. The results obtained from this experiment are shown in Figure B.1. The transmitted signal which has the highest peak at the beginning and the captured received signal are represented in Figure B.1(a) and B.1(b) respectively. The captured received signal is then cropped according to the procedure described in Chapter 4, Section 4.3 (shown in Figure B.1(c)). The received signal has a different shape than the transmitted signal due to the effects of the transducer and noise. After performing equalization on the cropped received signal (according to the procedure described in Chapter 4, Section 4.3) the shape of the received signal (shown in Figure B.1(d))) is returned to a shape similar to that of the transmitted signal. This means that the distance between the transmitter and hydrophone can accurately be determined by finding the first peak of this equalized received signal. The three-dimensional (3D) location of the transmitter can be determined using the proposed steepest decent optimization algorithm once multiple hydrophones are placed in the system in a similar configuration to that used indoors.

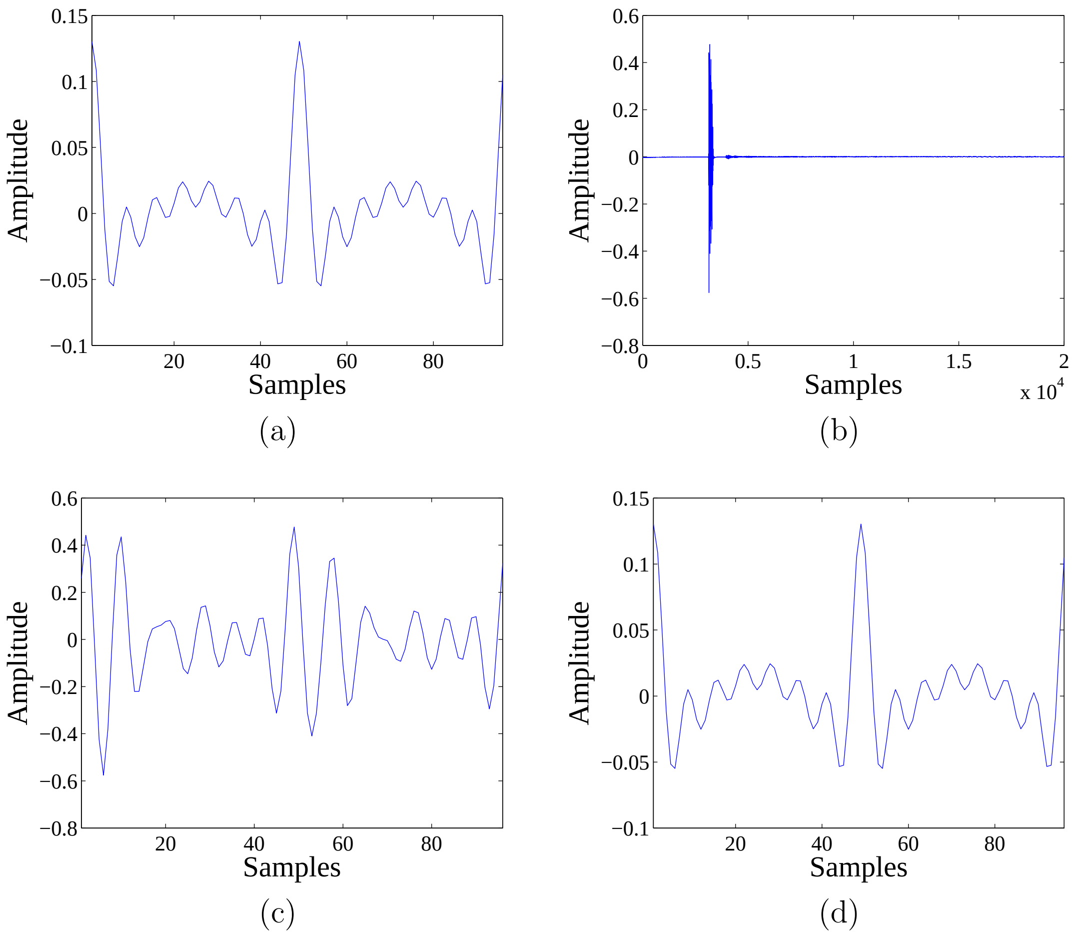

Figure B.1: Steps in OFDM-based TOF estimation method for underwater communication: (a) transmitted signal; (b) received signal; (c) cropped received signal; and (d) equalized received signal.

Bibliography

[1] "The bat ultrasonic location system," [Online]. Available: http://www.cl.cam.ac.uk/research/dtg/attarchive/spirit/.

[2] "The cricket indoor location system," [Online]. Available: http://cricket.csail.mit.edu.

[3] S. Park, I. Locher, A. Savvides, M. Srivastava, A. Chen, R. Muntz, and S. Yuen, "Design of a wearable sensor badge for smart kindergarten," in *Proceedings of the 6th International Symposium on Wearable Computers*, 2002, pp. 231–238.

[4] K. Whitehouse, C. Karlof, A. Woo, F. Jiang, and D. Culler, "The effects of ranging noise on multihop localization: an empirical study," in *Proceedings of the 4th international symposium on Information processing in sensor networks*, 2005.

[5] G. Oberholzer, P. Sommer, and R. Wattenhofer, "SpiderBat: augmenting wireless sensor networks with distance and angle information," in *Proceedings of the 10th International Conference on Information Processing in Sensor Networks*, 2011, pp. 211–222.

[6] S. J. Kim and B. Kim, "Dynamic ultrasonic hybrid localization system for indoor mobile robots," *IEEE Transactions on Industrial Electronics*, vol. 60, no. 10, pp. 4562–4573, 2013.

[7] C. D. Whitehouse, "The design of calamari: an ad-hoc localization system for sensor networks," Master's thesis, University of California at Berkeley, 2002.

[8] M. Kushwaha, "Sensor node localization using mobile acoustic beacons," Master's thesis, Vanderbilt University, 2005.

[9] A. Mandal, C. Lopes, T. Givargis, A. Haghighat, R. Jurdak, and P. Baldi, "Beep: 3D indoor positioning using audible sound," in *Proceedings of the 2nd IEEE Consumer Communications and Networking Conference*, Jan. 2005, pp. 348–353.

[10] L. Holger, "On aspects of indoor localization," Ph.D. dissertation, Department of Electrical Engineering, University of Dortmund, 2006.

[11] R. Bud and D. J. Warner, *Instruments of science: an historical encyclopedia.* Taylor & Francis, 1998.

[12] J. Last, "Radionavigation in a time of change," *Electronics Communication Engineering Journal*, vol. 1, no. 6, pp. 281–287, Nov. 1989.

[13] I. Getting, "Perspective/navigation-the global positioning system," *IEEE Spectrum*, vol. 30, no. 12, pp. 36–38, Dec. 1993.

[14] H. A. El-Natour, C. Macabiau, M. Boucheret, and A. Escher, "Impact of multipath and cross–correlation on GPS acquisition in indoor environments," *Institute of Navigation, National Technical Meeting, San Diego, CA*, 2005.

[15] A. Savvides, C.-C. Han, and M. B. Strivastava, "Dynamic fine-grained localization in ad-hoc networks of sensors," in *Proceedings of the 7th annual International Conference on Mobile computing and networking*, 2001, pp. 166–179.

[16] P. K. Misra, "Acoustical localization techniques in embedded wireless sensor networked devices," Ph.D. dissertation, The University of New South Wales, 2012.

[17] S. Ghosh, "Wirless sensor networks by resolving flip ambiguity," Ph.D. dissertation, The University of New South Wales, 2012.

[18] S. Bamberg, A. Benbasat, D. Scarborough, D. Krebs, and J. Paradiso, "Gait analysis using a shoe-integrated wireless sensor system," *IEEE Transactions on Information Technology in Biomedicine*, vol. 12, no. 4, pp. 413–423, Jul. 2008.

[19] C. Sertatl, M. A. Altnkaya, and K. Raoof, "A novel acoustic indoor localization system employing CDMA," *Digital Signal Processing*, vol. 22, no. 3, pp. 506–517, 2012.

[20] R. B. Davis III, S. Ounpuu, D. Tyburski, and J. R. Gage, "A gait analysis data collection and reduction technique," *Human Movement Science*, vol. 10, no. 5, pp. 575–587, 1991.

[21] Y. Zejie, Y. Yanming, W. Qihang, and L. Wenlian, "A new system for three–dimensional kinematic trajectory acquisition and analysis–I. The application of an ultrasonic technique to human gait analysis," *Medical engineering & physics*, vol. 18, no. 5, pp. 420–426, 1996.

[22] Y. Zejie, Y. Yanming, L. Wenlian, and W. Qihang, "A new system for three–dimensional kinematic trajectory acquisition and analysis–II. Digital

orthogonal integration phase–detection technique," *Medical engineering & physics*, vol. 18, no. 5, pp. 427–432, 1996.

[23] R. B. Huitema, A. L. Hof, and K. Postema, "Ultrasonic motion analysis system–measurement of temporal and spatial gait parameters," *Journal of biomechanics*, vol. 35, no. 6, pp. 837–842, 2002.

[24] L. Vogt, M. Portscher, K. Brettmann, K. Pfeifer, and W. Banzer, "Cross–validation of marker configurations to measure pelvic kinematics in gait," *Gait & posture*, vol. 18, no. 3, pp. 178–184, 2003.

[25] R. M. Kiss, L. Kocsis, and Z. Knoll, "Joint kinematics and spatial–temporal parameters of gait measured by an ultrasound-based system," *Medical engineering & physics*, vol. 26, no. 7, pp. 611–620, 2004.

[26] A. Putzhammer, B. Heindl, K. Broll, L. Pfeiff, M. Perfahl, and G. Hajak, "Spatial and temporal parameters of gait disturbances in schizophrenic patients," *Schizophrenia research*, vol. 69, no. 2, pp. 159–166, 2004.

[27] A. Putzhammer, M. Perfahl, L. Pfeiff, and G. Hajak, "Gait disturbances in patients with schizophrenia and adaptation to treadmill walking," *Psychiatry and clinical neurosciences*, vol. 59, no. 3, pp. 303–310, 2005.

[28] G. Ogris, T. Stiefmeier, H. Junker, P. Lukowicz, and G. Troster, "Using ultrasonic hand tracking to augment motion analysis based recognition of manipulative gestures," in *Proceedings of the 9th IEEE International Symposium on Wearable Computers*, 2005, pp. 152–159.

[29] T. Stiefmeier, G. Ogris, H. Junker, P. Lukowicz, and G. Troster, "Combining motion sensors and ultrasonic hands tracking for continuous activity recognition in a maintenance scenario," in *Proceedings of the 10th IEEE International Symposium on Wearable Computers*, 2006, pp. 97–104.

[30] Y. Wahab, "Design and implementation of MEMS biomechanical sensors for real-life measurements of gait parameters," Ph.D. dissertation, Victoria University, Australia., 2009.

[31] N. Hemmati and P. Rangraz, "Design of ultrasonic motion analysis system for estimating segment's stabilization during dynamic condition," in *IEEE EUROCON*, May 2009, pp. 134–137.

[32] T. Sato, S. Nakamura, K. Terabayashi, M. Sugimoto, and H. Hashizume, "Design and implementation of a robust and real-time ultrasonic motion-capture system," in *Proceedings of the International Conference on Indoor Positioning and Indoor Navigation*, Sept. 2011, pp. 1–6.

[33] Y. Wahab and N. Bakar, "Gait analysis measurement for sport application based on ultrasonic system," Jun. 2011, pp. 20–24.

[34] J. Roggendorf, S. Chen, S. Baudrexel, S. van de Loo, C. Seifried, and R. Hilker, "Arm swing asymmetry in parkinson's disease measured with ultrasound based motion analysis during treadmill gait," *Gait & posture*, vol. 35, no. 1, pp. 116–120, 2012.

[35] M. Domagalska, A. Szopa, M. Syczewska, S. Pietraszek, Z. Kidoń, and G. Onik, "The relationship between clinical measurements and gait analysis data in children with cerebral palsy," *Gait & posture*, vol. 38, no. 4, pp. 1038–1043, 2013.

[36] C. A. Macleod, B. A. Conway, D. B. Allan, and S. S. Galen, "Development and validation of a low-cost, portable and wireless gait assessment tool," *Medical engineering & physics*, vol. 36, no. 4, pp. 541–546, 2014.

[37] Y. Qi, C. B. Soh, E. Gunawan, K.-S. Low, and A. Maskooki, "A novel approach to joint flexion/extension angles measurement based on wearable

UWB radios," *IEEE Journal of Biomedical and Health Informatics*, vol. 18, no. 1, pp. 300–308, Jan. 2014.

[38] Y. Qi, C. Soh, E. Gunawan, and K. Low, "Ambulatory measurement of 3–Dimensional foot displacement during treadmill walking using wearable wireless ultrasonic sensor network," *IEEE Journal of Biomedical and Health Informatics*, no. 99, pp. 1–8, 2014.

[39] Y. Wahab, M. Mazalan, N. Bakar, A. Anuar, M. Zainol, and F. Hamzah, "Low power shoe integrated intelligent wireless gait measurement system," *Journal of Physics: Conference Series*, vol. 495, p. 012044, 2014.

[40] F. Tatar, J. Mollinger, J. Bastemeijer, and A. Bossche, "Time of flight technique used for measuring position and orientation of laparoscopic surgery tools," in *Proceedings of the IEEE on Sensors*, vol. 3, Oct. 2004, pp. 1480–1483.

[41] N. Priyantha, A. Chakraborty, and H. Balakrishnan, "The cricket location-support system," in *Proceedings of the of the 6th Annual International Conference on Mobile computing and networking*, 2000, pp. 32–43.

[42] N. B. Priyantha, A. K. L. Miu, H. Balakrishnan, and S. Teller, "The cricket compass for context-aware mobile applications," in *Proceedings of the 7th annual International Conference on Mobile computing and networking*, 2001, pp. 1–14.

[43] Y. Fukuju, M. Minami, H. Morikawa, and T. Aoyama, "DOLPHIN: an autonomous indoor positioning system in ubiquitous computing environment," in *Proceedings of the IEEE Workshop on Software Technologies for Future Embedded Systems*, 2003, pp. 53–56.

[44] T. Hori and Y. Nishida, "Improvement of position estimation of the ultrasonic 3D tag system," in *Proceedings of the 17th IEEE International Symposium on Robot and Human Interactive Communication*, Aug. 2008, pp. 436–441.

[45] A. Ward, A. Jones, and A. Hopper, "A new location technique for the active office," *IEEE journal on Personal Communications*, vol. 4, pp. 42–47, Oct. 1997.

[46] M. Saad, C. Bleakley, T. Ballal, and S. Dobson, "High–accuracy reference-free ultrasonic location estimation," *IEEE Transactions on Instrumentation and Measurement*, vol. 61, no. 6, pp. 1561–1570, Jun. 2012.

[47] M. Alloulah and M. Hazas, "An efficient CDMA core for indoor acoustic position sensing," in *Proceedings of the International Conference on Indoor Positioning and Indoor Navigation*, 2010, pp. 1–5.

[48] K. Mizutani, T. Ito, M. Sugimoto, and H. Hashizume, "Fast and accurate ultrasonic 3D localization using the TSaT-MUSIC algorithm," in *Proceedings of the International Conference on Indoor Positioning and Indoor Navigation*, 2010, pp. 1–5.

[49] S. Lopes, J. Vieira, and D. Albuquerque, "High accuracy 3D indoor positioning using broadband ultrasonic signals," in *Proceedings of the 11th IEEE International Conference on Trust, Security and Privacy in Computing and Communications*, Jun. 2012, pp. 2008–2014.

[50] S. Holm and C. Nilsen, "Robust ultrasonic indoor positioning using transmitter arrays," in *Proceedings of the International Conference on Indoor Positioning and Indoor Navigation*, 2010, pp. 1–5.

[51] S. Widodo, T. Shiigi, N. Hayashi, H. Kikuchi, K. Yanagida, Y. Nakatsuchi, Y. Ogawa, and N. Kondo, "Moving object localization using sound-based positioning system with doppler shift compensation," *Robotics*, vol. 2, no. 2, pp. 36–53, 2013.

[52] A. Yazici, U. Yayan, and H. Yucel, "An ultrasonic based indoor positioning system," in *Proceedings of the International Symposium on Innovations in Intelligent Systems and Applications*, 2011, pp. 585–589.

[53] A. Sanchez, A. Castro, S. Elvira, G. Glez-de Rivera, and J. Garrido, "Autonomous indoor ultrasonic positioning system based on a low-cost conditioning circuit," *Measurement*, vol. 45, no. 3, pp. 276–283, 2012.

[54] H. Schweinzer and M. Syafrudin, "LOSNUS: an ultrasonic system enabling high accuracy and secure TDOA locating of numerous devices," in *Proceedings of the International Conference on Indoor Positioning and Indoor Navigation*, 2010, pp. 1–8.

[55] J. Tapson, "High precision, short range ultrasonic sensing by means of resonance mode-locking," *Ultrasonics*, vol. 33, no. 6, pp. 441–444, 1995.

[56] R. Queiros, F. Alegria, P. Girao, and A. Serra, "Cross–correlation and sine–fitting techniques for high–resolution ultrasonic ranging," *IEEE Transactions on Instrumentation and Measurement*, vol. 59, no. 12, pp. 3227–3236, 2010.

[57] K. Pahlavan, X. Li, and J.-P. Makela, "Indoor geolocation science and technology," *IEEE Communications Magazine*, vol. 40, no. 2, pp. 112–118, 2002.

[58] P. Misra, N. Kottege, B. Kusy, D. Ostry, and S. Jha, "Acoustical ranging techniques in embedded wireless sensor networked devices," *ACM Transactions on Sensor Networks*, vol. 10, no. 1, pp. 15:1–15:38, Dec. 2013.

[59] J. Jackson, R. Summan, G. Dobie, S. Whiteley, S. Pierce, and G. Hayward, "Time–of–flight measurement techniques for airborne ultrasonic ranging," *IEEE Transactions on Ultrasonics, Ferroelectrics and Frequency Control*, vol. 60, no. 2, pp. 343–355, Feb. 2013.

[60] H. L. B. Hoffman, Wellenhof and J. Collins, *Global positioning system: Theory and Practice.* 4th Ed. Springer Verlag, 1997.

[61] J. Figueiras and S. Frattasi, *Mobile positioning and tracking: From conventional to cooperative techniques.* John Wiley & Sons, 2011.

[62] G. Mao, B. Fidan, and B. Anderson, "Wireless sensor network localization techniques," *Computer networks*, vol. 51, no. 10, pp. 2529–2553, 2007.

[63] N. B. Priyantha, H. Balakrishnan, E. Demaine, and S. Teller, "Anchor-free distributed localization in sensor networks," in *Proceedings of the 1st International Conference on Embedded Networked Sensor Systems*, 2003, pp. 340–341.

[64] C. Randell, C. Djiallis, and H. Muller, "Personal position measurement using dead reckoning," in *Proceedings of the 7th IEEE International Symposium on Wearable Computers*, Oct. 2003, pp. 166–173.

[65] R. Jirawimut, P. Ptasinski, V. Garaj, F. Cecelja, and W. Balachandran, "A method for dead reckoning parameter correction in pedestrian navigation system," *IEEE Transactions on Instrumentation and Measurement*, vol. 52, no. 1, pp. 209–215, Feb. 2003.

[66] L. Fang, P. Antsaklis, L. Montestruque, M. McMickell, M. Lemmon, Y. Sun, H. Fang, I. Koutroulis, M. Haenggi, M. Xie, and X. Xie, "Design of a wireless assisted pedestrian dead reckoning system - the navmote experience," *IEEE*

Transactions on Instrumentation and Measurement, vol. 54, no. 6, pp. 2342–2358, Dec. 2005.

[67] C. loic Tisse, T. Fauvel, and H. Durrant-Whyte, "A micro aerial vehicle motion capture system," in *Proceedings of the 1st International Conference on Sensing Technology*, 2005, pp. 533–538.

[68] L. Klingbeil and T. Wark, "A wireless sensor network for real-time indoor localisation and motion monitoring," in *Proceedings of the International Conference on Information Processing in Sensor Networks*, 2008, pp. 39–50.

[69] A. Smith, H. Balakrishnan, M. Goraczko, and N. B. Priyantha, "Tracking moving devices with the cricket location system," in *Proceedings of the 2nd International Conference on Mobile Systems, Applications and Services*, Jun. 2004.

[70] J. Hightower and G. Borriello, "Location systems for ubiquitous computing," *Computer*, vol. 34, no. 8, pp. 57–66, 2001.

[71] A. Harter, A. Hopper, P. Steggles, A. Ward, and P. Webster, "The anatomy of a context-aware application," *Journal of Wireless Networks*, vol. 8, no. 2/3, pp. 187–197, Mar. 2002.

[72] C. Peng, G. Shen, Y. Zhang, Y. Li, and K. Tan, "Beepbeep: a high accuracy acoustic ranging system using cots mobile devices," in *Proceedings of the 5th International Conference on Embedded Networked Sensor Systems*, 2007, pp. 1–14.

[73] L. Girod and D. Estrin, "Robust range estimation using acoustic and multimodal sensing," in *Proceedings of the IEEE/RSJ International Conference on Intelligent Robots and Systems*, vol. 3, 2001, pp. 1312–1320.

[74] M. Youssef, A. Youssef, C. Rieger, U. Shankar, and A. Agrawala, "Pinpoint: an asynchronous time-based location determination system," in *Proceedings of the 4th International Conference on Mobile systems, applications and services*, 2006, pp. 165–176.

[75] R. J. Fontana and S. J. Gunderson, "Ultra-wideband precision asset location system," in *Proceedings of the IEEE Conference on Ultra Wideband Systems and Technologies*, 2002, pp. 147–150.

[76] N. Alsindi, X. Li, and K. Pahlavan, "Analysis of time of arrival estimation using wideband measurements of indoor radio propagations," *IEEE Transactions on Instrumentation and Measurement*, vol. 56, no. 5, pp. 1537–1545, Oct. 2007.

[77] E. Xu, Z. Ding, and S. Dasgupta, "Source localization in wireless sensor networks from signal time-of-arrival measurements," *IEEE Transactions on Signal Processing*, vol. 59, no. 6, pp. 2887–2897, Jun. 2011.

[78] S. Venkateswaran and U. Madhow, "Localizing multiple events using times of arrival: a parallelized, hierarchical approach to the association problem," *IEEE Transactions on Signal Processing*, vol. 60, no. 10, pp. 5464–5477, Oct. 2012.

[79] T. Wang, Y. Sekercioglu, A. Neild, and J. Armstrong, "Position accuracy of time-of-arrival based ranging using visible light with application in indoor localization systems," *Journal of Lightwave Technology*, vol. 31, no. 20, pp. 3302–3308, Oct. 2013.

[80] Y. Chan and K. Ho, "A simple and efficient estimator for hyperbolic location," *IEEE Transactions on Signal Processing*, vol. 42, no. 8, pp. 1905–1915, 1994.

[81] N. Liu, Z. Xu, and B. Sadler, "Low–complexity hyperbolic source localization with a linear sensor array," *IEEE Signal Processing Letters*, vol. 15, pp. 865–868, 2008.

[82] C. Randell and H. L. Muller, "Low cost indoor positioning system," in *Proceedings of the International Symposium on Ubiquitous Computing*, 2001, pp. 42–48.

[83] S.-J. Kim and B.-K. Kim, "Accurate hybrid global self-localization algorithm for indoor mobile robots with two-dimensional isotropic ultrasonic receivers," *IEEE Transactions on Instrumentation and Measurement*, vol. 60, no. 10, pp. 3391–3404, 2011.

[84] R. Zhang, F. Hoflinger, and L. Reindl, "TDOA–based localization using interacting multiple model estimator and ultrasonic transmitter/receiver," *IEEE Transactions on Instrumentation and Measurement*, vol. 62, no. 8, pp. 2205–2214, 2013.

[85] B. Liu, H. Chen, Z. Zhong, and H. Poor, "Asymmetrical round trip based synchronization-free localization in large-scale underwater sensor networks," *IEEE Transactions on Wireless Communications*, vol. 9, no. 11, pp. 3532–3542, Nov. 2010.

[86] M. Parrilla, J. Anaya, and C. Fritsch, "Digital signal processing techniques for high accuracy ultrasonic range measurements," *IEEE Transactions on Instrumentation and Measurement*, vol. 40, no. 4, pp. 759–763, 1991.

[87] B. Barshan and R. Kuc, "A bat–like sonar system for obstacle localization," *IEEE Transactions on Systems, Man and Cybernetics*, vol. 22, no. 4, pp. 636–646, 1992.

[88] W. MaMullen, B. Delaughe, and J. Bird, "A simple rising–edge detector for time–of–arrival estimation," *IEEE Transactions on Instrumentation and Measurement*, vol. 45, no. 4, pp. 823–827, 1996.

[89] B. Barshan, "Fast processing techniques for accurate ultrasonic range measurements," *Measurement Science and Technology*, vol. 11, no. 1, p. 45, 2000.

[90] B. Barshan and B. Ayrulu, "Performance comparison of four methods of time–of–flight estimation for sonar waveforms," *Electronics Letters*, vol. 34, no. 16, pp. 1616–1617, 1998.

[91] D. Marioli, C. Narduzzi, C. Offelli, D. Petri, E. Sardini, and A. Taroni, "Digital time-of-flight measurement for ultrasonic sensors," *IEEE Transactions on Instrumentation and Measurement*, vol. 41, no. 1, pp. 93–97, 1992.

[92] K. Nakahira, T. Kodama, S. Morita, and S. Okuma, "Distance measurement by an ultrasonic system based on a digital polarity correlator," *IEEE Transactions on Instrumentation and Measurement*, vol. 50, no. 6, pp. 1748–1752, Dec. 2001.

[93] S. W. Smith, *Digital Signal Processing: A Practical Guide for Engineers and Scientists*. Oxford, UK: Newnes, 2003.

[94] A. J. Weiss and E. Weinstein, "Fundamental limitations in passive time delay estimation–part I: narrow–band systems," *IEEE Transactions on Acoustics, Speech and Signal Processing*, vol. 31, no. 2, pp. 472–486, 1983.

[95] S. Aalemian, H. Keivani, and O. Mahdiyar, "Comparison of radar pulse compression techniques," in *Proceedings of the IEEE International Symposium on Microwave, Antenna, Propagation and EMC Technologies for Wireless Communications*, vol. 2, 2005.

[96] P. Atkins, T. Collins, and K. Foote, "Transmit-signal design and processing strategies for sonar target phase measurement," *IEEE Journal of Selected Topics in Signal Processing*, vol. 1, no. 1, pp. 91–104, 2007.

[97] B. Sharif, J. Neasham, O. Hinton, and A. Adams, "A computationally efficient doppler compensation system for underwater acoustic communications," *IEEE Journal of Oceanic Engineering*, vol. 25, pp. 52–61, Jan. 2000.

[98] F. Álvarez, T. Aguilera, J. Fernandez, J. Moreno, and A. Gordillo, "Analysis of the performance of an ultrasonic local positioning system based on the emission of kasami codes," in *Proceedings of the International Conference on Indoor Positioning and Indoor Navigation*, Sept. 2010, pp. 1–5.

[99] J. A. Paredes, T. Aguilera, F. J. Álvarez, J. Lozano, and J. Morera, "Analysis of doppler effect on the pulse compression of different codes emitted by an ultrasonic LPS," *Sensors*, vol. 11, no. 11, pp. 10 765–10 784, 2011.

[100] F. J. Alvarez, T. Aguilera, J. A. Paredes, J. Morera, and J. A. Fernández, "Effect of receiver movement on signal detection in an ultrasonic LPS," in *Proceedings of the International Conference on Indoor Positioning and Indoor Navigation*, 2011, pp. 21–23.

[101] F. J. Álvarez, Álvaro Hernández, J. A. Moreno, M. C. Pérez, J. Urea, and C. D. Marziani, "Doppler-tolerant receiver for an ultrasonic LPS based on kasami sequences," *Sensors and Actuators A: Physical*, vol. 189, pp. 238 – 253, 2013.

[102] H. Liu, H. Darabi, P. Banerjee, and J. Liu, "Survey of wireless indoor positioning techniques and systems," *IEEE Transactions on Systems, Man, and Cybernetics, Part C: Applications and Reviews*, vol. 37, no. 6, pp. 1067–1080, 2007.

[103] N. Patwari, A. Hero, M. Perkins, N. Correal, and R. O'Dea, "Relative location estimation in wireless sensor networks," *IEEE Transactions on Signal Processing*, vol. 51, no. 8, pp. 2137–2148, 2003.

[104] H. Hashemi, "The indoor radio propagation channel," *Proceedings of the IEEE*, vol. 81, no. 7, pp. 943–968, 1993.

[105] T. Rappaport, *Wireless Communications: Principles and Practice*, 2nd ed. Prentice Hall PTR, 2001.

[106] P. Bahl and V. Padmanabhan, "RADAR: an in-building rf-based user location and tracking system," in *Proceedings of the 19th IEEE Annual Joint Conference of the IEEE Computer and Communications Societies*, vol. 2, 2000, pp. 775–784.

[107] E. Elnahrawy, X. Li, and R. P. Martin, "The limits of localization using signal strength: a comparative study," in *Proceedings of the 1st Annual IEEE Communications Society Conference on Sensor and Ad Hoc Communications and Networks*, 2004, pp. 406–414.

[108] K. Whitehouse, C. Karlof, and D. Culler, "A practical evaluation of radio signal strength for ranging-based localization," *SIGMOBILE Mobile Computing and Communications Review*, vol. 11, no. 1, pp. 41–52, Jan. 2007.

[109] P. Krishnan, A. Krishnakumar, W.-H. Ju, C. Mallows, and S. Gamt, "A system for LEASE: location estimation assisted by stationary emitters for indoor RF wireless networks," in *Proceedings of the 23rd Annual Joint Conference of the IEEE Computer and Communications Societies*, vol. 2, 2004, pp. 1001–1011.

[110] D. Niculescu and B. Nath, "Ad hoc positioning system (APS)," in *Proceedings of the IEEE Global Telecommunications Conference*, vol. 5, 2001, pp. 2926–2931.

[111] D. Koks, "Numerical calculations for passive geolocation scenarios, Edinburgh, SA, Australia," Defense Science and Technology Organization, Department of Defence, Australian Government, Tech. Rep., 2005.

[112] J. H. Winters, "Smart antenna techniques and their application to wireless ad hoc networks," *IEEE Wireless Communications*, vol. 13, no. 4, pp. 77–83, 2006.

[113] M. Boushaba, A. Hafid, and A. Benslimane, "High accuracy localization method using AoA in sensor networks," *Computer Networks*, vol. 53, no. 18, pp. 3076–3088, 2009.

[114] N. Patwari, J. Ash, S. Kyperountas, A. Hero, R. Moses, and N. Correal, "Locating the nodes: cooperative localization in wireless sensor networks," *IEEE Signal Processing Magazine*, vol. 22, no. 4, pp. 54–69, 2005.

[115] W. Murphy and W. Hereman, "Determination of a position in three dimensions using trilateration and approximate distances," *Department of Mathematical and Computer Sciences, Colorado School of Mines, Golden, Colorado, MCS-95-07*, vol. 19, 1995.

[116] D. Manolakis, "Efficient solution and performance analysis of 3D position estimation by trilateration," *IEEE Transactions on Aerospace and Electronic Systems*, vol. 32, no. 4, pp. 1239–1248, Oct. 1996.

[117] L. Hu and D. Evans, "Localization for mobile sensor networks," in *Proceedings of the 10th Annual International Conference on Mobile Computing and Networking*, 2004, pp. 45–57.

[118] Z. Yang and Y. Liu, "Quality of trilateration: confidence-based iterative localization," *IEEE Transactions on Parallel and Distributed Systems*, vol. 21, no. 5, pp. 631–640, 2010.

[119] A. Savvides, H. Park, and M. B. Srivastava, "The bits and flops of the n-hop multilateration primitive for node localization problems," in *Proceedings of the 1st ACM International Workshop on Wireless Sensor Networks and Applications*, 2002, pp. 112–121.

[120] D. Moore, J. Leonard, D. Rus, and S. Teller, "Robust distributed network localization with noisy range measurements," in *Proceedings of the 2nd International Conference on Embedded Networked Sensor Systems*, 2004, pp. 50–61.

[121] D. K. Goldenberg, P. Bihler, M. Cao, J. Fang, B. Anderson, A. S. Morse, and Y. R. Yang, "Localization in sparse networks using sweeps," in *Proceedings of the 12th Annual International Conference on Mobile Computing and Networking*, 2006, pp. 110–121.

[122] J. A. Costa, N. Patwari, and A. O. Hero, III, "Distributed weighted-multidimensional scaling for node localization in sensor networks," *ACM Transactions on Sensor Networks*, vol. 2, no. 1, pp. 39–64, Feb. 2006.

[123] H. Lim, L.-C. Kung, J. C. Hou, and H. Luo, "Zero-configuration indoor localization over IEEE 802.11 wireless infrastructure," *Wireless Networks*, vol. 16, no. 2, pp. 405–420, Feb. 2010.

[124] N. B. Priyantha, "The cricket indoor location system," Ph.D. dissertation, Massachusetts Institute of Technology, 2005.

[125] D. Estrin, R. Govindan, J. Heidemann, and S. Kumar, "Next century challenges: scalable coordination in sensor networks," in *Proceedings of the 5th*

annual ACM/IEEE International Conference on Mobile computing and networking, 1999, pp. 263–270.

[126] X. Xu, N. S. Rao, and S. Sahni, "A computational geometry method for localization using differences of distances," *ACM Transactions on Sensor Networks*, vol. 6, no. 2, p. 10, 2010.

[127] C. S. J. Rabaey and K. Langendoen, "Robust positioning algorithms for distributed ad-hoc wireless sensor networks," in *Proceedings of the USENIX technical annual conference*, 2002.

[128] H. Krim and M. Viberg, "Two decades of array signal processing research: the parametric approach," *IEEE Signal Processing Magazine*, vol. 13, no. 4, pp. 67–94, 1996.

[129] J. C. Chen, K. Yao, and R. E. Hudson, "Source localization and beamforming," *IEEE Signal Processing Magazine*, vol. 19, no. 2, pp. 30–39, 2002.

[130] A. Nasipuri and K. Li, "A directionality based location discovery scheme for wireless sensor networks," in *Proceedings of the 1st ACM international Workshop on Wireless Sensor networks and Applications*, 2002, pp. 105–111.

[131] J. J. Pan, J. T. Kwok, Q. Yang, and Y. Chen, "Multidimensional vector regression for accurate and low-cost location estimation in pervasive computing," *IEEE Transactions on Knowledge and Data Engineering*, vol. 18, no. 9, pp. 1181–1193, 2006.

[132] J. Rajamaki, P. Viinikainen, J. Tuomisto, T. Sederholm, and M. Saarnanen, "Laureapop personalized indoor navigation service for specific user groups in a WLAN environment," *WSEAS Transactions on Communications*, vol. 6, no. 4, pp. 524–531, 2007.

[133] M. Takashima, D. Zhao, K. Yanagihara, K. Fukui, S. Fukunaga, S. Hara, and K.-I. Kitayama, "Location estimation using received signal power and maximum likelihood estimation in wireless sensor networks," *Electronics and Communications in Japan (Part I: Communications)*, vol. 90, no. 12, pp. 62–72, 2007.

[134] A. Kushki, K. N. Plataniotis, and A. N. Venetsanopoulos, "Kernel-based positioning in wireless local area networks," *IEEE Transactions on Mobile Computing*, vol. 6, no. 6, pp. 689–705, 2007.

[135] U. Ahmad, A. V. Gavrilov, S. Lee, and Y.-K. Lee, "A modular classification model for received signal strength based location systems," *Neurocomputing*, vol. 71, no. 13, pp. 2657–2669, 2008.

[136] S.-H. Fang and T.-N. Lin, "Indoor location system based on discriminant-adaptive neural network in IEEE 802.11 environments," *IEEE Transactions on Neural Networks*, vol. 19, no. 11, pp. 1973–1978, 2008.

[137] C. Gao, Z. Yu, Y. Wei, S. Russell, and Y. Guan, "A statistical indoor localization method for supporting location-based access control," *Mobile Networks and Applications*, vol. 14, no. 2, pp. 253–263, 2009.

[138] L. M. Ni, Y. Liu, Y. C. Lau, and A. P. Patil, "LANDMARC: indoor location sensing using active RFID," *Wireless networks*, vol. 10, no. 6, pp. 701–710, 2004.

[139] Y. Gu, A. Lo, and I. Niemegeers, "A survey of indoor positioning systems for wireless personal networks," *IEEE Communications Surveys Tutorials*, vol. 11, no. 1, pp. 13–32, 2009.

[140] T.-N. Lin and P.-C. Lin, "Performance comparison of indoor positioning techniques based on location fingerprinting in wireless networks," in *Proceedings of the International Conference on Wireless Networks, Communications and Mobile Computing*, vol. 2, 2005, pp. 1569–1574.

[141] P. Kontkanen, P. Myllymaki, T. Roos, H. Tirri, K. Valtonen, and H. Wettig, "Topics in probabilistic location estimation in wireless networks," in *Proceedings of the 15th IEEE International Symposium on Personal, Indoor and Mobile Radio Communications*, vol. 2, 2004, pp. 1052–1056.

[142] P. Bahl, V. N. Padmanabhan, and A. Balachandran, "Enhancements to the RADAR user location and tracking system," Microsoft Research, Tech. Rep., 2000.

[143] P. Prasithsangaree, P. Krishnamurthy, and P. Chrysanthis, "On indoor position location with wireless LANs," in *Proceedings of the 13th IEEE International Symposium on Personal, Indoor and Mobile Radio Communications*, vol. 2, 2002, pp. 720–724.

[144] N. Cristianini and J. Shawe-Taylor, *An introduction to support vector machines and other kernel-based learning methods.* Cambridge University Press, 2000.

[145] H. Liu, A. Kshirsagar, J. Ku, D. Lamb, and C. Niederberger, "Computational models of intracytoplasmic sperm injection prognosis." in *Proceedings of the European Symposium on Artificial Neural Networks, Computational Intelligence and Machine Learning*, 2005, pp. 115–120.

[146] V. Kecman, *Learning and Soft Computing: Support Vector Machines, Neural Networks, and Fuzzy Logic Models.* Cambridge, MA, USA: MIT Press, 2001.

[147] V. N. Vapnik, *The Nature of Statistical Learning Theory.* New York, NY, USA: Springer-Verlag New York, Inc., 1995.

[148] M. Brunato and R. Battiti, "Statistical learning theory for location fingerprinting in wireless LANs," *Comput. Netw.*, vol. 47, no. 6, pp. 825–845, Apr. 2005.

[149] C.-L. Wu, L.-C. Fu, and F.-L. Lian, "WLAN location determination in e-home via support vector classification," in *Proceedings of the IEEE International Conference on Networking, Sensing and Control*, vol. 2, 2004, pp. 1026–1031.

[150] J. C. Hassab, B. W. Guimond, and S. C. Nardone, "Estimation of location and motion parameters of a moving source observed from a linear array," *The Journal of the Acoustical Society of America*, vol. 70, no. 4, pp. 1054–1061, 1981.

[151] H. Cox, "Resolving power and sensitivity to mismatch of optimum array processors," *The Journal of the acoustical society of America*, vol. 54, no. 3, pp. 771–785, 2005.

[152] J. Rickett and J. Claerbout, "Acoustic daylight imaging via spectral factorization: helioseismology and reservoir monitoring," *The leading edge*, vol. 18, no. 8, pp. 957–960, 1999.

[153] M. Siderius, C. H. Harrison, and M. B. Porter, "A passive fathometer technique for imaging seabed layering using ambient noise," *The Journal of the Acoustical Society of America*, vol. 120, no. 3, pp. 1315–1323, 2006.

[154] P. Gerstoft, W. S. Hodgkiss, M. Siderius, C.-F. Huang, and C. H. Harrison, "Passive fathometer processing," *The Journal of the Acoustical Society of America*, vol. 123, no. 3, pp. 1297–1305, 2008.

[155] M. Siderius, H. Song, P. Gerstoft, W. S. Hodgkiss, P. Hursky, and C. Harrison, "Adaptive passive fathometer processing," *The Journal of the Acoustical Society of America*, vol. 127, no. 4, pp. 2193–2200, 2010.

[156] "Current GPS constellation," [Online]. Available: http://www.usno.navy.mil/USNO/time/gps/current-gps-constellation/.

[157] Á. Lédeczi and M. Maróti., "Wireless sensor node localization," *A Philosophical Transactions of the Royal Society*, vol. 370(1958), pp. 85–99, 2012.

[158] M. Philipose, J. R. Smith, B. Jiang, A. Mamishev, S. Roy, and K. Sundara-Rajan, "Battery–free wireless identification and sensing," *IEEE Pervasive Computing*, vol. 4, no. 1, 2005.

[159] K. Finkenzeller, *Radio-Frequency Identification Fundamentals and Applications.*

[160] H. D. Chon, S. Jun, H. Jung, and S. W. An, "Using RFID for accurate positioning," *Journal of Global Positioning Systems*, vol. 1, pp. 32–39, 2004.

[161] Y. Wang, X. Jia, H. Lee, and G. Li, "An indoors wireless positioning system based on wireless local area network infrastructure," in *Proceedings of the 6th International Symposium on Satellite Navigation Technology Including Mobile Positioning & Location Services.*

[162] T. Kitasuka, K. Hisazumi, and T. Nakanishi, "Wips: location and motion sensing technique of IEEE 802.11 devices," in *Proceedings of the 3rd International Conference on Information Technology and Applications*, vol. 2, 2005, pp. 346–349.

[163] T. King, S. Kopf, T. Haenselmann, C. Lubberger, and W. Effelsberg, "Compass: a probabilistic indoor positioning system based on 802.11 and digital

compasses," in *Proceedings of the 1st international workshop on Wireless network Testbeds, Experimental Evaluation & Characterization*, 2006, pp. 34–40.

[164] "Ekahau," [Online]. Available: http://www.ekahau.com.

[165] M. Maróti, P. Völgyesi, S. Dóra, B. Kusý, A. Nádas, A. Lédeczi, G. Balogh, and K. Molnár, "Radio interferometric geolocation," in *Proceedings of the 3rd International Conference on Embedded Networked Sensor Systems*, 2005, pp. 1–12.

[166] R. Halmshaw, *Non-Destructive Testing.* London, UK: Edward Arnold, 1997.

[167] "Piezoelectric ceramics (piezotite) sensors," [Online]. Available: http://www.murata.com/ catalog at http://lib.chipdip.ru/250/doc000250624.pdf.

[168] "UA-25EX 24Bit/96kHz Audio Capture," [Online]. Available: http://www.rolandus.com/products/details/970.

[169] "USB-1604HS-2AO DAQ user's guide," [Online]. Available: http://www.mccdaq.com/PDFs/Manuals/USB-1604HS-2AO.pdf.

[170] P. K. Misra, D. Ostry, N. Kottege, and S. Jha, "TWEET: an envelope detection based broadband ultrasonic ranging system," 2011, pp. 409–416.

[171] M. McCarthy, H. L. Muller, A. Calway, and R. E. Wilson, "Position and velocity recovery from independent ultrasonic beacons," in *Proceedings of the 14th European Signal Processing Conference*, 2006, pp. 4–8.

[172] K. E. Nolan, "Reconfigurable OFDM systems," Ph.D. dissertation, Trinity College Dublin, 2005.

[173] X. Li, K. Pahlavan, M. Latva-aho, and M. Ylianttila, "Comparison of indoor geolocation methods in DSSS and OFDM wireless LAN systems," in *Proceedings of the 52nd IEEE Vehicular Technology Conference*, vol. 6, 2000, pp. 3015–3020.

[174] J. Li, "Characterization of WLAN Location Fingerprinting Systems," Master's thesis, Institute of Computing Systems Architecture, School of Informatics, University of Edinburgh, 2003.

[175] T. Kitasuka, T. Nakanishi, and A. Fukuda, "Design of wips: WLAN–based indoor positioning system," *Korea Multimedia Society*, vol. 7, no. 4, pp. 15–29, 2003.

[176] J. D. Gupta, H. Suzuki, and K. Ziri-Castro, "Effect of pedestrian movement on MIMO–OFDM channel capacity in an indoor environment," *IEEE Antennas and Wireless Propagation Letters*, vol. 8, pp. 682–685, 2009.

[177] T. J. S. Khanzada, "Wireless communication techniques for indoor positioning and tracking applications," Ph.D. dissertation, Magdeburg University, 2010.

[178] B. Pricope and H. Haas, "Experimental validation of a new pedestrian speed estimator for ofdm systems in indoor environments," in *Proceedings of the IEEE Global Telecommunications Conference*, Dec. 2011, pp. 1–5.

[179] J. Xiao, K. Wu, Y. Yi, and L. Ni, "FIFS: fine-grained indoor fingerprinting system," in *Proceedings of the 21st International Conference on Computer Communications and Networks*, Jul. 2012, pp. 1–7.

[180] K. Wu, J. Xiao, Y. Yi, D. Chen, X. Luo, and L. Ni, "CSI–based indoor localization," *IEEE Transactions on Parallel and Distributed Systems*, vol. 24, no. 7, pp. 1300–1309, Jul. 2013.

[181] B. Pricope and H. Haas, "Positioning using terrestrial wireless systems," Ph.D. dissertation, IRC-Library, Information Resource Center der Jacobs University Bremen, 2013.

[182] M. Shafiee, "WiFi-based fine Timing fssistance for GPS fcquisition," Ph.D. dissertation, Department of Geomatics Engineering Calgary, Alberta, 2003.

[183] J. Ashdown, G. Saulnier, T. Lawry, K. Wilt, and H. Scarton, "High–rate ultrasonic communication through metallic barriers using MIMO–OFDM techniques," in *Proceedings of the Military Communications Conference*, Oct. 2012, pp. 1–6.

[184] K. Wanuga, M. Bielinski, R. Primerano, M. Kam, and K. Dandekar, "High-data-rate ultrasonic through-metal communication," *IEEE Transactions on Ultrasonics, Ferroelectrics and Frequency Control*, vol. 59, no. 9, pp. 2051–2053, Sept. 2012.

[185] T. Lawry, K. Wilt, J. Ashdown, H. Scarton, and G. Saulnier, "A high–performance ultrasonic system for the simultaneous transmission of data and power through solid metal barriers," *IEEE Transactions on Ultrasonics, Ferroelectrics and Frequency Control*, vol. 60, no. 1, pp. 194–203, Jan. 2013.

[186] W. M. D. Wright, O. Doyle, and C. T. Foley, "P2I-9 multi-channel data transfer using air-coupled capacitive ultrasonic transducers," in *Proceedings of the IEEE Ultrasonics Symposium*, Oct. 2006, pp. 1805–1808.

[187] M. Khyam, M. Alam, and M. Pickering, "OFDM based low-complexity time of arrival estimation in active sonar," in *Proceedings of the OCEANS MT-S/IEEE Conference*, 2014, p. in IEEE press.

[188] H. Shaban, M. El-Nasr, and R. M. Buehrer, "Toward a highly accurate ambulatory system for clinical gait analysis via UWB radios," *IEEE Transactions on Information Technology in Biomedicine*, vol. 14, no. 2, pp. 284–291, Mar. 2010.

[189] M. Addlesee, R. Curwen, S. Hodges, J. Newman, P. Steggles, A. Ward, and A. Hopper, "Implementing a sentient computing system," *Computer*, vol. 34, no. 8, pp. 50–56, 2001.

[190] M. Hazas and A. Ward, "A high performance privacy-oriented location system," in *Proceedings of the 1st IEEE International Conference on Pervasive Computing and Communications*, 2003, pp. 216–223.

[191] M. Hazas and A. Hopper, "Broadband ultrasonic location systems for improved indoor positioning," *IEEE Transactions on Mobile Computing*, vol. 5, pp. 536–547, 2006.

[192] J. Hernandez and C. Bleakley, "High–precision robust broadband ultrasonic location and orientation estimation," *IEEE Journal of Selected Topics in Signal Processing*, vol. 3, no. 5, pp. 832–844, 2009.

[193] Y. Zhao and S.-G. Haggman, "Intercarrier interference self-cancellation scheme for OFDM mobile communication systems," *IEEE Transactions on Communications*, vol. 49, no. 7, pp. 1185–1191, Jul. 2001.

[194] T. Wang, J. Proakis, E. Masry, and J. Zeidler, "Performance degradation of OFDM systems due to Doppler spreading," *IEEE Transactions on Wireless Communications*, vol. 5, no. 6, pp. 1422–1432, June 2006.

[195] M. Morelli, C.-C. Kuo, and M.-O. Pun, "Synchronization techniques for orthogonal frequency division multiple access (OFDMA): a tutorial review," *Proceedings of the IEEE*, vol. 95, no. 7, pp. 1394–1427, Jul. 2007.

[196] M. Erol-Kantarci, H. Mouftah, and S. Oktug, “A survey of architectures and localization techniques for underwater acoustic sensor networks,” *IEEE Communications Surveys Tutorials*, vol. 13, no. 3, pp. 487–502, 2011.

[197] C. D. Whitehouse, “Understanding the prediction gap in multi-hop localization,” Ph.D. dissertation, University of California, Berkeley, 2006.

[198] R. Want, A. Hopper, V. Falcão, and J. Gibbons, “The active badge location system,” *ACM Transaction on Information Systems*, vol. 10, no. 1, pp. 91–102, Jan. 1992.

[199] G. Borriello, A. Liu, T. Offer, C. Palistrant, and R. Sharp, “WALRUS: wireless acoustic location with room-level resolution using ultrasound,” in *Proceedings of the 3rd International Conference on Mobile systems, Applications, and Services*, 2005, pp. 191–203.

[200] M. R. McCarthy, “The BUZZ: narrowband ultrasonic positioning for wearable computers,” Ph.D. dissertation, University of Bristol, 2007.

[201] “Sonitor system,” [Online]. Available: http://www.sonitor.com.

[202] F. J. Álvarez, Á. Hernández, J. A. Moreno, M. C. Pérez, C. D. Marziani *et al.*, “Doppler-tolerant receiver for an ultrasonic LPS based on Kasami sequences,” *Sensors and Actuators A: Physical*, vol. 189, pp. 238–253, 2013.

[203] N. Aloui, K. Raoof, A. Bouallegue, S. Letourneur, and S. Zaibi, “Performance evaluation of an acoustic indoor localization system based on a fingerprinting technique,” *EURASIP Journal on Advances in Signal Processing*, vol. 2014, no. 1, pp. 1–16, 2014.

[204] Y. Kwon, K. Mechitov, S. Sundresh, W. Kim, and G. Agha, “Resilient localization for sensor networks in outdoor environments,” in *Proceedings of*

the 25th IEEE International Conference on Distributed Computing Systems, 2005, pp. 643–652.

[205] M. Kushwaha, K. Molnár, J. Sallai, P. Völgyesi, M. Maróti, and A. Lédeczi, "Sensor node localization using mobile acoustic beacons," in *Proceedings of the IEEE International Conference on Mobile Ad-Hoc and Sensor Systems Conference*, 2005.

[206] G. Simon, M. Maróti, A. Lédeczi, G. Balogh, B. Kusy, A. Nádas, G. Pap, J. Sallai, and K. Frampton, "Sensor network-based countersniper system," in *Proceedings of the 2nd International Conference on Embedded Networked Sensor Systems*, 2004, pp. 1–12.

[207] L. Girod, M. Lukac, V. Trifa, and D. Estrin, "The design and implementation of a self-calibrating distributed acoustic sensing platform," in *Proceedings of the 4th International Conference on Embedded Networked Sensor Systems*, 2006, pp. 71–84.

[208] L. D. Girod, "A self-salibrating system of dsistributed scoustic srrays," Ph.D. dissertation, University of California, Los Angeles, 2005.

[209] J. Sallai, G. Balogh, M. Maróti, Á. Lédeczi, and B. Kusy, "Acoustic ranging in resource-constrained sensor networks," in *Proceedings of the International Conference on Wireless and Mobile Computing*, 2004.

[210] C. V. Lopes, A. Haghighat, A. Mandal, T. Givargis, and P. Baldi, "Localization of off-the-shelf mobile devices using audible sound: architectures, protocols and performance assessment," *Mobile Computing and Communications Review*, vol. 10, no. 2, pp. 38–50, Apr. 2006.

[211] N. M. Vallidis, "WHISPER: a spread spectrum approach to occlusion in acoustic tracking," Ph.D. dissertation, University of North Carolina at Chapel Hill, 2002.

[212] J. Hightower, R. Want, and G. Borriello, "SpotON: an indoor 3D location sensing technology based on RF signal strength," University of Washington, Department of Computer Science and Engineering, Tech. Rep., 2000.

[213] "Zebra technology company," [Online]. Available: http://www.wherenet.com.

[214] M. Youssef, A. Agrawala, and A. Udaya Shankar, "WLAN location determination via clustering and probability distributions," in *Proceedings of the 1st IEEE International Conference on Pervasive Computing and Communications*, 2003, pp. 143–150.

[215] M. Youssef and A. Agrawala, "Handling samples correlation in the Horus system," in *Proceedings of the 23th Annual Joint Conference of the IEEE Computer and Communications Societies, 2004*, vol. 2, 2004, pp. 1023–1031.

[216] ——, "The Horus WLAN location determination system," in *Proceedings of the 3rd International Conference on Mobile Systems, Applications, and Services*, 2005, pp. 205–218.

[217] B. Kusy, A. Ledeczi, M. Maroti, and L. Meertens, "Node density independent localization," in *Proceedings of the 5th International Conference on Information Processing in Sensor Networks*, 2006, pp. 441–448.

[218] B. Kusý, A. Lédeczi, and X. Koutsoukos, "Tracking mobile nodes using RF Doppler shifts," in *Proceedings of the 5th International Conference on Embedded Networked Sensor Systems*, 2007, pp. 29–42.

[219] A. Lédeczi, P. Volgyesi, J. Sallai, and R. Thibodeaux, "A novel RF ranging method," in *Proceedings of the International Workshop on Intelligent Solutions in Embedded Systems*, 2008, pp. 1–12.

[220] H.-L. Chang, J.-B. Tian, T.-T. Lai, H.-H. Chu, and P. Huang, "Spinning beacons for precise indoor localization," in *Proceedings of the 6th ACM Conference on Embedded Network Sensor Systems*, 2008, pp. 127–140.

[221] "Topaz local positioning solution," [Online]. Available: http://www.tadlys.com.

[222] A. Kotanen, M. Hannikainen, H. Leppakoski, and T. Hamalainen, "Experiments on local positioning with bluetooth," in *Proceedings of the International Conference on Information Technology: Coding and Computing (Computers and Communications)*, Apr. 2003, pp. 297–303.

[223] J. Hallberg, M. Nilsson, and K. Synnes, "Positioning with bluetooth," in *Proceedings of the 10th International Conference on Telecommunications*, vol. 2, Feb. 2003, pp. 954–958.

[224] "Ubisense," [Online]. Available: http://www.ubisense.net.

[225] A. Smailagic and D. Kogan, "Location sensing and privacy in a context-aware computing environment," *IEEE Wireless Communications*, vol. 9, no. 5, pp. 10–17, 2002.

[226] G. Welch, G. Bishop, L. Vicci, S. Brumback, K. Keller, and D. Colucci, "The HiBall Tracker: high-performance wide-area tracking for virtual and augmented environments," in *Proceedings of the ACM Symposium on Virtual Reality Software and Technology*, 1999, pp. 1–10.

[227] "Coda motion analysis system," [Online]. Available: http://codamotion.com.

[228] "Qualisys motion capture system," [Online]. Available: http://www.qualisys.com.

[229] "Vicon motion analysis system," [Online]. Available: http://www.vicon.com.

[230] B. Brumitt, B. Meyers, J. Krumm, A. Kern, and S. Shafer, "Easyliving: technologies for intelligent environments," in *Handheld and ubiquitous computing*, 2000, pp. 12–29.

[231] SRD, United Kingdom. *SRD Acoustic Equipment Guide.*

[232] Bruel & Kjael, DK-2850 Naerum, Denmark. *Product Data: Hydrophones-Types 8103, 8104, 8105 and 8106.*

[233] ROLAND CORPORATION, 5100 S. Eastern Avenue Los Angeles. CA 90040-2938. *UA-101: Edirol Hi Speed USB Audio Capture.*